NUREG/CR-6534, Vol. 4
PNNL–11513

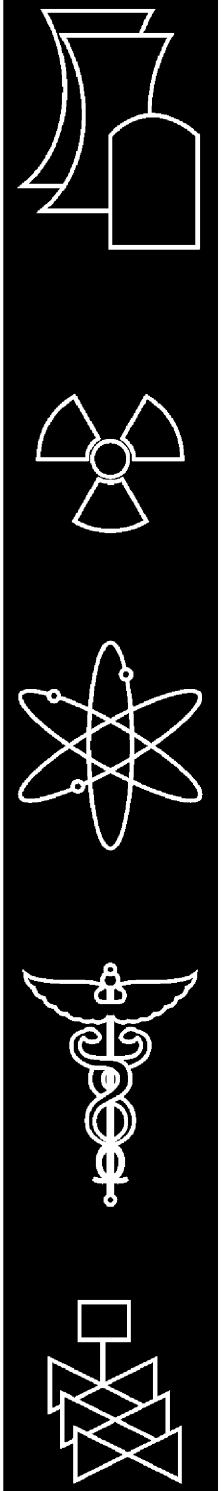

FRAPCON-3 Updates, Including Mixed-Oxide Fuel Properties

Pacific Northwest National Laboratory

U.S. Nuclear Regulatory Commission
Office of Nuclear Regulatory Research
Washington, DC 20555-0001

AVAILABILITY OF REFERENCE MATERIALS IN NRC PUBLICATIONS

NRC Reference Material

As of November 1999, you may electronically access NUREG-series publications and other NRC records at NRC's Public Electronic Reading Room at http://www.nrc.gov/reading-rm.html. Publicly released records include, to name a few, NUREG-series publications; *Federal Register* notices; applicant, licensee, and vendor documents and correspondence; NRC correspondence and internal memoranda; bulletins and information notices; inspection and investigative reports; licensee event reports; and Commission papers and their attachments.

NRC publications in the NUREG series, NRC regulations, and *Title 10, Energy*, in the Code of *Federal Regulations* may also be purchased from one of these two sources.

1. The Superintendent of Documents
   U.S. Government Printing Office
   Mail Stop SSOP
   Washington, DC 20402–0001
   Internet: bookstore.gpo.gov
   Telephone: 202-512-1800
   Fax: 202-512-2250
2. The National Technical Information Service
   Springfield, VA 22161–0002
   www.ntis.gov
   1–800–553–6847 or, locally, 703–605–6000

A single copy of each NRC draft report for comment is available free, to the extent of supply, upon written request as follows:

Address: Office of the Chief Information Officer,
Reproduction and Distribution
Services Section
U.S. Nuclear Regulatory Commission
Washington, DC 20555-0001
E-mail: DISTRIBUTION@nrc.gov
Facsimile: 301–415–2289

Some publications in the NUREG series that are posted at NRC's Web site address http://www.nrc.gov/reading-rm/doc-collections/nuregs are updated periodically and may differ from the last printed version. Although references to material found on a Web site bear the date the material was accessed, the material available on the date cited may subsequently be removed from the site.

Non-NRC Reference Material

Documents available from public and special technical libraries include all open literature items, such as books, journal articles, and transactions, *Federal Register* notices, Federal and State legislation, and congressional reports. Such documents as theses, dissertations, foreign reports and translations, and non-NRC conference proceedings may be purchased from their sponsoring organization.

Copies of industry codes and standards used in a substantive manner in the NRC regulatory process are maintained at—

The NRC Technical Library
Two White Flint North
11545 Rockville Pike
Rockville, MD 20852–2738

These standards are available in the library for reference use by the public. Codes and standards are usually copyrighted and may be purchased from the originating organization or, if they are American National Standards, from—

American National Standards Institute
11 West 42nd Street
New York, NY 10036–8002
www.ansi.org
212–642–4900

Legally binding regulatory requirements are stated only in laws; NRC regulations; licenses, including technical specifications; or orders, not in NUREG-series publications. The views expressed in contractor-prepared publications in this series are not necessarily those of the NRC.

The NUREG series comprises (1) technical and administrative reports and books prepared by the staff (NUREG–XXXX) or agency contractors (NUREG/CR–XXXX), (2) proceedings of conferences (NUREG/CP–XXXX), (3) reports resulting from international agreements (NUREG/IA–XXXX), (4) brochures (NUREG/BR–XXXX), and (5) compilations of legal decisions and orders of the Commission and Atomic and Safety Licensing Boards and of Directors' decisions under Section 2.206 of NRC's regulations (NUREG–0750).

NUREG/CR-6534, Vol. 4
PNNL-11513

FRAPCON-3 Updates, Including Mixed-Oxide Fuel Properties

Manuscript Completed: May 2005
Date Published: May 2005

Prepared by
D. D. Lanning, C. E. Beyer, K.J.Geelhood

Pacific Northwest National Laboratory
Richland, WA 99352

Prepared for
Division of Systems Analysis and Regulatory Effectiveness
Office of Nuclear Regulatory Research
U.S. Nuclear Regulatory Commission
Washington, DC 20555-0001
NRC Job Code Y6586

ABSTRACT

The FRAPCON-3 code has been altered by a number of additions to form version FRAPCON-3.3. The major changes include an improved model for the urania fuel pellet thermal conductivity; the addition of mixed plutonia-urania oxide (MOX) fuel pellet thermal properties and other parameters to facilitate analysis of MOX fuel rod performance; and the addition of corrosion and hydrogen pickup parameters appropriate to advanced cladding types. This volume contains descriptions and discussions of these and other revisions.

The document also contains code-data comparisons of MOX fuel temperatures used to verify the MOX fuel pellet thermal conductivity model, and similar comparisons for urania fuel rods. The total sequence of code revisions that have led from the last-published version of FRAPCON-3 (NUREG/CR-6534, Volume 2, 1997) to the latest issued version, FRAPCON-3.3, is also given.

FOREWORD

Computer codes related to fuel performance have played an important role in the work of the U.S. Nuclear Regulatory Commission (NRC) since the agency's inception in 1975. Formal requirements for fuel performance analysis appear in several of the agency's regulatory guides and regulations, including those related to emergency core cooling system evaluation models, as set forth in Appendix K to Title 10, Part 50, of the *Code of Federal Regulations* (10 CFR Part 50), "Domestic Licensing of Production and Utilization Facilities." Nonetheless, these codes and requirements must evolve to reflect changes in the reactor fuel design. For example, recent initiatives in the U.S. Department of Energy's Surplus Plutonium Disposition Program will incorporate urania-plutonia or mixed-oxide (MOX) fuel for the first time in a commercial nuclear power plant. This made it necessary to seek new experimental data, and to modify and validate the code predictions for proposed new fuel designs.

FRAPCON-3.3, described in this report, is the most recent addition to the series of fuel performance codes developed by Pacific Northwest National Laboratory (PNNL) and used by the NRC. This version of the FRAPCON code incorporates modifications to predict the behavior of material used in the Surplus Plutonium Disposition Program. Although similar in many respects to more traditional low-enrichment urania fuel, MOX fuel exhibits some differences. For fuel performance, the most notable difference is thermal conductivity, which is suppressed with the addition of plutonia. This difference results in higher fuel temperatures at a given linear heat generation rate and must be accounted for in fuel performance analyses.

Changes in the FRAPCON code to account for the addition of plutonia were documented and made public during the MOX hearings for the Catawba Nuclear Station. This report formally captures that information along with other recent code changes, and reviews the experimental data used to validate the code predictions. In so doing, this report supplements three previous volumes of information on FRAPCON in the NUREG/CR-6534 series.

The current report is also noteworthy because of its extensive use of experimental data from test reactor programs (particularly the Halden Reactor Project sponsored by the Nuclear Energy Agency of the Organization for Economic Cooperation and Development). These data, which the NRC obtained under an international agreement, demonstrate that the analytical tools used by the NRC staff are more than adequate for a wide variety of fuel designs and reactor conditions. As presented in this report, these data and the PNNL analyses have contributed significantly to our understanding of nuclear fuel behavior.

Carl J. Paperiello, Director
Office of Nuclear Regulatory Research
U.S. Nuclear Regulatory Commission

CONTENTS

LIST OF FIGURES

LIST OF TABLES

EXECUTIVE SUMMARY

The FRAPCON-3 fuel rod performance code is sponsored by the U.S. Nuclear Regulatory Commission (NRC) for evaluating light water reactor (LWR) fuel performance and is maintained by Pacific Northwest National Laboratory (PNNL). The code is used by fuel experts from a large number of organizations worldwide.

This document discusses the modifications and additions to the FRAPCON-3 code that results in the currently issued version FRAPCON-3.3. The major modifications include an improved thermal conductivity model for urania that provides a better prediction of fuel temperatures at high burnups and at high temperatures. The improved model contains the same adjustment for urania-gadolinia conductivity as provided in the previous conductivity correlation for urania documented in Volume 1 of NUREG/CR6534. This adjustment for gadolinia additions to the current urania correlation was confirmed to provide a good prediction to out-of reactor measurements of unirradiated urania-gadolinia thermal conductivity.

The improved thermal conductivity model also required that the fission gas release (FGR) model be recalibrated and verified. Several new fuel temperature and FGR data were used to recalibrate and verify the thermal conductivity and FGR models including new data from the Halden test reactor with fuel burnups up to 70 GWd/MTU and beyond (temperature only). The modifications to the UO_2 models have shown that the code provides a good prediction of UO_2 fuel temperatures and FGR up to rod-average burnups of 62 GWd/MTU. The code has been verified against a small amount of data beyond this burnup level but these data are not judged to be of sufficient quantity to provide confidence in predictions beyond this burnup level.

Additions and modifications were also performed to model the performance of mixed oxide (MOX) fuel in LWRs. The most important were adding a new thermal conductivity model and increasing the diffusion coefficient in the FGR model to better predict the measured fuel temperature and FGR data from MOX fuel. The modifications have shown that the code provides a good prediction of MOX fuel temperatures up to rod-average burnups of 62 GWd/MTU. While there are FGR data from MOX fuel up to 65 GWd/MTU the code's predictions of MOX fission gas release are of much greater uncertainty than the UO_2 FGR model due to the scarcity of the MOX data. Helium production and release models used for urania are not presently altered for MOX fuel.

The corrosion and hydrogen pickup characteristics of the advanced new alloys of ZIRLO™ and M5™ were added to the code by modifying the current corrosion model for Zircaloy-4 by multiplication factors (< 1.0) appropriate to each alloy, and by reducing the current hydrogen pickup fraction. It is anticipated that a more comprehensive corrosion model will be developed in the future for the code but this simple modification has been shown to provide a good prediction of corrosion for these advanced alloys.

This document also describes additional updates and corrections to existing models and provides traceability for all corrections and updates made since the last published code description documentation (NUREG/CR-6534 Volumes 1, 2 and 3).

ABBREVIATIONS

ALHR	average linear heat rate
at.%	atom percent
atm	atmosphere
ATR	advanced test reactor
BOL	beginning-of-life
BWR	boiling-water reactor
°C	degrees Celsius
cm	centimeters
DOE	U.S. Department of Energy
EOL	end-of-life
°F	degrees Fahrenheit
FDI	fuel duty index
ft	feet
FGR	fission gas release
Gd_2O_3	gadolinia
GWd/MTHM	gigawatt days per metric ton of heavy metal, referring to MOX fuel
GWd/MTU	gigawatt days per metric ton of uranium
$GWd/MTUO_2$	gigawatt days per metric ton of uranium dioxide
GWd/tU	gigawatt days per tonne of uranium
HBWR	Halden Boiling-Water Reactor
HUHB	Halden Ultra High Burnup
in.	inches
ITU	Institute for Transuranium Elements
K	kelvin
kg	kilograms
kW/ft	kilowatts per foot
kW/m	kilowatts per meter
LHGR	linear heat generation rate
LSQ	least-squares
LWR	light-water reactor
MCWO	Monte Carlo N-particle (transport) code Coupled With ORIGEN-2
mm	millimeters

MOX	mixed oxide
MPa	megapascal
NFI	Nuclear Fuels Industries
NRC	U.S. Nuclear Regulatory Commission
PIE	postirradiation examination
PNNL	Pacific Northwest National Laboratory
ppm	parts per million
psi	pounds per square inch
PWR	pressurized water reactor
PuO_2	plutonia
SBR	short binderless route
TD	theoretical density
Torr	unit of pressure equaling approximately 133.3 pascals (after Torrcelli)
UO_2	urania
wt.%	weight percent

1.0 INTRODUCTION

The FRAPCON-3 fuel rod performance computer code is sponsored by the U.S. Nuclear Regulatory Commission (NRC) and maintained by Pacific Northwest National Laboratory (PNNL). The code is used in original or modified form by fuel experts worldwide (see for example, Hodge and Ott, 2004; Vallejo et al., 2004; In de Betou et al., 2004; Kim and Lee, 2004; Hejzlar et al., 2004; Long et al., 2004; Khoruzhii et al., 2004).

The FRAPCON-3 code has been altered by a number of modifications and additions to form version FRAPCON-3.3. The major changes include an improved model choice for the urania fuel pellet thermal conductivity, the addition of mixed PuO_2-UO_2 (plutonia-urania) oxide (MOX) fuel pellet thermal properties and other parameters to facilitate analysis of MOX fuel rod performance, and the addition corrosion and hydrogen pickup parameters appropriate to advanced cladding types. Those models and subroutines in the code not modified are described in Volumes 1 and 2 of NUREG/CR-6534.

MOX light-water reactor (LWR) fuel pellets are high-density, low plutonia-content mixtures of plutonia and urania. This MOX fuel has been produced in France, England, Japan, and Germany and irradiated in European and Japanese power reactors for several decades (Blanpain et al., 2000; Lippens, 1988). In the United States, interest in LWR MOX fuel has been limited since 1978 due to the prohibition on fuel recycle. However, interest has revived recently because special MOX rods will be fabricated to irradiate (fission) excess weapons-grade plutonium in pressurized water reactors (PWRs), rendering the plutonium non-weapons grade and very difficult to access, and extracting nuclear electricity in the process (U.S. Department of Energy, 1999). The U.S. Nuclear Regulatory Commission (NRC) supports MOX fuel performance prediction capability in order to assess vendor assertions of the performance of special MOX rods.

FRAPCON-3 (Berna et al., 1997) and its antecedents, FRAPCON-1 and FRAPCON-2, contained a plutonium content dependency for fuel pellet-specific heat and conductivity. However, these dependencies, reflected in MATPRO-11 Rev. 2 (Hagrman et al., 1981) were drawn from relatively old fast-reactor fuel data that utilized much higher plutonia contents than are currently planned for LWR MOX for weapons-grade plutonium disposition. In addition, FRAPCON-3 lacked any accommodation for input of initial Pu isotopic distribution and calculation of Pu isotopic shift sufficient to accurately track the development of radial power and burnup profiles for MOX fuel.

The NRC, which sponsors the FRAPCON-3 (steady-state) and FRAPTRAN (transient) fuel performance codes, has requested Pacific Northwest National Laboratory (PNNL) to update the FRAPCON-3 code with fuel pellet properties and parameters appropriate for the LWR MOX planned for Pu disposition. This effort also includes confirmation of whether the current subcode used for calculating radial power/burnup distributions (TUBRNP) will adequately predict these profiles when given initial (as-fabricated) plutonium content and weapons-grade isotopic distributions.

Section 2 of this volume contains the description of the revised urania fuel thermal conductivity model, which is shown to better reflect credible recent data both at high temperatures (>2500 K) and at nominal to high burnup (> 30 GWd/tU). Section 3 contains the revisions that have been made to update the FRAPCON-3 code for LWR MOX applications. This section addresses fuel pellet thermal

conductivity, fission gas release (FGR), helium production, Xe/Kr ratio for stable fission gas, radial power/burnup profile predictions, fuel heat capacity, fuel melting, and fuel thermal expansion and swelling. In each section where an update is described, background is given for the update, the updated model is described, the verification against measured data is shown, and the limits and uncertainties are stated.

Updates to the FGR model for urania fuel (in response to the revised urania fuel pellet thermal conductivity model) are described and confirmed against the FGR data base in Section 4.

The updates to cladding corrosion and hydriding to apply to advanced Zircaloy cladding materials (ZIRLO™ and M5™) are discussed in Section 5, together with model corrections for cladding wall thinning due to corrosion. Specific code capability enhancements are described in Section 6. References are given in Section 7.

Appendix A contains code-data comparisons on MOX fuel temperatures used to verify the MOX fuel pellet thermal conductivity model. Appendix B describes the code updates made from the first published version (described in Volumes 1 and 2 of NUREG/CR-6534) up to the present version, FRAPCON-3.3. Appendix C describes the revised code input instructions.

Errata to the various volumes of this NUREG are collected as a list on the PNNL FRAPCON/FRAPTRAN website, www.pnl.gov/frapcon3.

2.0 URANIA FUEL PELLET THERMAL CONDUCTIVITY UPDATE

The Lucuta formula for urania pellet thermal conductivity (Lucuta et al., 1996) used in previous versions of FRAPCON-3 was found to have two inaccuracies: It predicts values at high temperature (> 2200 K) that are too large relative to credible modern data for unirradiated fuel pellet material (Ronchi et al., 1999), and it had too little burnup degradation (and hence was non-conservative above ~30 GWd/tU burnup) compared to both in-cell laser-flash diffusivity measurements on high-burnup pellet samples and in-reactor fuel temperatures measured at nominal to high burnup. The form of the Lucuta equations was also non-standard and did not facilitate comparisons between models. A revised model was developed, as described below.

2.1 Revised Urania Pellet Thermal Conductivity Model

Following examination of several thermal conductivity models, the Nuclear Fuels Industries (NFI) model (Ohira and Itagaki, 1997) (with modifications) was selected as a replacement for the Lucuta model in FRAPCON-3 and FRAPTRAN. This model, as published, applies to urania fuel pellets at ~95% of theoretical density (TD). Similar to most other fuel thermal conductivity models utilized in fuel performance codes, the NFI model consists of a lead term that is inversely proportional to the temperature function A + BT (phonon term), with burnup dependence factors in its denominator, plus terms that model the electronic contribution to fuel heat transfer at high temperature. In the revised model, the temperature-dependent portion of the burnup function in the phonon term is altered, and the form of the electronic term is changed, as shown below:

UNMODIFIED NFI MODEL (for 95% TD pellet material)

$$K = \frac{1}{A + BT + f(Bu) + g(Bu)h(T)} - CT^2 + DT^4 \qquad (2.1)$$

MODIFIED NFI MODEL

$$K = \frac{1}{A + BT + f(Bu) + \left(1 - 0.9\exp(-0.04Bu)\right)g(Bu)h(T)} + \frac{E}{T^2}\exp(-F/T) \qquad (2.2)$$

where:

K	=	thermal conductivity, W/m-K
T	=	temperature in Kelvin
Bu	=	burnup in GWd/MTU
f(Bu)	=	effect of fission products in crystal matrix (solution)
	=	0.00187•bu
g(Bu)	=	effect of irradiation defects, = $0.038 \cdot Bu^{0.28}$,
h(T)	=	temperature dependence of annealing on irradiation defects

$$= \frac{1}{1 + 396e^{-Q/T}}$$

Q = temperature dependence parameter ("Q/R") = 6380 K
A = 0.0452 m-K/W
B = 2.46E-4 m-K/W/K
C = 5.47E-9 W/m-K^3
D = 2.29E14 W/m-K^5
E = 3.5E9 W-K/m
F = 16361 K

As applied in FRAPCON-3, the above model is adjusted for as-fabricated fuel density (in fraction of TD) using the Lucuta recommendation for spherical-shaped pores (Lucuta et al., 1996), as follows:

$$K_d = 1.0789 * K_{95} * [d/\{1.0 + 0.5(1-d)\}] \quad (2.3)$$

where:

d = density in fraction of TD
K_{95} = as-given conductivity (reported to apply at 95% TD)

The factor 1.0789 adjusts the conductivity back to that for 100% TD material.

This model is activated when the user-input integer flag IMOX has the value 0 (the code defaults to IMOX = 0)

The phonon-term modification applies nearly full irradiation defect annealing at low burnup but restores the temperature-dependent annealing at higher burnups such that for burnups greater than 30 GWd/MTU, the phonon term is equivalent to that in the original NFI model. The electronic terms (which in either case become significant only above ~1500 K) are altered to a more theoretically based equation (see Hagrman et al., 1981; Popov et al., 2000). The magnitude is slightly lower than the original NFI model at high temperature. This adjustment was indicated by Institute for Transuranium Elements (ITU) data at on unirradiatied PWR pellet material at temperatures approaching fuel melting (Ronchi et al., 1999).

At low burnup (<20 GWd/MTU) and low temperatures (< 1000 K), the modified model is higher than the unmodified NFI model and roughly equivalent to the Lucuta model without its radiation term. At higher burnup (> 30 GWd/MTU), the revised model is equivalent to the original NFI model with the exception of the small reduction at very high temperatures. These trends are demonstrated in Figures 2.1 through 2.3.

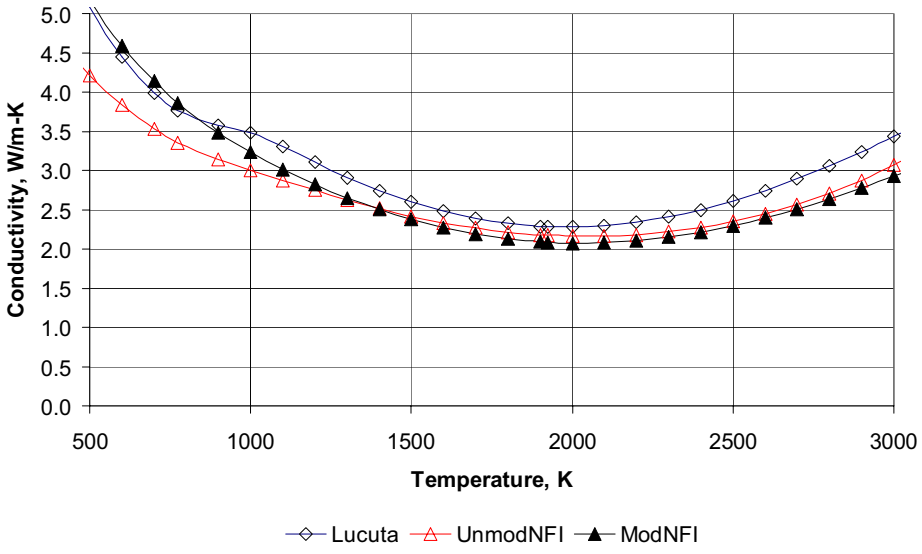

Figure 2.1 The Lucuta, Unmodified NFI, and Modified NFI Fuel Pellet Thermal Conductivity Models Compared at 5 GWd/tU Burnup

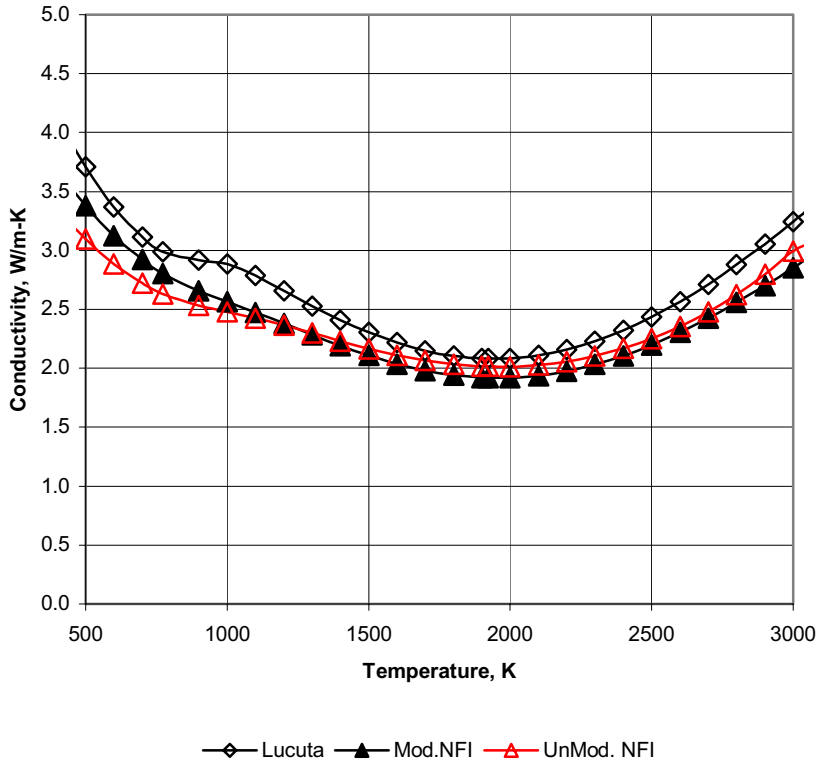

Figure 2.2 The Lucuta, Unmodified NFI, and Modified NFI Fuel Pellet Thermal Conductivity Models Compared at 30 GWd/tU Burnup

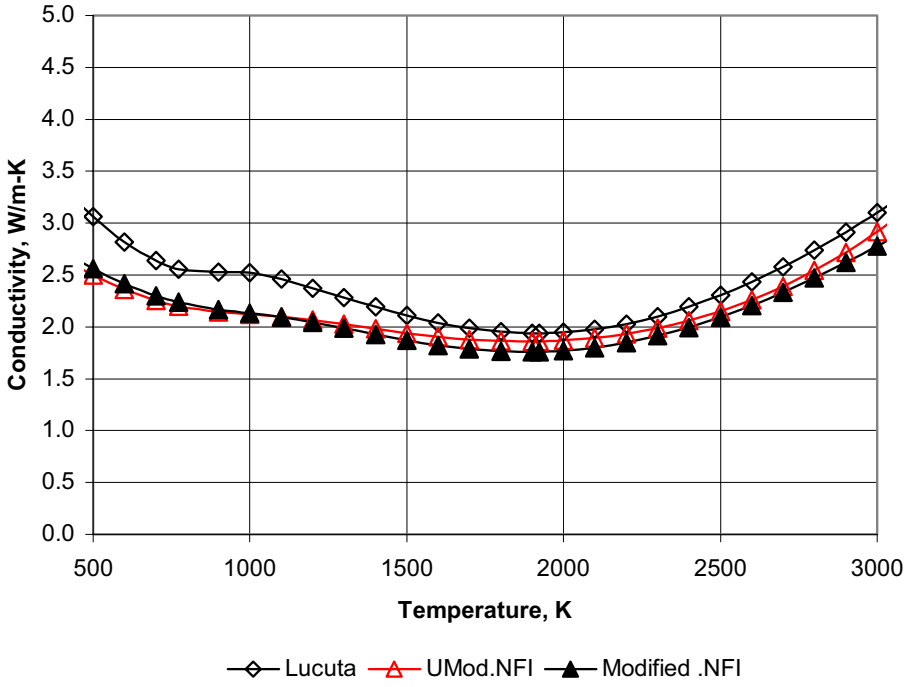

Figure 2.3 The Lucuta, Unmodified NFI, and Modified NFI Fuel Pellet Thermal Conductivity Models Compared at 60 GWd/tU Burnup

2.2 Adjustment for Gadolinia Additions

Gadolinia (Gd_2O_3) additions to reactor fuel provide a burnable absorber for power peaking control early in the life of a fuel assembly. The additions are typically limited to less than 10 wt.%. The impact of limited gadolinia additions on the unirradiated fuel thermal conductivity is somewhat significant due to its disturbance of the lattice and of phonon-type heat transfer. Various commercial fuel vendors have their own data sets and proprietary modeling approaches. In FRAPCON, it will suffice to have a model that captures the effect, and is publicly available. The data correlation in Massih et al. (1992) provides such a model.

Massih found a parameter to be used the denominator in the phonon term of standard equations for urania conductivity that correlated the laser-flash diffusivity data for urania gadolinia conductivity reported by Babcock and Wilcox in Newman et al. (1984). The form of the Massih adder to the phonon term denominator is simply "a" times "g,"

where

a = constant = 1.1599
gad = weight fraction of gadolinia.

Therefore, the modified NFI model with the gadolinia term becomes

$$K = \frac{1}{A + a \cdot gad + BT + f(Bu) + \left(1 - 0.9\exp(-0.04Bu)\right)g(Bu)h(T)} + \frac{E}{T^2}\exp(-F/T) \qquad (2.4)$$

2.3 Verification of the Urania Pellet Thermal Conductivity

In Figure 2.4, the model predictions at zero burnup (unirradiated) are shown in comparison to the Ronchi (1999) data on unirradiated pellet material at nominal and high temperatures to demonstrate that the revised model accounts for the high-temperature portion of that data better than the Lucuta model.

The modified NFI model was also compared to recent laser-flash diffusivity/conductivity data taken post irradiation at ITU on both high-burnup PWR fuel pellet samples and on flat, thin urania disks irradiated at constant temperature to varying burnup levels in the Halden Reactor under the High Burnup Rim Project (Ronchi et al., 2004). The data were compared to the model only at the irradiation temperatures, although data were taken over a large range of temperatures (from room temperature to 1500 K). The comparison is tabled in Table 2.1 and plotted in Figure 2.5. On average, the model overpredicts the data for unannealed material by 8% relative. Since some in-reactor annealing is expected at temperatures of interest, especially in overpower transients when fuel pellet temperatures themselves are of interest, the FRAPCON (modified NFI) model is considered adequate.

The modified NFI model was also compared to postirradiation conductivity from laser flash diffusivity data reported by Carrol et al. (1994) on test fuel irradiated in the Halden Reactor to 40 GWd/tU burnup. The results again show improvement over the Lucuta model (Figure 2.6).

FRAPCON-3 predictions (with the modified NFI pellet thermal conductivity model) are compared to in-reactor test fuel center temperatures in Figure 2.7. The data in this figure come from the Halden Ultra High Burnup instrumented fuel assembly (Wiesenack and Tverberg, 2000). The tendency for the over-prediction at low burnup with the unmodified NFI model and for underprediction at high burnup with the Lucuta model has both been significantly reduced by the revised thermal conductivity model.

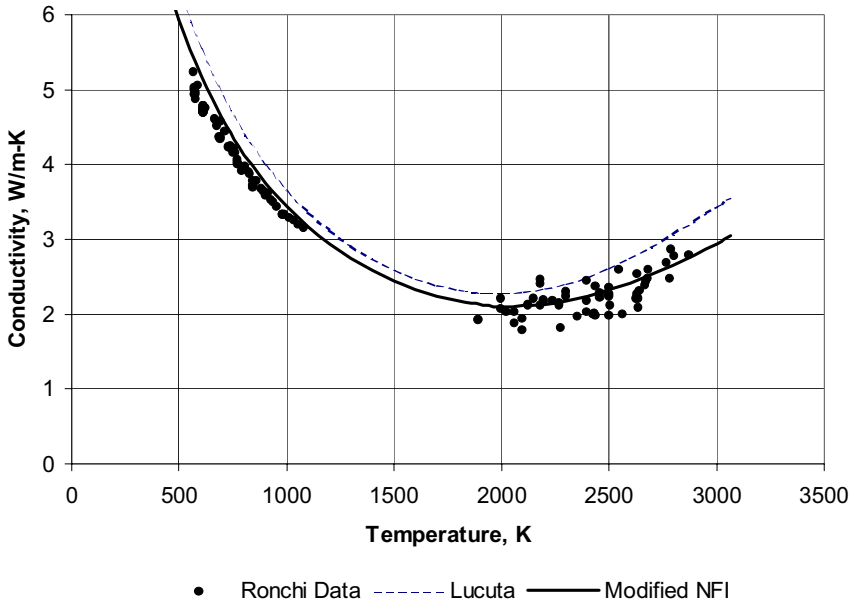

Figure 2.4 Modified NFI and Lucuta Model Predictions Compared to Measured Conductivity on Unirradiated Pellet Material (Ronchi et al., 1999 ITU Data)

Table 2.1 Measured High Burnup Fuel Pellet Material Thermal Conductivity and Calculated Values (see also Figure 2.5)

Burnup GWd/tU	Reported Irradiation Temperature, K	Measured Conductivity (before annealing) W/cm-K	Calculated Conductivity, W/m-K
34	730	2.57	2.76
34	860	2.41	2.60
33	1020	2.16	2.49
34	1210	1.86	2.31
55	680	2.24	2.28
51	890	2.14	2.22
51	1100	1.86	2.11
51	1300	1.92	2.00
82	700	2.10	1.83
96	730	1.98	1.63
92	1490	1.49	1.52

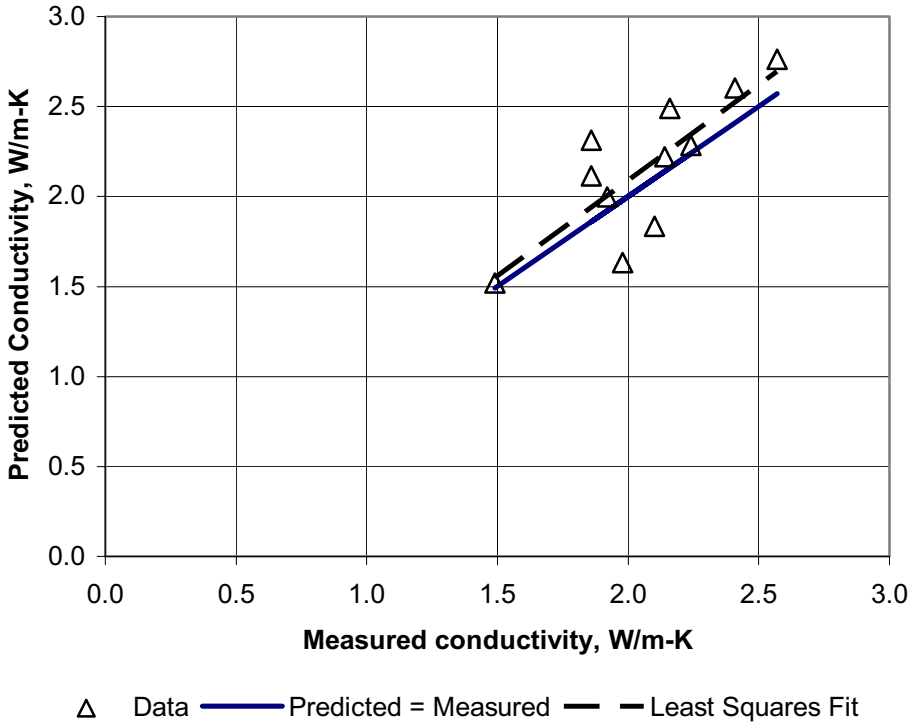

Figure 2.5 Comparison of Modified NFI Fuel Pellet Thermal Conductivity to Ronchi et al. (2004) ITU Data for High Burnup Pellet Material

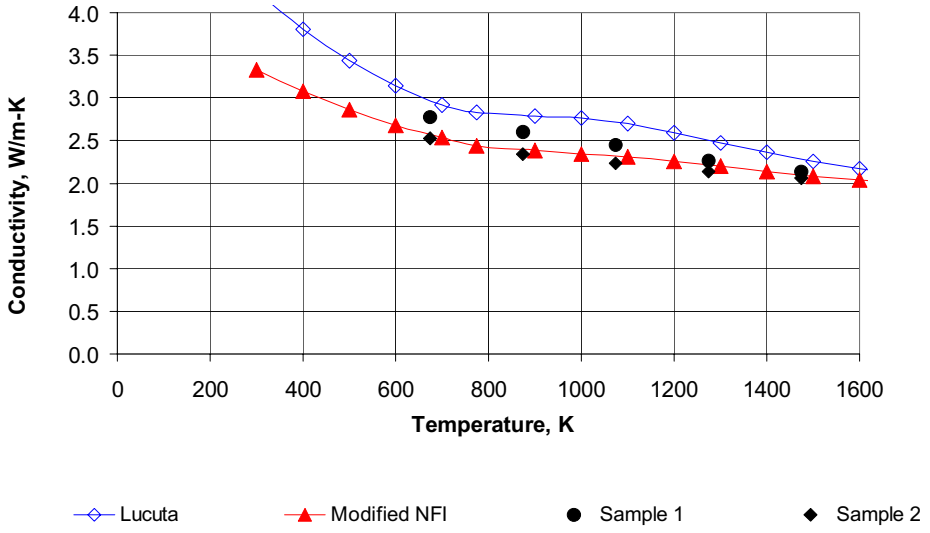

Figure 2.6 The Lucuta and Modified NFI Models Compared to Postirradiation Thermal Conductivity Measurements from Carrol et al. (1994) for BWR Pellet Samples with 40 GWd/tU Burnup

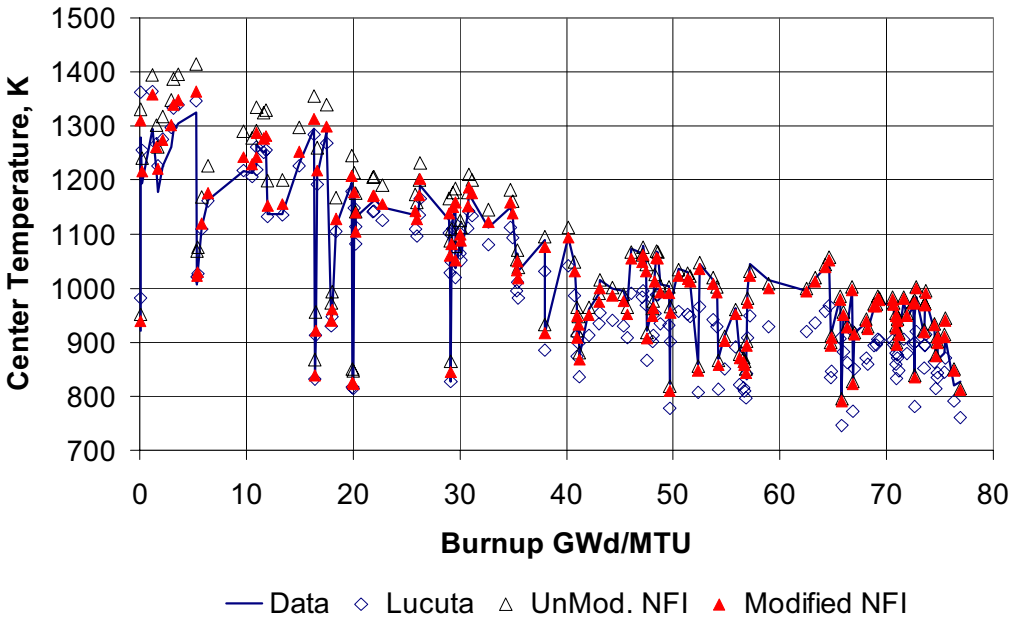

Figure 2.7 FRAPCON-3 Fuel Temperature Predictions Compared to the Halden Ultra High Burnup (HUHB) Data with the Indicated Thermal Conductivity Models in the Code (Wiesenack and Tverberg, 2000)

Code-data comparisons for test fuel center temperatures have been made for two other experiments in Halden. The center temperatures from the lower thermocouple in a small-gap boiling-water reactor (BWR)-type test rod (Rod 3 of IFA-432) (Lanning, 1986) are compared to code prediction in Figure 2.8. In this case, use of the modified NFI model results in a slight overprediction of the temperatures at ~40 GWd/tU, but this could be partly due to overprediction of the FGR for this test rod. A similar comparison is made in Figure 2.9 for a test involving a re-fabricated instrumented high-burnup BWR fuel section, IFA-597.3, with base-irradiation burnup at ~66 GWd/tU. (Matsson and Turnbull, 1998). In this case, due to the refabrication process and the pellet cladding gap closure in the high burnup fuel section, uncertainties in predicted fuel temperature due to uncertainty in gap size and FGR/gap gas composition are minimized. The use of the modified NFI model results in improved code-data comparison in this case.

Based on these comparisons, the FRAPCON-3 code with the Modified NFI model is considered a best-estimate predictor (i.e., not intentionally conservative) for fuel temperatures.

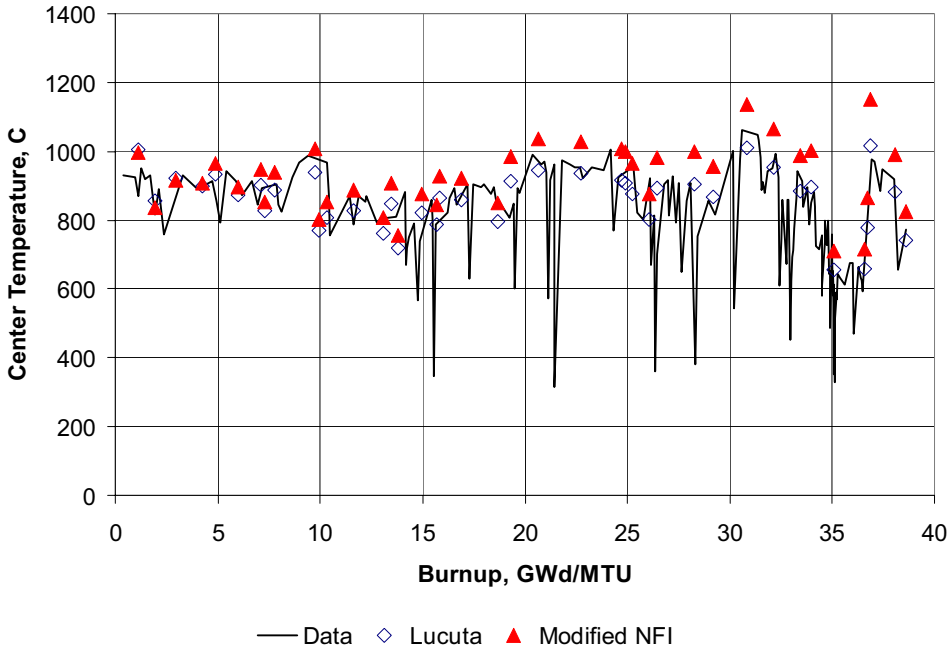

Figure 2.8 Code-Data Comparison for Fuel Center Temperatures for Rod-3 of Halden Experiment IFA-432 (Small-Gap BWR-Style Test Rod)

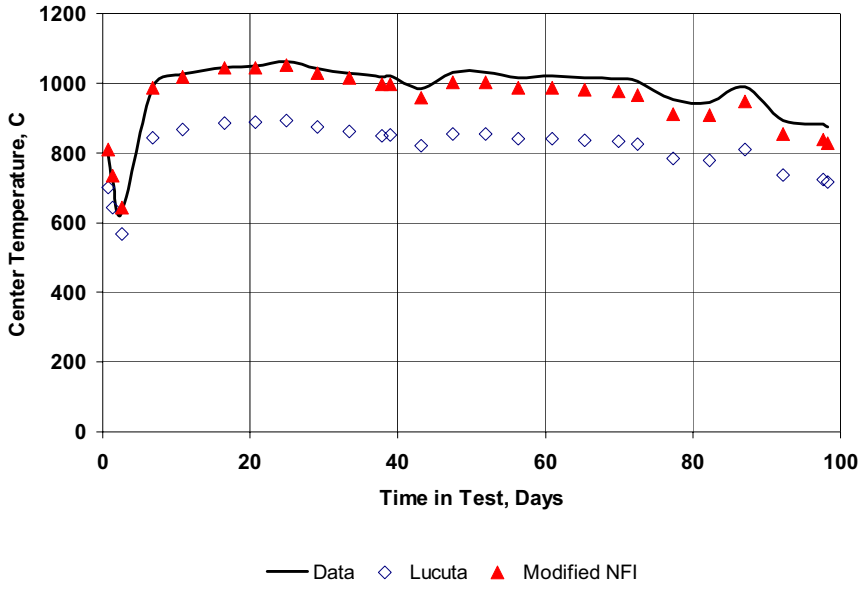

Figure 2.9 Code Data Comparison for Fuel Center Temperatures for Halden Experiment IFA-597.3 Rod 8 (Re-fabricated, Instrumented BWR Fuel Section with ~66 GWd/tU Burnup)

2.3.1 Verification of the Urania-Gadolinia Model

Because the data base for the Massih model only includes gadolinia contents up to 5.66% (Newman, 1984), the model was also compared to data correlations from other studies that included higher gadolinia contents. Hirai and Ishimoto (1991) measured thermal conductivities by the laser-flash diffusion method on sintered samples containing 0, 3, 5, 7, and 10 wt.% gadolinia over the temperature range from 20 to 1750°C. These authors developed a thermal conductivity correlation using a special form for the phonon term that includes point-defect interactions and adding a high-temperature term that fit their data with a standard error of only 6% relative. In an earlier study, Fukushima et al. (1982) measured thermal diffusivities and deduced conductivities in the temperature range from 400 to 1335°C for gadolinia contents of 0 to 10.3 wt.%. A thermal conductivity correlation was also developed by Fukushima et al. (1982) based on their data.

The modified NFI model is compared to the Hirai and Ishimoto (1991), Massih et al. (1992), and Fukushima et al. (1982) data correlations at an example gadolinia content of 8.0 wt.% in Figure 2.10. The Massih model, and the modified NFI model with the Massih gadolinia adjustment, are very similar and show the same qualitative degradation of the thermal conductivity with increasing gadolinia content as the other two correlations and remain intermediate between them in the operating temperature range (above 300°C). The Fukushima et al. (1982) data have been found to be low relative to results of other investigations such as that of Hirai and Ishimoto (1991). We recommend using the Massih correction for gadolinia in FRAPCON, both because of its slightly conservative predictions and its straightforward application within the existing MATPRO fuel thermal conductivity equations.

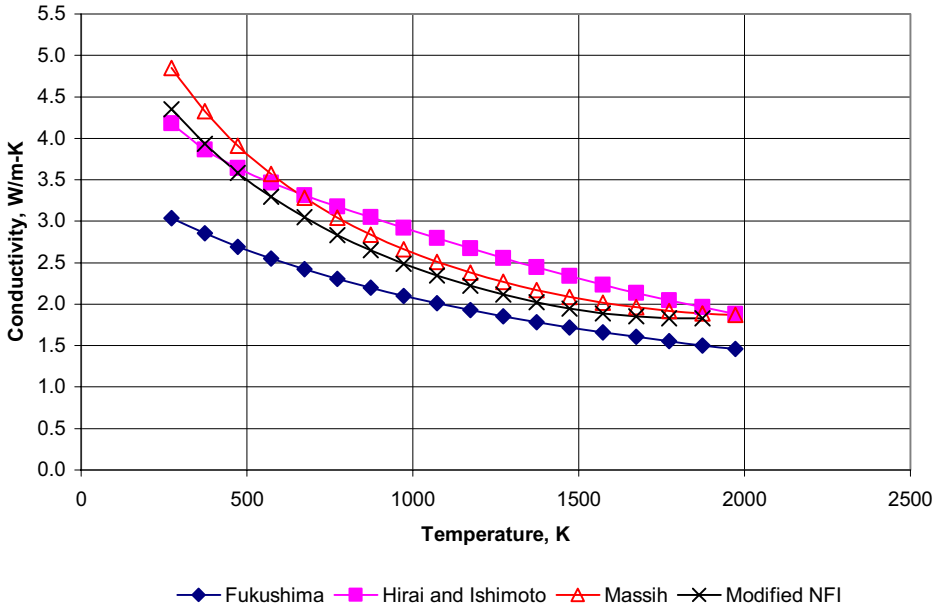

Figure 2.10 The Modified NFI Model with the Massih Adjustment for Gadolinia, Compared to Various Data Correlations at 8.0 Wt.% Gadolinia

The modified NFI model with the Massih adjustment for the phonon term was also compared to data from Hirai and Ishimoto (1991). The comparison, for example at 8.5 wt.%, is shown in Figure 2.11. This is further confirmation that the model is not overpredicting the thermal conductivity at this level of gadolinia content.

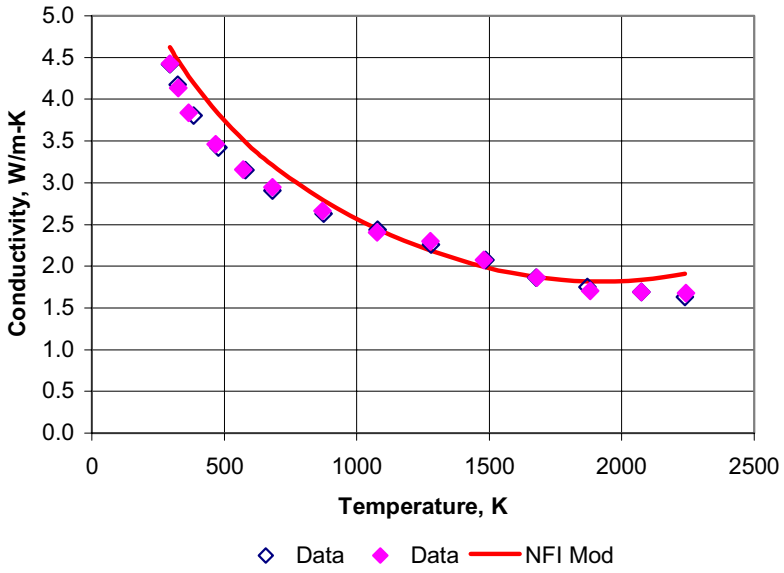

Figure 2.11 Comparison between Modified NFI (with Massih correction for Gadolinia) and Unirradiated Urania Gadolinia Data Trend from Hirai and Ishimoto (1991) at 8.5 wt.% Gadolinia Content

All these comparisons are shown for unirradiated pellet material. As burnup progresses, there is mounting evidence from comparative fuel temperature data taken in the Halden Reactor that a synergism exists between burnup-induced conductivity degradation and that induced from gadolinia addition, such that the two effects are not completely additive. At present, the model in FRAPCON treats these effects as additive, and hence it is likely low (conservative) for high-burnup urania-gadolinia fuel. This aspect is a subject for continued data monitoring and model adjustment in the future.

2.4 Range of Application and Uncertainties

The recommended ranges of application for the urania and urania-gadolinia fuel pellet thermal conductivity expressions are given below. These ranges represent PNNL-estimated limits for reliable model-to-data comparisons to-date, and not necessarily the outer bounds of all available data. No attempt has been made to bias the conductivity in any direction.

Temperature: 300 to 3000 K
Rod-Average Burnup: 0 to 62 GWd/MTU (Urania only*)
As-fabricated Density: 92 to 97% TD
Gadolinia Content: 0 to 10 wt.%

*The current model underestimates thermal conductivity at nominal to high burnup for urania-gadolinia pellets. The Halden Reactor Project currently has integral experiments (fuel centerline temperature data) of urania-gadolinia fuel at nominal burnups that demonstrate some conservatism in the current model. Further Halden experiments are planned that will measure fuel temperatures in urania-gadolinia fuel up to high burnups.

The uncertainty on the thermal conductivity is on the order of the uncertainty of verification for fuel temperature rise from pellet surface to pellet center, i.e., from about 10 to 15%.

3.0 MODELING CHANGES FOR EXTENSION TO MOX FUEL

This section contains the various model and code changes that have been made or considered to extend the code to apply to MOX fuel. In the United States, the introduction of MOX fuel into LWRs is planned solely as part of the conversion and disposition effort for plutonium metal contained in excess weapons parts. The changes described below are limited, in part, by that sole application.

3.1 Thermal Conductivity Model for MOX Fuel Pellets

The major modification to FRAPCON-3.3 for application to MOX fuel was the addition of a fuel thermal conductivity model specific to MOX fuel. This was selected as a combination of the Duriez stoichiometry-dependent correlation, derived from diffusivity measurements on unirradiated fuel pellets (Duriez et al., 2000), plus the burnup degradation contained in a modified version of the NFI fuel thermal conductivity model (Lanning and Beyer, 2002; Ohira and Itagaki, 1997). Background on MOX fuel pellet thermal conductivity considerations is given in Section 3.1.1. The combined model is described in Section 3.1.2.

The model was verified by inserting it into the FRAPCON-3.3 code and comparing predicted fuel center temperatures to measured values for several instrumented Halden Reactor test irradiations on fuel segments, which were re-fabricated from irradiated full-length MOX PWR rods and instrumented with centerline thermocouples. The results of this verification process are described in Section 3.1.3. The ranges of application for the MOX model and the estimated uncertainty are stated in Section 3.1.4.

3.1.1 Background on MOX Fuel Thermal Conductivity

Significant experimental investigations and modeling efforts are ongoing concerning the thermal conductivity of LWR-type MOX fuel pellets. Thermal diffusivity/conductivity measurements at Cadarache Laboratory on unirradiated hypostoichiometric MOX pellets have confirmed a strong dependence of the MOX thermal conductivity on deviations from stoichiometry, but only a minor dependence on plutonia content over the range of 1 to 15 wt.% (Duriez et al., 2000). Duriez et al. (2000) reported measurements on unirradiated pellets only and did not discuss burnup-induced thermal conductivity degradation. In contrast, the Halden Reactor Project recommends a function for burnup degradation, derived from their extensive data base on measured urania and MOX fuel temperatures (Wiesenack and Tverberg, 2000). However, the Halden Reactor Project model overpredicts recently published urania thermal conductivity data at high temperatures (> 2500 K), and the Halden adaptation of their model for MOX fuel lacks an explicit dependence on stoichiometry. Various organizations are proposing models that combine the current understanding of stoichiometry, plutonia content, burnup degradation, and high temperature effects on MOX fuel pellet thermal conductivity.

PNNL has installed an LWR MOX fuel pellet thermal conductivity model in FRAPCON 3.3. The key features of this model are as follows:

(a) The previous dependence in the model on plutonia content (derived from MATPRO-11) is eliminated, especially since FRAPCON-3 applications for MOX will be at less than 15 wt.% plutonia while the MATPRO model is based on ~ 25% plutonia data

(b) The Duriez model for unirradiated fuel is applied, with its stoichiometry dependence

(c) Revised functions are used for burnup degradation and high-temperature thermal conductivity based on urania data.

3.1.2 Description of the MOX Fuel Thermal Conductivity Models

At the request of the NRC, two thermal conductivity models for MOX fuel are made available in FRAPCON-3.3. The first, the Duriez-Modified NFI model (described in Section 3.1.2.1), is the recommended model and the one that PNNL has verified against in-reactor fuel temperature data. The second is the Halden MOX fuel model (described in section 3.1.2.2), which has not been verified by PNNL but has been verified by Halden Reactor Project staff against a similar set of in-reactor MOX fuel temperature data. The two models are similar at normal operating fuel temperatures (< 2000 K) but diverge at higher temperatures. The burnup degradation in the recommended model is also somewhat stronger than in the Halden model.

3.1.2.1 The Duriez-Modified NFI Model

The Duriez model for the thermal conductivity, K_{95}, of unirradiated MOX fuel pellets at a nominal density of 95% TD, is as follows:

$$K_{95} = \frac{1}{A(x) + B(x)T} + \frac{C}{T^2}\exp(-\frac{D}{T}) \tag{3.1}$$

where:

K95	=	Conductivity in W/m-K, at 95% TD
x	=	2.00 – O/M (i.e., oxygen-to-metal ratio)
T	=	temperature in K
A(x)	=	2.85x + 0.035 m-K/W
B(x)	=	(2.86 - 7.15x)*1E-4 m/W
C	=	1.689E9 W-K/m
D	=	13520 K.

PNNL has modified this model to include a burnup dependence, a gadolinia dependence, and a slightly reduced high-temperature term, as follows:

$$K_{95} = \frac{1}{A(x) + a \cdot gad + B(x)T + f(Bu) + \left(1 - 0.9\exp(-0.04Bu)\right)g(Bu)h(T)} + \frac{C_{\text{mod}}}{T^2}\exp(-\frac{D}{T}) \qquad (3.2)$$

where:

x, T, A(x), B(x), and D are as defined above

a = 1.1599, "gad" = weight fraction gadolinia (not expected in MOX)

Bu = burnup in GWd/tHM

f(Bu) = effect of fission products in crystal matrix (solution) = 0.00187•Bu

g(Bu) = effect of irradiation defects = 0.038•Bu0.28

h(T) = temperature dependence of annealing on irradiation defects $= \frac{1}{1 + 396\exp(-\frac{Q}{T})}$

Q = temperature dependence parameter ("Q/R") = 6380K

Cmod = 1.5E9 W-K/m.

In the first term of the modified model (the "phonon conduction" term), the expressions describing the effect of dissolved fission products [f(Bu)], irradiation induced defects [g(Bu)], and the temperature-dependent defect healing (annealing) [h(T)] are the original functions put forward by Ohira and Itagaki (1997) of NFI. The term multiplying the product g(Bu)h(T) is a PNNL modification that reduces the annealing at low burnup (<20 GWd/MTM) and brings it back at nominal-to-high burnup (see Lanning and Beyer, 2002).

The second term in the model describes high-temperature electronic heat conduction. The constant "C" has been reduced in the modified model to agree with recent high-temperature diffusivity-derived conductivity measurements on unirradiated fuel pellets (Ronchi et al., 1999). These data are lower than previously measured values, but the older values have high uncertainty, and the more recent data appear to be very credible.

As applied in FRAPCON-3, the above model is adjusted for as-fabricated fuel density (in % of TD) using the Lucuta recommendation for spherical-shaped pores (Lucuta et al., 1996) as follows:

In the first term of the modified model (the "phonon conduction" term), the expressions describing the effect of dissolved fission products [f(Bu)], irradiation induced defects [g(Bu)], and the temperature-dependent defect healing (annealing) [h(T)] are the original functions put forward by Ohira and Itagaki (1997) of NFI. The term multiplying the product g(Bu)h(T) is a PNNL modification that reduces the annealing at low burnup (<20 GWd/MTM) and brings it back at nominal-to-high burnup (see Lanning and Beyer, 2002).

The second term in the model describes high-temperature electronic heat conduction. The constant "C" has been reduced in the modified model to agree with recent high-temperature diffusivity-derived conductivity measurements on unirradiated fuel pellets (Ronchi et al., 1999). These data are lower than previously measured values, but the older values have high uncertainty, and the more recent data appear to be very credible.

As applied in FRAPCON-3, the above model is adjusted for as-fabricated fuel density (in % of TD) using the Lucuta recommendation for spherical-shaped pores (Lucuta et al., 1996) as follows:

$$K_d = 1.0789 * K_{95} * [d/\{1.0 + 0.5(1-d)\}] \quad (3.3)$$

where:

d = density in fraction of TD.

The factor 1.0789 adjusts the conductivity back to that for 100% TD material.

This model is activated when the user-input integer flag IMOX has the value 1.

3.1.2.2 The Halden Project MOX Fuel Thermal Conductivity Model

The Halden Reactor Project has developed a variant of their urania fuel pellet thermal conductivity model for MOX fuel, based on their extensive in-reactor data base for fuel temperatures and linear heat generation rates (LHGRs) for both fuel types. This model is included in the FRAPCON-3.2 code as a user option (utilized when the user-input integer flag IMOX has the value 2).

The structure of the Halden model for urania fuel is very straightforward, consisting of a phonon conduction term plus an electronic conduction term. The effects of burnup are contained solely in the phonon conduction term, as follows:

$$K_{95} = \frac{1}{0.1148 + a \cdot gad + 1.1599x + 0.0040 \cdot B + 2.475 \cdot 10^{-4} \cdot (1 - 0.00333 \cdot B) \cdot \vartheta} + 0.0132 \cdot e^{0.00188 \cdot T} \quad (3.4)$$

where:

K_{95} = conductivity in W/m-K, at 95% TD
T = temperature in degrees Celsius
B = burnup, MWd/kg urania
ϑ = Minimum of: 1650°C or current temperature in degrees Celsius
a = 1.1599, "gad" = weight fraction gadolinia (not expected in MOX).

In applying this equation, one must recognize that the units for temperature and for burnup (degrees C and MWd/kg urania) deviate from the units used for most models in the literature (degrees Kelvin and MWd/kgU or atom % burnup) and adjust accordingly.

The change to the above equation for MOX is to multiply the phonon term by the factor 0.92. The Halden equation for MOX fuel conductivity is thus:

$$K_{95} = \frac{0.92}{0.1148 + a \cdot gad + 1.1599x + 0.0040 \cdot B + 2.475 \cdot 10^{-4} \cdot (1 - 0.00333 \cdot B) \cdot \vartheta} + 0.0132 \cdot e^{0.00188 \cdot T} \quad (3.5)$$

The above conductivity is adjusted for fuel pellet density by the same K_d factor applied above to the Duriez-NFI model.

3.1.3 Verification of the Duriez/NFI Combined Model

Code-data comparisons were made with the combined MOX model (Equation 3.3) added to FRAPCON 3.3 for three instrumented MOX fuel tests in the Halden Reactor: IFA-629.1, IFA-610.2,4 and IFA-648.1 and also for IFA-629.3 (the ramp-test extension of IFA-648.1) and for IFA-606. All these tests and their reference documents are briefly summarized in Table 3.1. Each test is described in more detail in Appendix A.

Table 3.1 Instrumented MOX Tests in Halden. All with re-fabricated PWR rod sections containing MIMAS MOX Fuel

Reactor/Full-Length Rod (and Rod Diameter in mm)	Base Irradiation Cycles	Burnup, GWd/MTM (and FGR%) at End of Base Irradiation	Halden Test (IFA No.) and Report (HWR No.)*	Test Type and Max. (Rod-Average LHGR , kW/m)	End of Test FGR % and Measurement Type
St. Laurent-B1/J09 (9.35)	2	27 (low)	629.1 HWR-586	Ramp (35)	25% (Puncture) 26% PT[(a)]
Gravelines-4/N06 (9.35)	4	48 (4.12)	610.2,4** HWR-603,650	Lift-off (10).	--
Gravelines-4/N12 (9.35)	4	57 (4.86) (64.5)[(b)]	648** (629.3) HWR-651 (HWR-714)	SS[(c)] (10) (Ramp, 25)	--
Gravelines-4/P16 (9.35)	4	53 (2.58) (59.5)[(b)]	648** (629.3) HWR-651 (HWR-714)	SS (10) (Ramp, 25)	7% (PT)
Beznau-1 (10.7)	5	50 (low)	606 (HPR-349/30)	Ramp (32)	13% (PT and puncture)

* HWR-664 contains design, precharacterization, and base irradiation data for the St. Laurent and Gravelines EdF rods.
** Note that IFAs 610.2,4, and IFA-648.1 operated in a PWR-condition loop within the Halden Reactor, thus at a coolant temperature and pressure of 310°C and 2250 psia instead of normal Halden Reactor conditions (240°C, 500 psia)
(a) Pressure transducer
(b) End of steady-state irradiation in Halden at ~10 kW/m
(c) SS means steady-state (steady operation at normal PWR core-average LHGR levels)

Predicted vs. measured results for all the comparisons are shown in Figure 3.1. The normalized temperature differences (predicted minus measured, divided by measured minus coolant temperature) are shown as a function of LHGR in Figures 3.2 and vs. burnup in Figure 3.3. The deviations between predicted and measured temperatures show no bias or trend vs. LHGR or burnup and are generally within +/- 10% relative, which is considered good agreement because this is near the uncertainty for LHGR in the Halden instrumented tests. Note that this bound on deviation is for the center temperature in Celsius. Since the coolant temperature for most Halden HBWR tests is ~240°C, and temperature typically rises ~100 to 200°C from coolant to pellet surface, the uncertainty in calculated fuel temperature increase from pellet surface to pellet center implied by Figures 3.2 and 3.3 is approximately 15 to 20%.

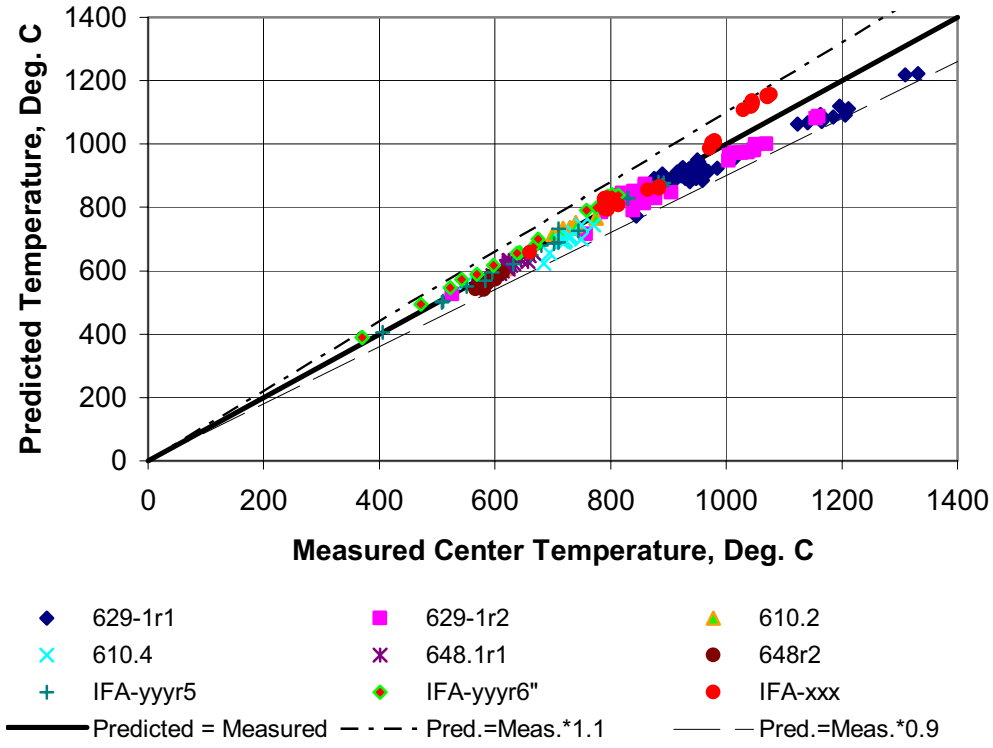

Figure 3.1 Predicted vs. Measured Fuel Center Temperatures for Halden MOX Tests

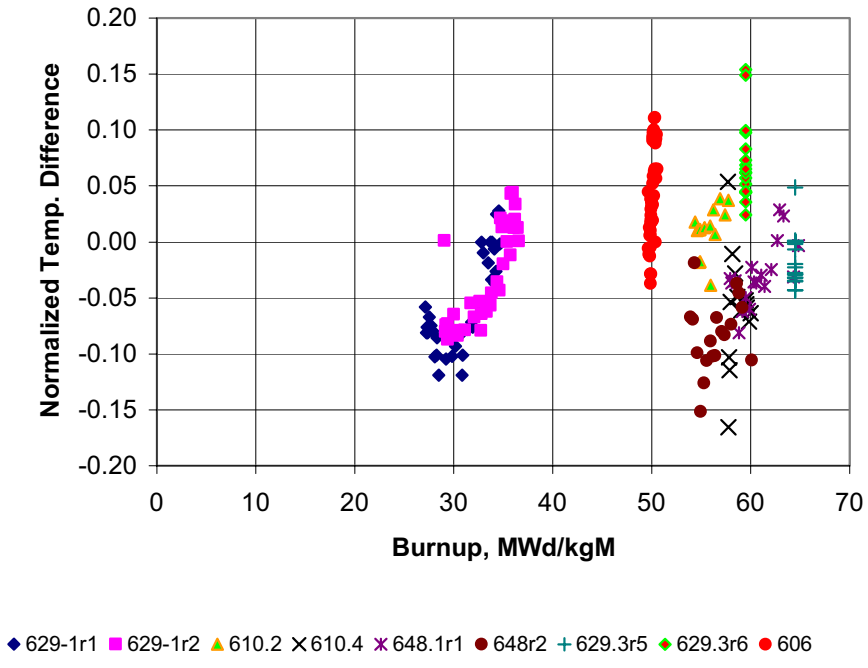

Figure 3.2 Predicted Minus Measured Normalized Temperature Difference for MOX Test Cases as a Function of Burnup

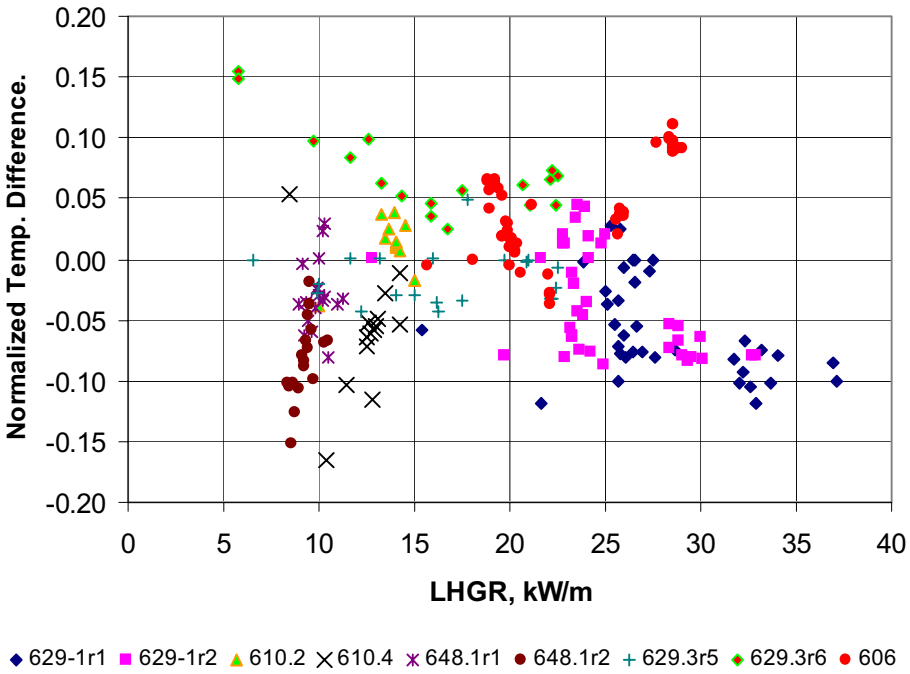

Figure 3.3 Predicted Minus Measured Normalized Temperature Difference for MOX Test Cases as a Function of LHGR

3.1.4 Range of Application and Uncertainties for MOX Thermal Conductivity

The recommended ranges of application for the MOX fuel pellet thermal conductivity models are given below. These ranges represent PNNL-estimated limits for reliable model-to-data comparisons to date and not necessarily the outer bounds of all available data. No attempt has been made to bias the conductivity in any direction:

Temperature: 300 to 3000 K
Rod-Average Burnup: 0 to 62 GWd/MTU
Plutonia Content: 0 to 7 wt.%
As-fabricated Density: 92 to 97% TD
Plutonia Particle Size < 20 microns*

*The majority of the code-data comparisons involves EdF fuel rod sections, for which the plutonia particle size is reported at 15 to 18 microns.

The uncertainty on the thermal conductivity is on the order of the uncertainty of verification for fuel temperature rise from pellet surface to pellet center, i.e., from 15 to 20%. This is greater uncertainty than that estimated for urania thermal conductivity because urania fuel thermal conductivity is verified not only from in-reactor instrumented fuel tests but also from ex-reactor diffusivity/conductivity on irradiated fuel samples. This latter data set is now becoming quite extensive for urania (see Ronchi et al., 2004, for example).

3.2 Fission Gas Release Model Changes for MOX

FGR model parameters have been modified for MOX fuel and verified against available data. Well-qualified FGR data for MOX fuel is rather sparse. What data have been reported have not suggested a large difference in FGR between urania and MOX, given equivalent duty cycles (Cook et al., 2003). This has been indicated again, in particular for LWR-weapons grade Pu source MOX tested to date in the Advanced Test Reactor (ATR) (Hodge et al., 2003). Therefore, only an incremental change in the existing FRAPCON-3 FGR model for urania (the Massih model) is proposed for MOX. This change takes the form of an altered diffusion constant for fission gas diffusing from the fuel grains to the grain boundary.

3.2.1 The Model Changes

The diffusion constant was increased by the factor 1.75 for MOX, based on preliminary comparisons of code predictions to data for Halden ramp tests.

3.2.2 Model Verification

Design, operation, and FGR data provided by Halden have provided an opportunity to compare code predictions to the steady-state FGR from three full-length MOX PWR rods (the "mother rods" N06, N12, and P16 used as sources for instrumented sections tested in Halden Reactor tests, IFAs 610.2,4, and IFA-648.1/629.3). Comparison has also been made to end-of-ramp FGR for the power-ramp tested instrumented fuel rod sections in IFAs 629.1, 629.3, and 606. The results, with and without the modification to the FGR model, are shown in Figure 3.4. It is clear that FRAPCON-3.2 is generally under predicting the FGR for these six cases. Multiplying the diffusion constant by 1.75 raises the FGR to a closer overall comparison with this available data and has been incorporated for MOX into FRAPCON-3.3.

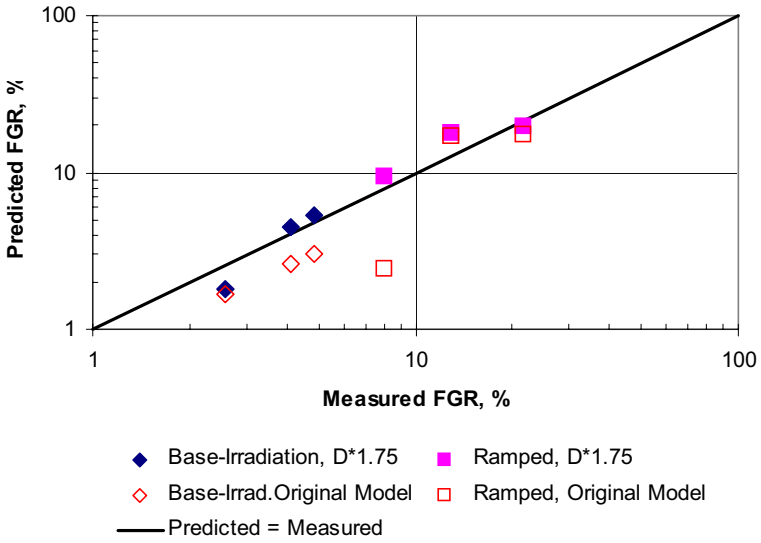

Figure 3.4 Predicted vs. Measured FGR, Diffusion Constant x 1.75

3.2.2.1 Ranges of Application and Uncertainties for MOX FGR

The recommended ranges of application for MOX fuel FGR are given below. The uncertainties on the present MOX FGR model, at all burnup levels, are considered large and indeterminate due to the scarcity of validation data. No attempt has been made to bias the FGR in any direction.

Temperature: 300 to 2300 K
Rod-Average Burnup: 0 to 62 GWd/MTU
Plutonia Content: 0 to 7 wt.%
As-fabricated Density: 92 to 97% TD

Mean Plutonia Particle Size < 20 microns*

*The majority if the code-data comparisons involve EdF fuel rod sections, for which the plutonia particle size is reported at 15 to 18 microns.

3.3 Xe/Kr Ratio

Ranges of application and uncertainties are not provided for Xe/Kr ratio or the other following models and correlations.

Fission gas is partitioned into krypton and xenon fractions within the code. Currently, the code uses Xe/Kr ratio of 5.67 in making this partition, which is appropriate for urania fuel at low burnup. For MOX fuel, the majority of fissions occur in plutonium, and the xenon stable isotope yields are higher. Halden gas analysis data from MOX rod punctures at nominal to high burnup indicate Xe/Kr ratios of approximately 19; however, Xe/Kr fission yields for plutonium indicate a value of 16 (White et al., 2001). The code has been altered to use the ratio of 16 when MOX fuel is being analyzed. The effects of this change are a small decrease in gas conductivity and a very small decrease in gap conductance for cases where fission gas concentration in the plenum gas becomes significant. However, the output gas species ratios now reflect a more realistic Xe/Kr ratio for MOX.

3.4 Helium Production and Release

Helium production in MOX rods can be expected to be higher than in urania rods due to higher actinide decay sources from the plutonium. Halden puncture data and gas analysis were provided for two of the three mother rods, N12 and P16. This permits evaluation of the change to rod helium inventory from beginning-of-life (BOL) to end of life (EOL). The results indicate negligible change (~1% relative) in the helium inventory from BOL to EOL. These results are summarized in Table 3.2. This is consistent with current FRAPCON-3.2 predictions, and no change to FRAPCON-3.2 regarding helium release is recommended at this time. It should be noted that the initial fill gas pressure for these rods was relatively high at 363 psia, vs. a somewhat smaller expected value for MOX rods used in the United States for plutonium disposition. There is some evidence and theory that suggests higher fill gas pressure will reduce helium release.

Examples where release of created helium was possibly detected in low-pressure rods (1 atmosphere fill gas pressure at room temperature) include the Pu-Disposition program MOX test rodlets irradiated in

the ATR. The rods were punctured, and the postirradiation pressure was measured. FGR was deduced from the Kr-85 activity in the gas. By difference, an additional source of pressurizing gas was deduced, on the order of 3E-5 moles per 82-gram (15-pellet) rodlet at 42 GWd/tHM. This corresponds to a release of created helium equal to 9E-9 mole He per gram fuel per GWd/tHM, which is a 5 to 6% increase in the helium inventory in an LWR MOX rod. However, this amounts to only about 10 psi pressure increase at room temperature or 20 to 25 psi increase at reactor operating temperatures. Due to the small amount of additional helium production and release that is expected and the lack of quantitative measured release data, **the previous helium release model in FRAPCON-3 is unaltered in the current version**.

Table 3.2 Helium Results from Halden Test High-Burnup PWR MOX "Mother Rods"

Reactor/Full-Length Rod (Rod Diameter in mm)	Base Irradiation Cycles	Initial Fill Pressure, MPa at Room Temperature	Burnup, GWd/MTM	BOL/EOL Helium inventory, STPcc
Gravelines-4/N12 (9.35)	4	2.6	50	449/454
Gravelines-4/P16 (9.35)	4	2.6	47	417/422

3.5 Input Plutonium Isotopes for Radial Power Profile

Input parameters have been added to signal when MOX fuel is being analyzed and to initialize the concentrations of plutonium isotopes in the TUBRNP subcode, which calculates radial power and burnup profiles within the fuel pellets. Given this isotope initialization, TUBRNP calculates the radial profiles for LWR MOX fuel with acceptable accuracy. This was assessed by comparing code calculations to Monte Carlo N-particle (transport) (MCNP) code calculations for radial power profiles (where the MCNP results were provided by Oak Ridge National Laboratory). The code MCWO (MCNP Coupled With ORIGEN-2) was used to analyze the detailed fuel rod radial burnup characteristics. This code was validated by comparing the MCWO-calculated concentration profiles with the postirradiation examination (PIE) data. For detailed radial profile analyses, a typical PWR unit cell model with a 0.915-cm-diameter fuel pin was set up. The radial mesh contained 100 subdivided, equal-volume sub-cells in the fuel rod. An example of the results of this code in comparison with TUBRNP is shown in Figure 3.5.

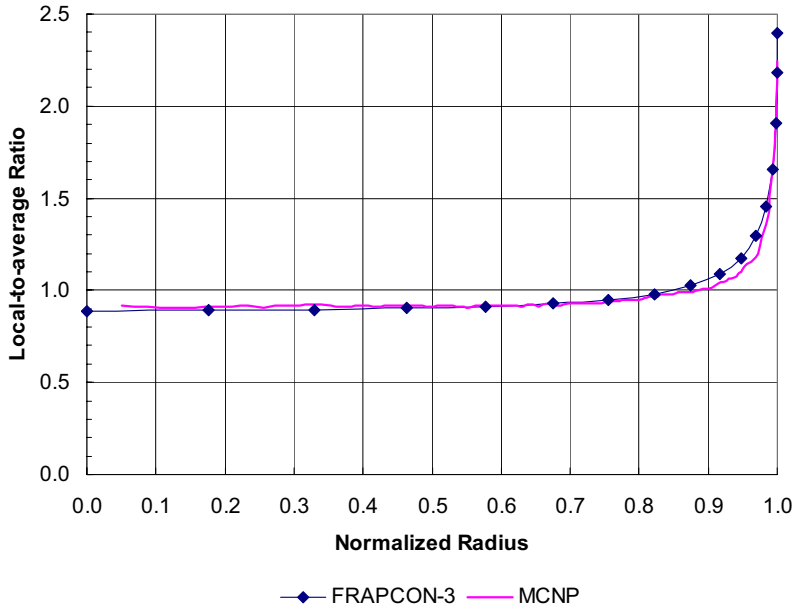

Figure 3.5 MCNP and FRAPCON-3 Calculations of Normalized Radial Power Profile in PWR MOX Fuel at 50 GWd/MTHM (Initial content = 5 wt.% WG Plutonia in MOX)

3.6 MOX Fuel Heat Capacity

The MATPRO-11 correlations for the heat capacity of urania, plutonia, and MOX have been retained in FRAPCON-3.2. The heat capacity equation was derived in MATPRO-11 as:

$$FCP = \frac{K_1\theta^2 \exp(\theta/T)}{T^2\left[\exp(\theta/T)-1\right]^2} + K_2 T \quad + \frac{YK_3E_D}{2RT^2}\exp(-E_D/RT) \tag{3.6}$$

and the fuel enthalpy is the integral of the above equation with respect to temperature:

$$FENTHL = \frac{K_1\theta}{\left[\exp(\theta/T)-1\right]} + \frac{K_2T^2}{2} \quad + \frac{Y}{2}K_3\exp(-E_D/RT) \tag{3.7}$$

In the above,

FCP = specific heat capacity (J/kg-K)
FENTHL = fuel enthalpy (J/kg)
T = temperature (K)
K1, K2, and K3 are constants (see Table 3)
Y = oxygen-to-metal ratio
R = universal gas constant = 8.315 J/mole-K
θ = Einstein temperature (K)
ED = Activation energy for Frenkel defects (J/mole).

The values for the urania and plutonia parameters are given in Table 3.3. At temperatures exceeding 200K, the urania heat capacity exceeds that of plutonia, which means that the heat capacity of MOX is less than that of urania. The enthalpy and heat capacity values for urania are adjusted to account for plutonia additions by the rule of mixtures; that is, X (MOX) = X(plutonia)*COMP + (1-COMP)*X(urania), where COMP is the weight fraction of plutonia in the mixed oxide, X is either heat capacity (in J/kg-K) or enthalpy (in J/kg), and Y is the plutonia weight fraction. However, for LWR MOX application with < 10 wt.% plutonia, the difference between MOX heat capacity and urania heat capacity is relatively small, as demonstrated in Figure 3.6.

Equations for heat capacity and enthalpy having the same form as the MATPRO equations (Eq. 6 and 7), but slightly differing parameter values, have been proposed by Popov et al. (2000). The deviations between the two sets for temperatures below melting are, however, extremely small particularly at the low-plutonia contents of interest for LWR applications, as demonstrated in Figure 3.7. Therefore, the heat capacity equations in FRAPCON-3.3 have not been altered to date.

Table 3.3 Parameter Values for Urania and Plutonia Fuel Heat Capacity and Enthalpy

Parameter and Units	Value for Urania	Value for Plutonia
K_1, J/kg-K	296.7	347.4
K_2, J/kg-K^2	0.0243	0.000395
K_3, J/kg	8.745×10^7	3.860×10^7
θ, in degrees K	535.285	571
E_D, J/mole	1.577×10^5	1.967×10^5

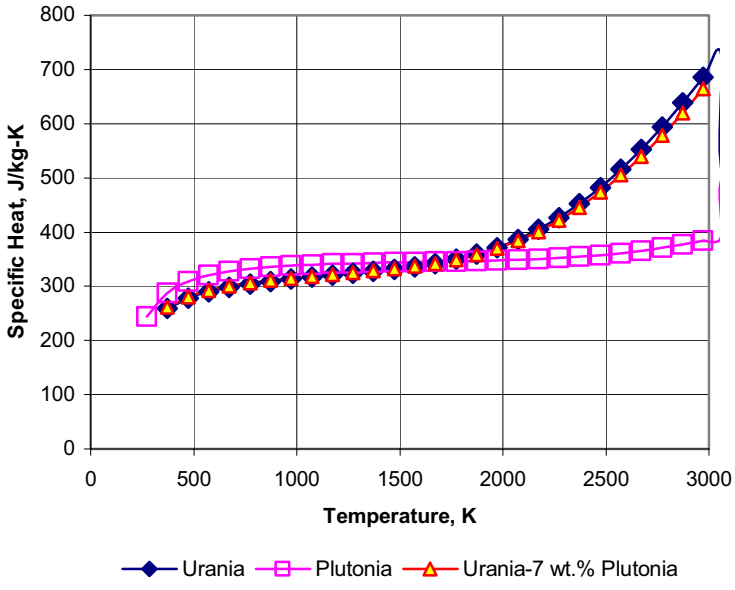

Figure 3.6 Urania and Plutonia Heat Capacities and Heat Capacity for 7 wt.% plutonia MOX

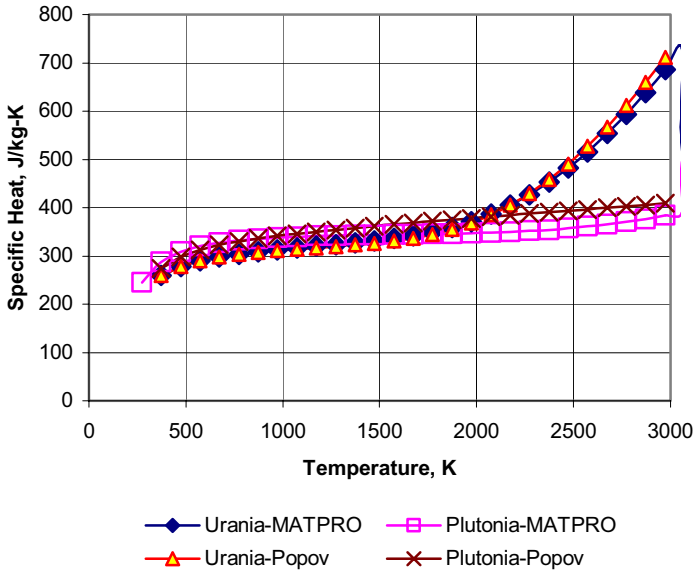

Figure 3.7 Urania and Plutonia Heat Capacities as Calculated by MATPRO-11 Correlation and by the Correlation of Popov et al. (2000)

3.7 Melting Temperature for MOX

FRAPCON-3 contains the MATPRO values for unirradiated urania and plutonia melt temperatures of 3113 K and 2647 K, respectively. Popov et al. (2000) recommend values of 3120 K and 2701 K for urania and plutonia, respectively. The code has not been altered with regard to the melt temperature of the unirradiated fuel because these differences are very small as applied to LWR MOX. The melt temperature Tmelt for MOX is calculated from the urania and plutonia contents in a manner similar to the calculation of fuel specific heat; that is,

$T_{melt}(MO) = Y*T_{melt}(plutonia) + (1-Y)*T_{melt}(urania)$,
where Y = the weight fraction of plutonia.

The MATPRO burnup dependence (reduction) in melt temperature is 3.2 K per MWd/kgU, whereas Popov et al. (2000) recommend 0.5 K per MWd/kgU on the basis of two references (Adamson et al., 1985; Komatsu et al. 1988). The code has been altered to include this lower burnup dependence because it is based on more reliable data.

3.8 Thermal Expansion, Densification, and Swelling for MOX

Following the comparisons and recommendations of Popov et al. (2000), the current (MATPRO-11) thermal expansion correlation for urania is also applied to LWR MOX fuel.

The current expressions for urania for in-reactor densification and solid fission product-induced swelling are also applied to MOX. MOX test rod irradiation experiments that include assessment of fuel densification are ongoing in the Halden Reactor and at the ATR reactor in the United States, but the

results to date are inconclusive regarding significant difference between LWR MOX and urania fuel (see for example, Tolonen et al., 2001; Hodge et al., 2003). Therefore, the current urania-fuel solid fission product-induced swelling rate is also applied to MOX fuel.

The in-reactor creep of MOX fuel has been demonstrated to be greater than that of urania fuel (see, for example, Petiprez, 2002). Therefore, the consequence of fuel swelling upon cladding outward strain and rod axial strain (once fuel-cladding hard contact has occurred) has been shown to be less for MOX fuel rods (see, for example, White, 1999). However, currently, FRAPCON-3 does not model fuel creep for either fuel type.

4.0 REVISED PARAMETERS FOR THE URANIA FGR MODEL

When a change is made to the code that significantly affects the predicted fuel temperature for the confirmation cases, the constants in the Massih FGR model must be re-tuned to fit data from steady-state and slow power ramp cases and thus keep the model best estimate. As discussed in Section 2.0, the urania thermal conductivity model was changed. As a result of this change, the fuel temperatures predicted by FRAPCON-3 will be significantly changed. Therefore, the constants in the Massih FGR model will also be re-tuned to a data base consisting of measured FGR from steady-state and power ramped rods.

4.1 Massih Diffusion Coefficient Model Changes

The following are the constants that were changed in the Massih FGR model:

- The multiplier on the recommended resolution rate was increased from 250 to 300
- The divisor on burnup in the adjustment to the diffusion constant for burnup was increased from 35 GWd/MTU to 40 GWd/MTU
- The multiplier on the diffusion constant was decreased from 14 to 12.

4.1.1 Model Verification

The current model changes were verified by comparing the model predictions to the measured gas release values from 23 steady-state rods and 18 power ramp cases. These cases were drawn from the "development data base" described in Volume 3 of this NUREG, plus additional verification cases. These steady-state and power-ramp cases are listed in Tables 4.1 and 4.2, respectively. The predicted vs. measured gas release values for the steady-state cases are shown in Figure 4.1. This figure shows that the FRAPCON-3 model fits these data quite well. The standard deviation on the predicted minus measured is 2.77% FGR. The predicted vs. measured gas release values for the power ramp cases are shown in Figure 4.2. This figure shows that the FRAPCON-3 model fits these data acceptably. The standard deviation on the predicted minus measured is 5.32% FGR.

The code-to-data comparison was also examined for bias or trend as a function of burnup. The predicted-minus measured FGR difference is plotted vs. test rod burnup for the steady-state and power ramp cases in Figures 4.3 and 4.4, respectively. No significant bias or trend is evident for the cases portrayed here.

Table 4.1 Steady-State Cases Used in the Assessment and Validation of FRAPCON-3.3

Case	Measured Rod Average Burnup GWd/MTU	Measured Fission Gas Release %	Predicted Fission Gas Release %	Reference
24i6	60.1	21.8	22.90	Balfour, 1982
3618	61.5	33.8	38.40	Balfour, 1982
111i5	48.6	14.4	15.07	Balfour, 1982
28i6	53.3	13.2	13.63	Balfour, 1982
30i8	57.85	34.5	36.76	Balfour, 1982
BNFL-DE	42	10.7	9.22	Lanning et al., 1987 See also Garlick et al.,1982
BNFL-DH	33.9	20	15.54	Lanning et al., 1987
LFF	3.29	17.3	19.81	Notley et al., 1965, 1967
CBP	2.61	14.1	14.82	Notley et al., 1965, 1967
CBR	2.7	14.1	17.96	Notley et al., 1965, 1967
CBY	2.65	16.8	19.80	Notley et al., 1965, 1967
4110-AE2	6.2	22.1	17.81	Janvier et al., 1967
4110-BE2	6.6	15.9	17.78	Janvier et al., 1967
332	56.8	20.9	17.44	Balfour et al., 1982
ELP-4	10.4	17.3	18.00	De Meulemeester et al., 1973
FUMEX 6F	55.45	45±5	43.02	Chantoin et al., 1997
FUMEX 6S	55.45	50±5	56.49	Chantoin et al., 1997
IFA 597.3	70	15.8	12.62	Matsson and Turnbull, 1998
IFA429DH	73	24	44.63	Devold and Wallin, 1994, Waterman, 1978
ANO TSQ002	53.2	1	1.78	Smith et al., 1994
Oconee 15309	50	0.8	1.25	Newman, 1986
M2-2C	43.75	35.6	41.16	Bagger et al., 1978
PA29-4	47.39	48.1	45.59	Bagger et al., 1978

Table 4.2 Power Ramp Cases Used in the Assessment and Validation of FRAPCON-3.3

Case	Measured Rod Average Burnup GWd/MTU	Measured Fission Gas Release %	Predicted Fission Gas Release %	Reference
D200	25	38	17.32	Barner et al., 1990
D226	44	44.1	32.19	Barner et al., 1990
PK6-2	36.8	3.5	9.30	Djurle, 1985
PK6-3	36.5	6.7	10.2	Djurle, 1985
PK6-S	35.9	6.1	10.36	Djurle, 1985
IRRMP 16	21	16	15.05	Mogard, 1979
IRRMP 18	18	4	6.40	Mogard, 1979
RISO F14-6	27	22.1	14.67	Knudsen, 1983
RISO F7-3	35	11.5	13.71	Knudsen, 1983
RISO F9-3	33	17.5	17.42	Knudsen, 1983
GE2	41.9	24.6	26.98	Chantoin et al., 1997
GE4	23.96	27	18.27	Chantoin et al., 1997
GE6	42.29	26	33.64	Chantoin et al., 1997
GE7	41	14.4	11.78	Chantoin et al., 1997
RISO AN1	41.3	31.16	26.15	Chantoin et al., 1997
RISO AN8	40.3	13.85	5.73	Chantoin et al., 1997
B&W Studsvik R1	62.3	9.4	11.88	Wesley et al., 1994
B&W Studsvik R3	62.1	11.3	13.60	Wesley et al., 1994

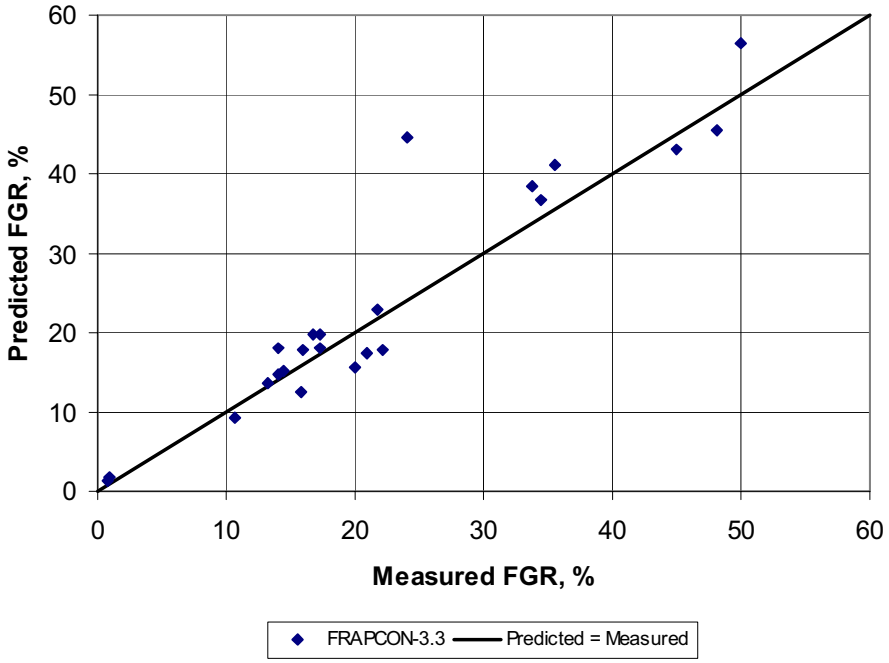

Figure 4.1 Predicted vs. Measured FGR for Steady-State Assessment Cases Using FRAPCON-3.3

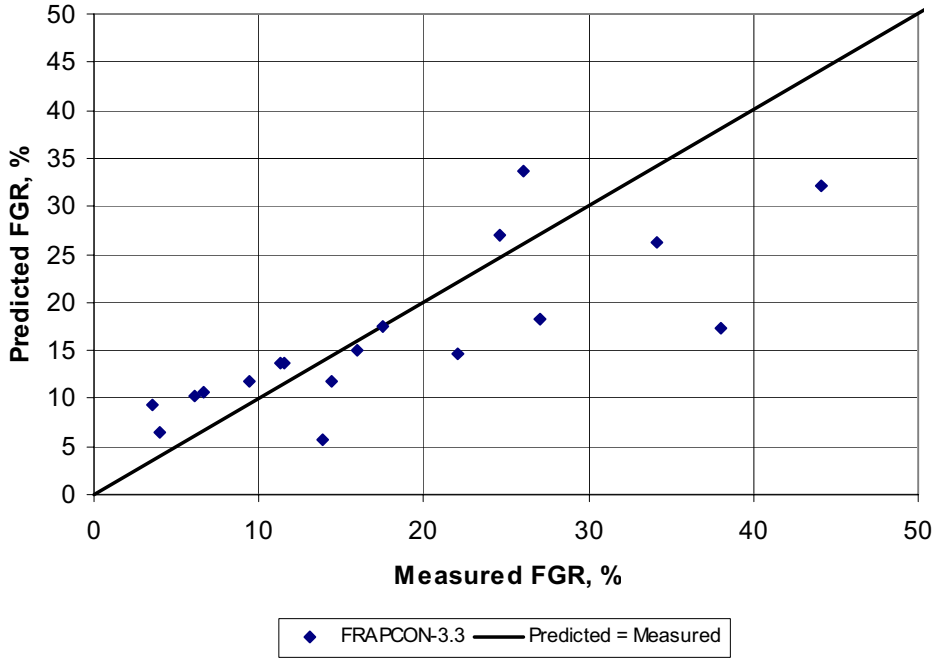

Figure 4.2 Predicted vs. Measured FGR for Power Ramp Assessment Cases Using FRAPCON-3.3

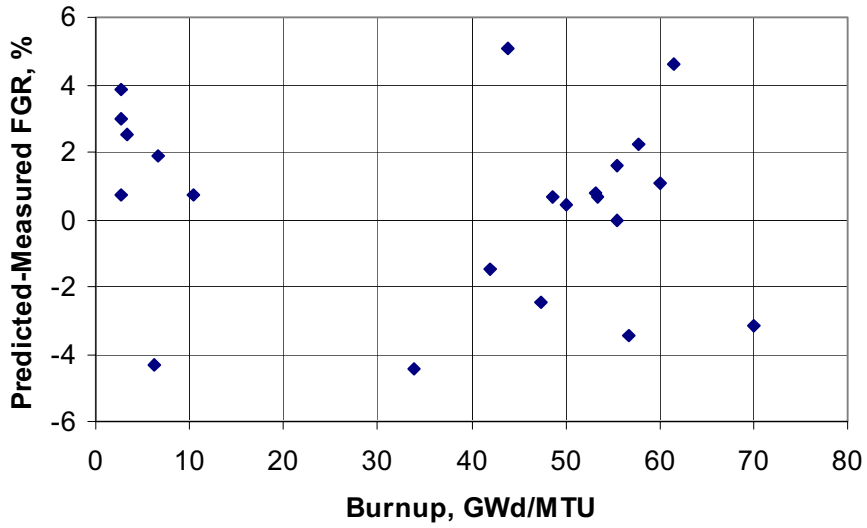

Figure 4.3 Predicted Minus Measured FGR as a Function of Burnup for Steady State Assessment Cases Using FRAPCON-3.3

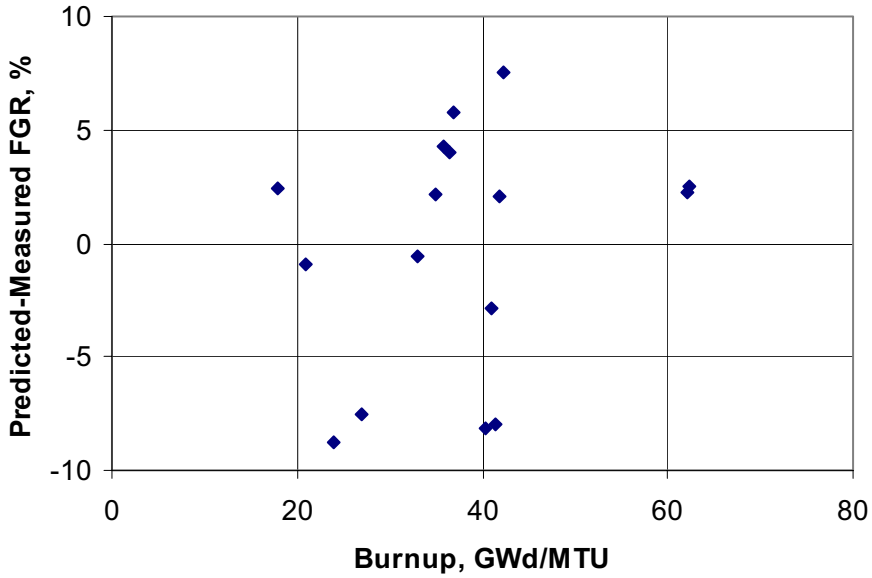

Figure 4.4 Predicted Minus Measured FGR as a Function of Burnup for Power Ramp Assessment Cases Using FRAPCON-3.3

4.1.2 Ranges of Application and Uncertainties for Urania FGR

The recommended ranges of application for the urania FGR model are given below. These ranges represent PNNL-estimated limits for reliable model-to-data comparisons to date and not necessarily the outer bounds of all available data. No attempt has been made to bias the FGR in any direction:

Temperature: 300 to 2300 K
Rod-Average Burnup: 0 to 62 GWd/MTU
As-fabricated Density: 92 to 97% TD.

The uncertainties on the present urania FGR model are considered good based on the comparison to assessment data. The standard deviation for the steady-state cases is 2.8% FGR, and the standard deviation for the power ramp cases is 5.3% FGR.

4.2 Numerical Solution Improvements

Several improvements were made to the Massih gas release model to increase the accuracy of the FGR predictions. The first change was to replace the three-term approximation to the integration kernel with a more accurate four-term approximation. The second change was to use the radial burnup profile rather than the radial power profile to weight the release from each radial ring in the calculation of the gas release for the current axial node.

4.2.1 Improved Numerical Solution

Hermansson and Massih have recently published a paper (Hermansson and Massih, 2002) where they use a four-term approximation to the integration kernel in their gas release model rather than the three-

term approximation that was used in the original publication of the model (Forsberg and Massih, 1985). The use of the four-term approximation in the Massih model in FRAPCON-3 resulted in negligible changes to the overall FGR prediction for the assessment cases.

4.2.2 Use of Radial Burnup Profile

The original version of FRAPCON-3 used the radial power profile to weight the contribution of released gas from each radial ring when calculating the total gas release from each axial node. This is not correct because the gas release value is a fraction of the total produced gas; therefore, a quantity proportional to the total produced gas should be used to weight the contribution of gas release from each radial ring. The radial power profile is proportional to the gas produced in the current time step, but since the power changes with time, it is not proportional to the total gas production. The radial burnup profile is proportional to the total gas production. For this reason, the code was changed to use the radial burnup profile to weight the gas release from each radial ring in the calculation of the total gas release from each axial node.

4.2.3 Modeling of Fission Gas Release During Power Ramps

A clarification is offered here on the recommended use of the code for power ramp cases, which relates to the current logic within the Massih FGR model. In the Massih gas release model, if the current time step is less than 1 day, the code assumes that no re-solution occurs during that time step. Thus, more gas will accumulate in the grain boundary bubbles, which in turn promotes grain boundary saturation and FGR from more nodes relative to the case where resolution is allowed. This behavior simulates the enhanced release that is known to occur during power ramps following significant burnup accumulation at steady-state power operation.

This enhanced release is not appropriate for steady-state power operation. Therefore, if steady-state operation is being modeled, then time steps greater than 1 day should be used so that the re-solution is modeled for the entire power-time history.

This guideline on the size of time steps will also be reflected in the input instructions for the latest version of FRAPCON-3 under the variable, 'ProblemTime.' Future issues of the code are expected to contain a revised version of the Massih model that will more robustly incorporate both high-burnup effects and power ramp-related effects.

4.3 Corrections to the ANS5.4 Model

Several errors were discovered and corrected in the alternate gas release model, ANS5.4:

- The ANS5.4 model was modified to calculate gas release based on the current time step radial power and burnup profile. In the previous version of FRAPCON-3, the BOL power and burnup profiles were used throughout life.

- A typographical error was discovered in an intermediate version of the code (FRAPCON-3.2), which resulted in the ANS5.4 subroutine excluding the thermal release portion in the calculation of the total gas release. The total gas release only reflected the athermal gas release fraction. This error was corrected, so both the thermal release and the athermal release are included in the calculation of total gas release.

Note: No adjustments have been made to the ANS5.4 gas release model parameters to account for the new thermal conductivity model or the addition of MOX fuel properties. PNNL has not assessed the impact of these code changes on ANS5.4 predictions relative to data. PNNL does not recommend the use of the ANS5.4 model to make quantitative estimates of FGR. The changes described in this section have been made simply to bring the ANS5.4 model in FRAPCON-3.3 into agreement with the original reference (ANSI/ANS-5.4-1982).

5.0 MODIFICATIONS FOR CLADDING CORROSION AND ITS EFFECTS

Improved zirconium alloys have now been developed and deployed for PWR fuel rod cladding that demonstrate significantly reduced corrosion and hydrogen pickup compared to Zircaloy-4. These include "ZIRLO™" (developed by Westinghouse) and "M5™" (developed by FRAMATOME). The extensive use of these new alloys, and the recent availability of published performance data for them, makes it both possible and necessary to make preliminary updates to the corrosion model and hydrogen uptake model in the FRAPCON-3 code to apply to cases where these cladding alloys are used.

Sections 5.1 and 5.2 describe the corrosion model updates that have been made for each of the new alloys. It should be emphasized that these changes are empirical corrections to the existing FRAPCON-3 models for Zircaloy-4 corrosion and hydrogen pickup, not new models.

Note that changes for the new alloys to other cladding models, such as axial growth, thermal expansion, mechanical properties, and thermal conductivity have not been made. The current Zircaloy-4 models continue in use for these properties because published data for the new alloys are sparse, and proprietary data indicate that the variations from the Zircaloy-4 models present in FRAPCON-3 are not large in general. (The exception to this is axial growth, which will be examined in a subsequent fuel code update.) Ranges of application and uncertainties for the advanced cladding corrosion models are given in Section 5.3.

NRC Staff questioned whether the existing corrosion and hydrogen pickup models for Zircaloy-2 cladding (used in BWR fuel rods) are applicable to the higher burnup and varying water chemistries typical of modern BWR fuel and operation. Section 5.4 demonstrates, by data comparisons drawn from recent references, that the existing models for Zircaloy-2 cladding on BWR rods are still applicable, even to higher burnup. Section 5.5 describes the adjustment now made to cladding stress calculation from corrosion-related wall thinning. The revised hydrogen solubility model in Zircaloy cladding is described in Section 5.6.

5.1 Modifications for ZIRLO™ Cladding: Changes and Verification

ZIRLO™ cladding differs from Zircaloy-4 primarily by the addition of 1% niobium and reduced iron and tin content. These changes result in significantly reduced corrosion (Knott et al., 2003) (see Figure 5.1) and slightly reduced hydrogen pickup fraction. The FRACPON-3 input signal ICM (cladding type indicator) is given the value 4 for Zircaloy-4. In the modified code, this variable can now be given the value 6 to indicate that modified corrosion appropriate for ZIRLO™ will be used.

It was found by trial that reducing the FRAPCON-3 calculated Zircaloy-4 corrosion rate by the factor 2.0 results in corrosion layer thickness predictions that compare closely to the ZIRLO™ corrosion data trend presented by Knott et al. (2003). (Much of these data were also presented earlier in Kaiser et al., [2000].) The least-squares (LSQ) curve presented with this data in Figures 5.1 and 5.2 represents the least squares fit to the ZIRLO™ data. Figure 5.2 demonstrates the effect of this change in FRAPCON-3

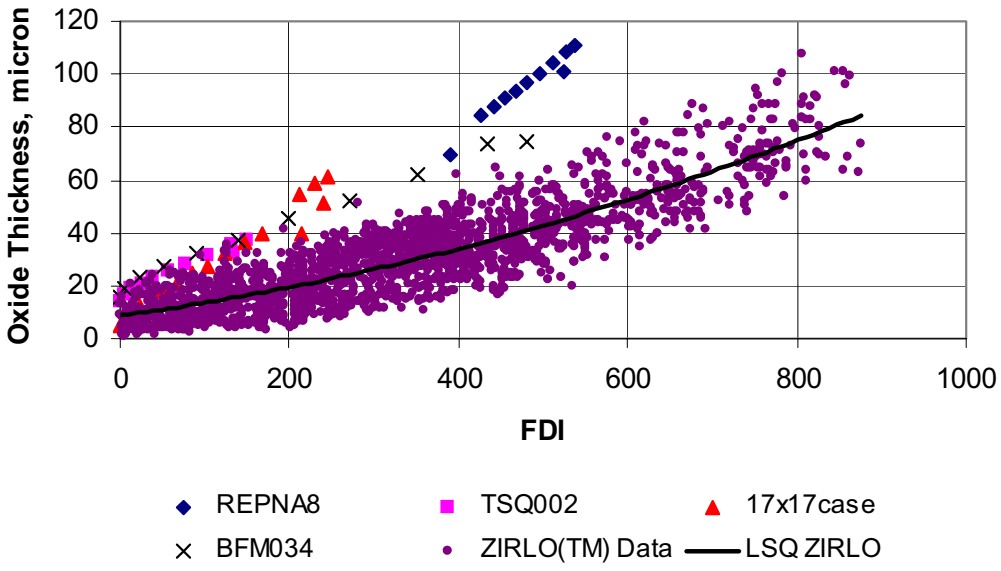

Figure 5.1 Comparison of FRAPCON-3 (Zircaloy-4) Calculated Corrosion (Various Symbols Noted in Legend) with Westinghouse Data (Small Dots) for ZIRLO™, as a Function of Fuel Duty Index (FDI)

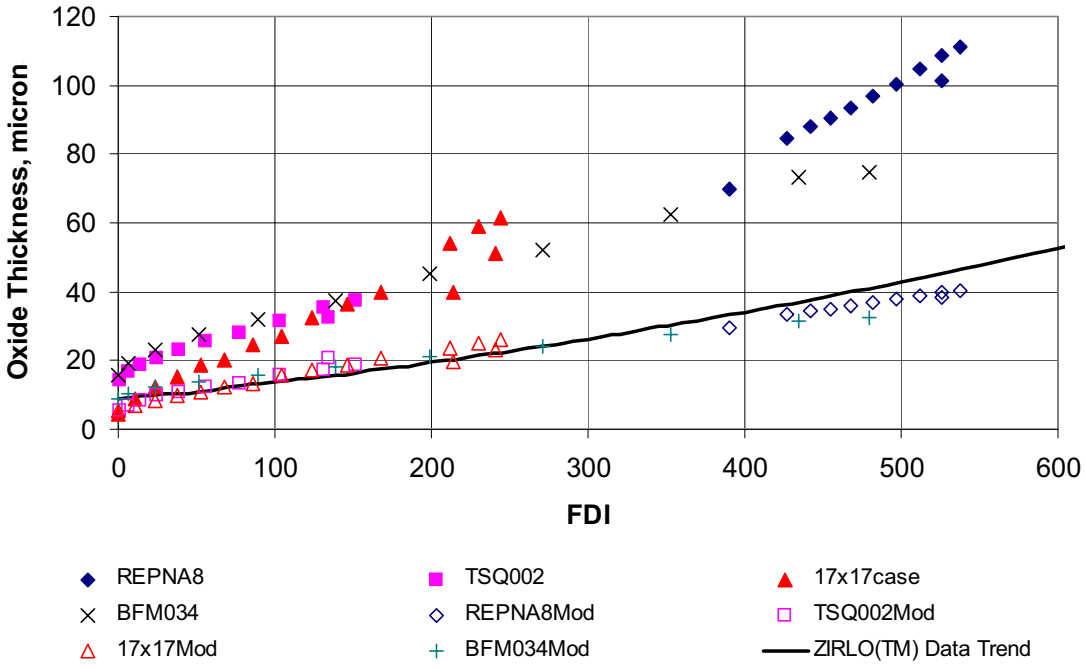

Figure 5.2 Comparison of FRAPCON-3 Calculated Zircaloy-4 Corrosion (Closed Symbols), Modified FRAPCON-3 (ZIRLO^{TM}) Calculated Corrosion (Open Symbols), and Westinghouse Data Trend for ZIRLO^{TM} (Solid Line), as a Function of FDI

predictions, relative to the ZIRLO™ corrosion data. The closed data points are FRAPCON-3 predictions for these fuel rods with Zircaloy-4 cladding, and the open data points and (+) symbols are for these same fuel rods with ZIRLO™ cladding.

Note that both Kaiser et al. (2000) and Knott et al. (2003) present the ZIRLO™ corrosion data as a function of the so-called fuel duty index (FDI), which is proportional to the product of cladding surface temperature and time, integrated over the operational history of the fuel rod segment corresponding with the cladding sample. Hence, the calculated oxide layer thicknesses are plotted against this same index, using the axial nodal cladding surface temperatures for each time step and the case power history time step sizes, and applying the formula for FDI given by Knott et al. (2003):

$$FDI = \int \frac{T_{ave} - 580}{100} \frac{t}{1000} dt \qquad (5.1)$$

where

t = time in hours
Tave = local average cladding oxide layer outer surface temperature in ºF.

The hydrogen pickup fraction for ZIRLO™ was reduced from the 15% derived for Zircaloy-4 to 12.5%, based on data from the irradiation tests reported in the Japanese/Spanish TopFuel paper (Tsukuda et al., 2003) (see Figure 5.3.) The overall hydrogen absorption is reduced significantly relative to that of Zircaloy-4 at equivalent duty factor because of the significant reduction in oxidation.

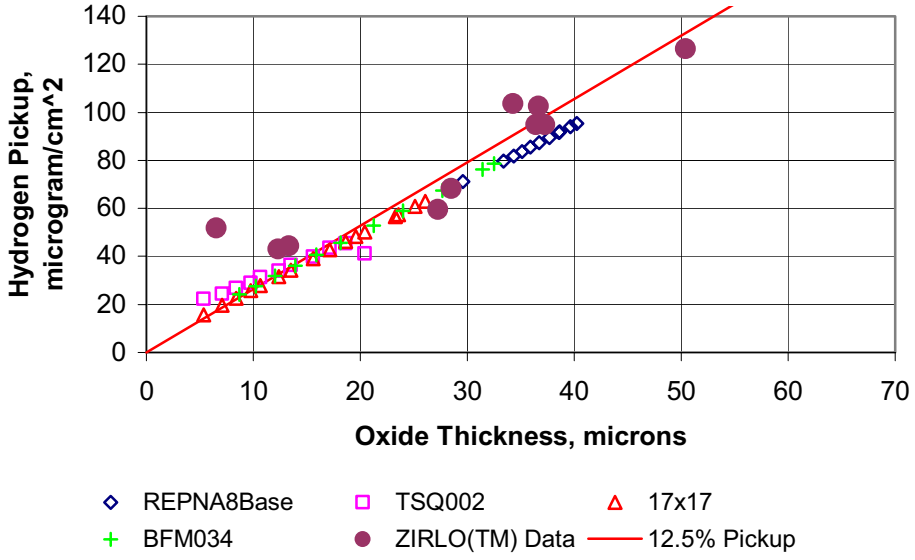

Figure 5.3 Hydrogen Pickup Data (Closed Circles) and Modified FRAPCON-3 Calculations (Open Symbols), for ZIRLO™ Cladding

5.2 Modifications for M5™ Cladding: Changes and Verification

M5™ cladding differs from Zircaloy-4 primarily by the addition of 1% niobium and alteration of annealing resulting in recrystallization of the grains. These changes result in significantly reduced corrosion (FRAMATOME website 2004; Mardon and Waeckel, 2003) (see Figure 5.4) and significantly reduced hydrogen pickup fraction. In the modified FRAPCON-3 code, the cladding type indicator ICM can now be given the value 5 to indicate that modified corrosion and hydrogen pickup fraction appropriate for M5™ cladding will be used.

In FRAPCON-3, it was found by trial that reducing the calculated Zircaloy-4 corrosion rate by the factor 2.3 results in corrosion layer thickness predictions that compare closely to the M5™ corrosion data trend presented by Mardon and Waeckel, (2003) and on the FRAMATOME website. Figure 5.5 demonstrates the effect of this change in FRAPCON-3 predictions, relative to the M5™ corrosion data. The open triangles, diamonds, and squares and the (+) symbols are the FRAPCON-3 predictions for these rods with M5™ cladding. The LSQ curve in this figure represents the least squares fit to the M5™ corrosion data.

The corrosion data are presented by FRAMATOME only as a function of fuel burnup. If the information were presented as a function of FDI, which incorporates the effect of cladding surface temperature, the data scatter likely would be reduced, and it is certain (from Section 5.1) that the scatter in the calculated oxide values would be reduced.

The hydrogen pickup fraction for M5™ was reduced from the 15% derived for Zircaloy-4 to 7.5%, based on data presented on the FRAMATOME website (see Figure 5.5).

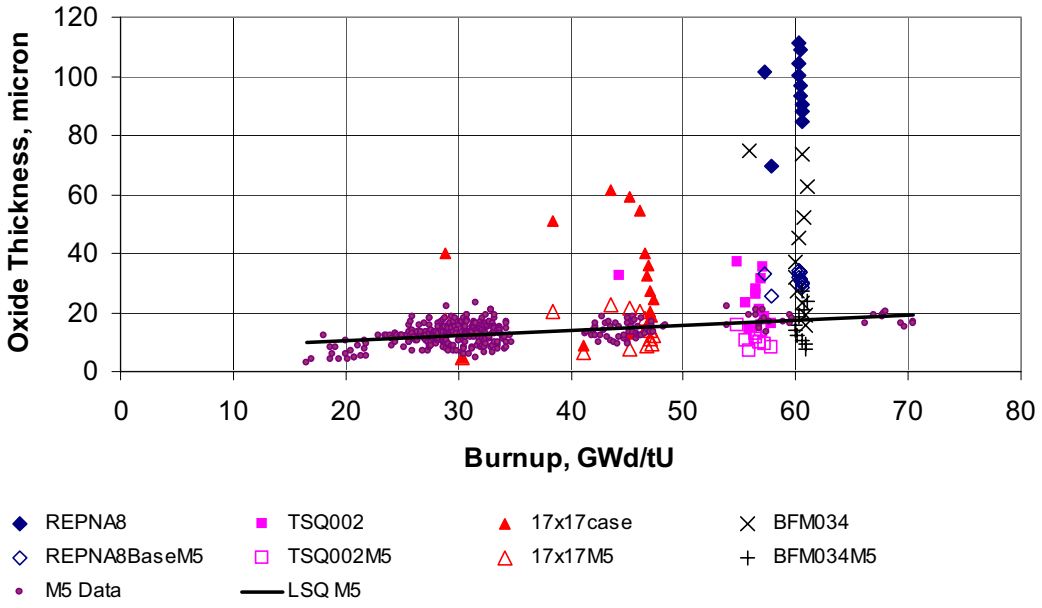

Figure 5.4 Comparison of Unmodified FRAPCON-3 Zircaloy-4 Corrosion (Solid Symbols, x Symbol, and Modified FRAPCON-3 [M5™] Corrosion (Open Symbols and + Symbol) Against FRAMATOME Corrosion Data for M5™ Cladding

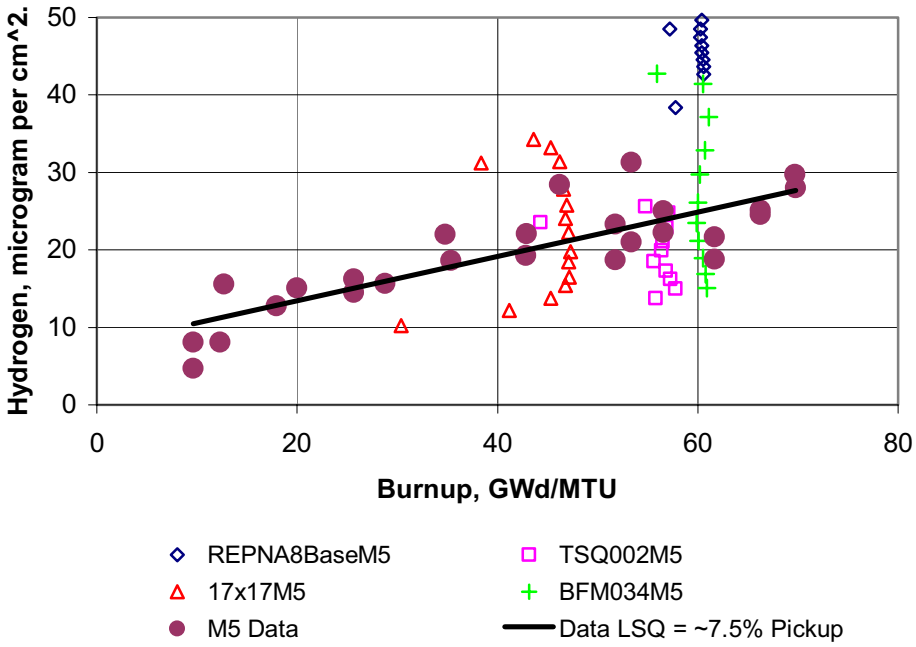

Figure 5.5 Hydrogen Pickup Data (Closed Circles) and Modified FRAPCON-3 Calculations for M5™ Cladding (Hydrogen Pickup Fraction is Reduced from 15% to 7.5%)

5.3 Ranges of Application and Uncertainty for Cladding Corrosion

The recommended ranges of application for the cladding corrosion models are given below. These ranges represent PNNL-estimated limits for reliable model-to-data comparisons to date and not necessarily the outer bounds of all available data:

Temperature: 570 to 650 K (PWR)
520 to 550 K (BWR)
Rod-Average Burnup: 0 to 62 GWd/MTU
Oxide Thickness: 1 to ~150 microns.

The uncertainty on oxide thickness is approximately 5 microns up to 50 microns layer thickness, and 10% relative for thicker oxide layers. The uncertainty on hydrogen content in the cladding (for a given oxide layer thickness) is approximately 15% relative.

5.4 Confirmation BWR Corrosion Rate and Hydrogen Pickup for Zircaloy-2

It is apparent that the current BWR-condition corrosion model in FRAPCON-3 (applied to Zircaloy 2) predicts well to high burnup and should be retained based on comparison to data from GE fuel presented by Potts (2000), and Japanese BWR and Zircaloy-2 corrosion data presented by Itagaki et al. (2003) and Ishimoto et al. (2000). This is demonstrated in Figures 5.6 - 5.8.

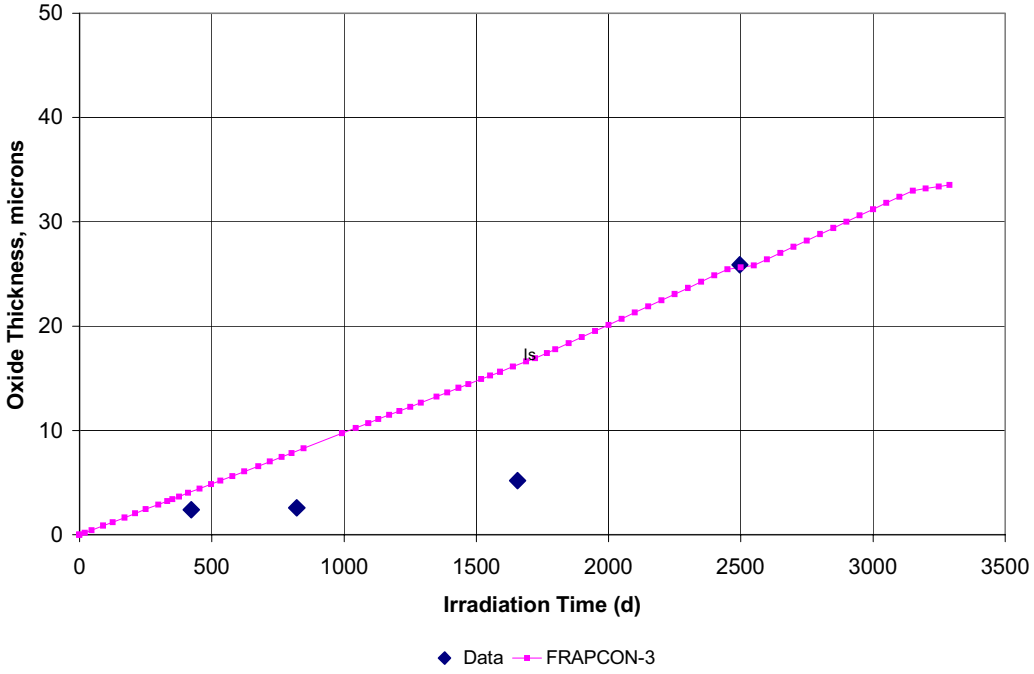

Figure 5.6 Japanese/Spanish BWR Zircaloy-2 Corrosion Data and FRAPCON 3 Calculations (from Ishimoto et al. [2003])

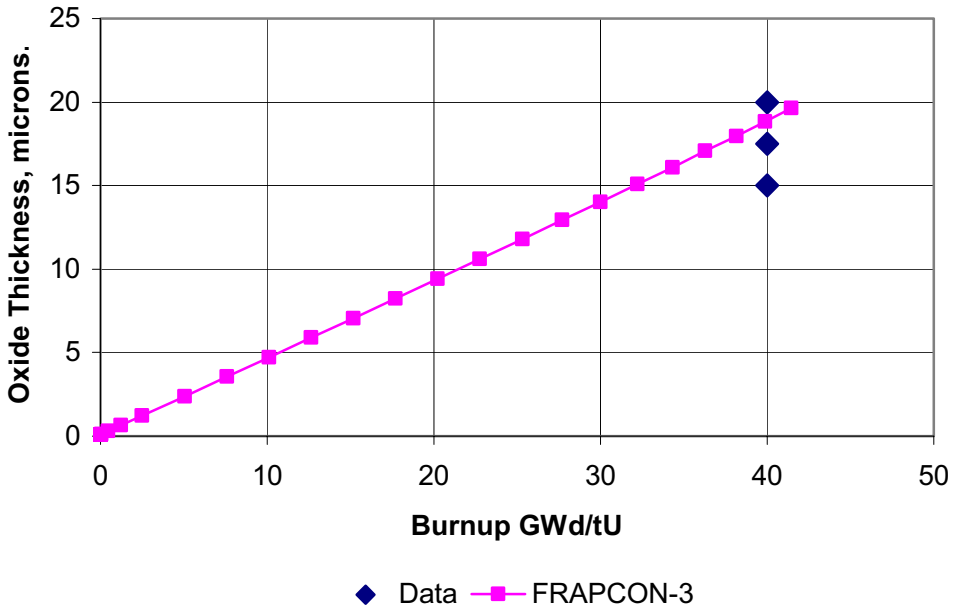

Figure 5.7 Japanese Halden Test BWR Zircaloy-2 Corrosion Data and FRAPCON-3 Calculations (from Itagaki et al. [2003])

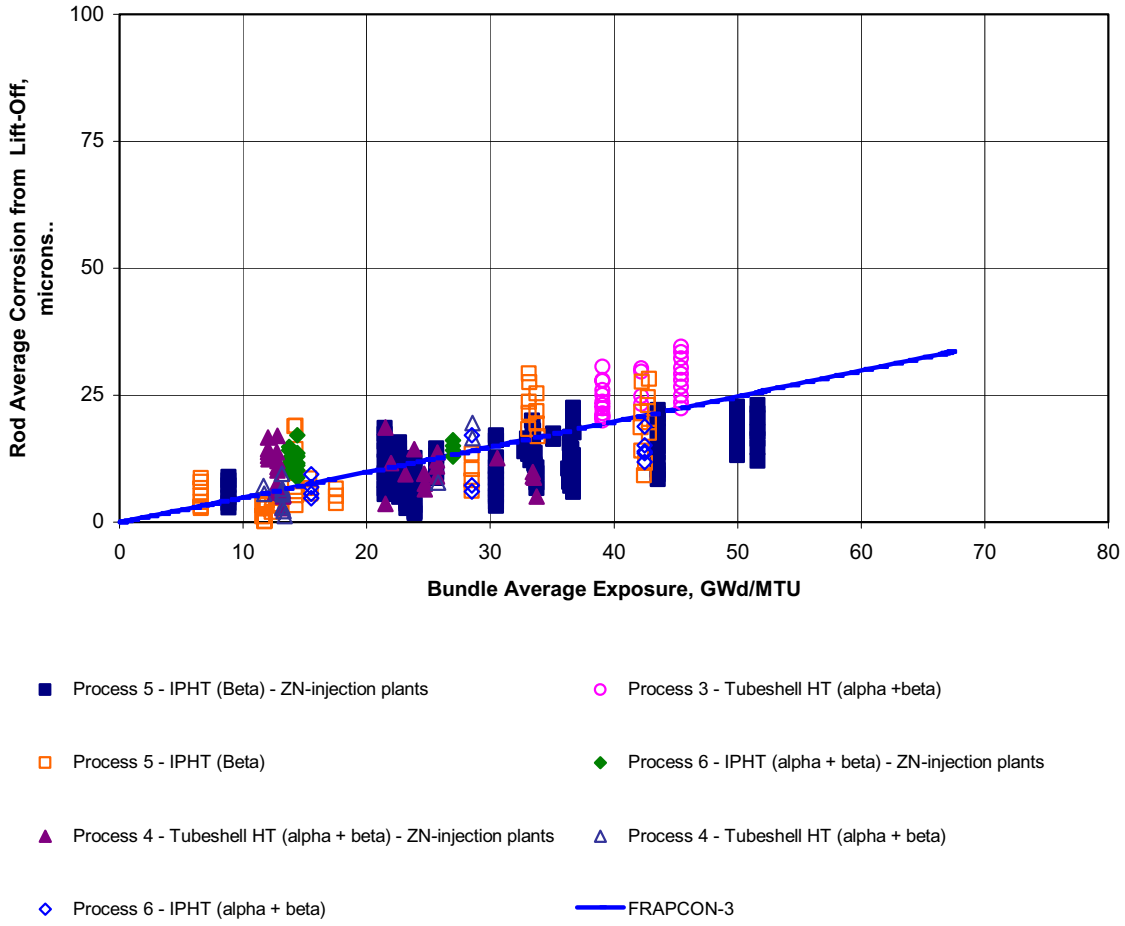

Figure 5.8 GE BWR Zircaloy-2 Corrosion Data and FRAPCON-3 Calculations (from Potts [2000])

It is also apparent that the current hydrogen pickup fraction of 29% used in FRAPCON 3 is appropriate to high burnup and should be retained, based on irradiation test data and autoclave test data presented by Itagaki et al. (2003), and Ishimoto et al. (2000) (see Figure 5.9).

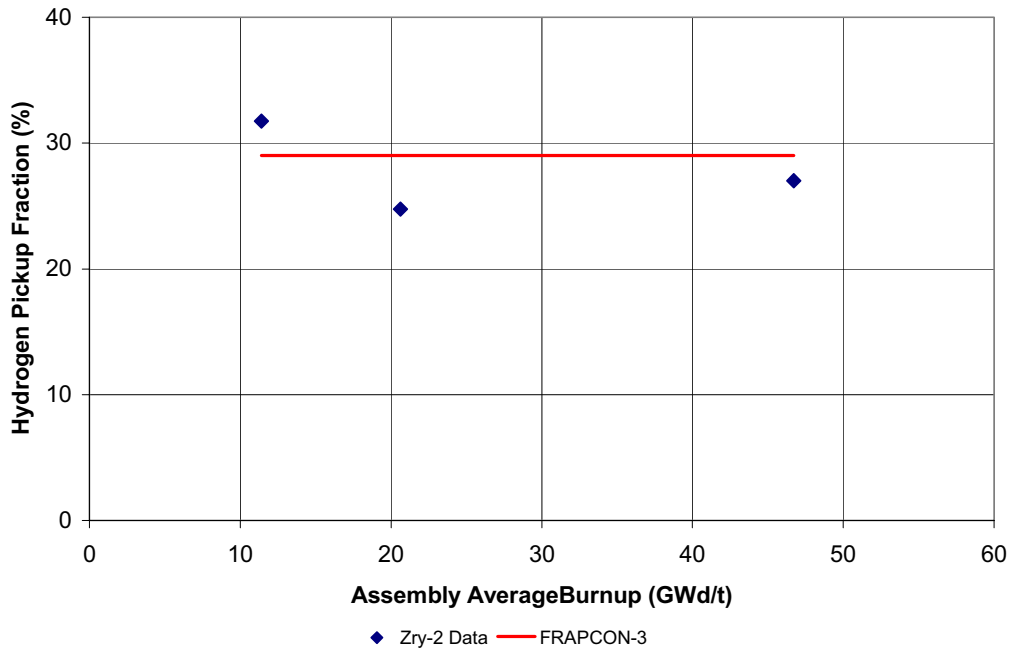

Figure 5.9 Measured In-Reactor Hydrogen Pickup Fractions in Zircaloy-2 Coupons (from Itagaki et al. [2003]) Compared to the FRAPCON-3 Value

5.5 Adjustment of Stress Calculations for Clad Wall Thinning Due to Corrosion

As the cladding oxidizes, the wall thickness that should be used to calculate stress decreases as more of the Zircaloy is consumed in the oxidation reaction. This thinning of the cladding had not been modeled in previous versions of FRAPCON-3. The latest version of FRAPCON-3 accounts for the effect of clad wall thinning due to corrosion on the calculation of stress.

To account for this wall thinning, at each time step the variable, 'dco', which stores the clad outer diameter, is reduced by the oxide thickness increase from the previous time step divided by 1.56, which is the ratio of the volume of ZrO_2 to the volume of Zircaloy. This value of 'dco' is stored for each axial node and goes into the mechanical calculations, so the cladding stress is calculated based on a reduced wall thickness.

In FRAPCON-3, the variable, 'dco', which is modified as described above, is used to convert surface heat flux to LHGR and back to surface heat flux in several places throughout the code. To keep the LHGR values consistent with the input values a new variable is defined as the initial cladding outer diameter, which was input, and this variable, which is not modified for the thinning due to oxidation, is used to convert between surface heat flux and LHGR.

It is known that at high burnup, as the cladding begins to pick up a significant quantity of hydrogen, the outer edge of the cladding begins to exhibit a structure known as a hydride rim, characterized by dense circumferential hydrides. This hydride rim is very brittle and most likely does not contribute to the

strength of the cladding. Currently in FRAPCON-3, this hydride rim is not modeled, and the stress in the cladding is divided equally across the entire thickness of the cladding that has not been consumed by oxidation.

5.6 New Hydrogen Solubility Function for Zircaloy Cladding

The model in FRAPCON-3 for the solubility of hydrogen in Zircaloy was changed from the Sawatzky model (Sawatzky and Wilkins, 1967) to the Kearns model (Kearns, 1967). FRAPCON 3 does not explicitly use the amount of hydrogen in solution in any of its calculations. It does, however, output the amount of precipitated hydrogen at each axial node that is calculated using a hydrogen solubility model. The transient companion code to FRAPCON-3, FRAPTRAN, uses the amount of precipitated hydrogen in the calculation of its strain-based failure criteria. To keep the two codes consistent with each other, the hydrogen solubility model in FRAPCON-3 was changed to the Kearns model used in FRAPTRAN, and that is more widely used in the literature.

The model for hydrogen solubility in Zircaloy in FRAPCON-3 is now given by the following equation.

$$H = 1.2 \times 10^{5} \exp(-8550/[1.986T]) \tag{5.2}$$

where:

HSol = Solubility of hydrogen in Zircaloy (ppm)
T = Zircaloy temperature (K).

6.0 CODE CAPABILITY ENHANCEMENTS

Several significant changes have been made to FRAPCON-3 since its original release that do not fall into the category of new or updated models. Rather, these changes represent enhancements to the basic code structure that allow the user to perform calculations that previously had not been possible without altering the code.

6.1 Input Option to Restrict Fission Gas Release

A new input variable was added to the data block, $frpcon, called 'igas.' The default value for 'igas' is 0. This variable is defined as the time step when FGR will begin. For all time steps prior to this value, the code will calculate a value of 0 for the gas release. For steps including and after the value specified in 'igas,' the calculation of FGR will proceed as if the rod had released gas in the prior steps, except the released gas from prior steps is not included in the rod void volume and therefore does not contribute to the gas mixture for gap gas thermal conductivity and gap conductance calculations or to the rod internal pressure.

This option is useful in performing a calculation where a rod is irradiated for some time, refabricated and refilled with gas, and then the refabricated rod is irradiated for another period of time. If the user is interested in the gas release behavior of the refabricated rod, the user can run the code with no gas release during the initial irradiation to calculate the burnup effects from the initial irradiation, and then specify a time step where gas release will begin for the second irradiation period.

This option only applies to the Massih FGR model. PNNL has not included this option in the ANS5.4 model.

6.2 Input Option to Impose Cladding Surface Temperature Profiles

In some cases, it may be necessary for the user to be able to specify the cladding surface temperature at each axial node (as a function of time). The previous version of the code did not facilitate this because it calculated the cladding temperature for each node based on the coolant inlet temperature, enthalpy rise, and film coefficient, where the latter two are in turn functions of input flow rate, LHGR (hence heat flux), and coolant system pressure. Potential applications of this option are analysis of a test rod irradiated within a capsule and simulation of an irradiated rod in cask storage conditions. The latest version of FRAPCON-3.3 has been modified as described below to allow the user to input the temperature profile for the cladding surface for use during specified time steps.

The application of this option follows a pattern similar to that for axial power shape input.

The following is a list of the new variables that were added to the $frpcon input block in order to add this capability.

- ifixedtsurf – default value =0, in order for the input surface temperature to be used for a time step, 'ifixedtsurf' must be equal to 1 and the input variable, 'go,' must be equal to 0.0 for that time step.

- xt(1) – input elevations for the first temperature profile. The first value must be 0.0 and the last value must equal 'totl.' Begin the input elevations for the second temperature profile at xt(n+1), where n is the number of values in the first profile. Input value in feet or meters, depending on the type of input units being used.

- cladt(1) – input cladding temperatures corresponding to the values in the 'xt' array. Begin the temperature values for the second temperature profile at cladt(n+1), where n is the number of values in the first profile. Input value in °F or K, depending on the type of input units being used.

- jstsurftemp – array of integer values that show which temperature profile to use for each time step. Similar to 'jst' for the axial power profiles.

- jnsurftemp – array of integer values that show how many values are in each temperature profile. Each temperature profile may have a different number of values. The number of values does not need to correspond with the number of axial nodes. The code will interpolate values for each axial node based on the input.

The plenum region rod outer surface temperature equals the top-node input surface temperature. The plenum (gas) heatup model remains unchanged (but that model adds no heat in a zero-power application).

6.3 FORTRAN 90 Compliance

The development and release of the FRAPCON-3 code has moved from a UNIX-based system to a PC-based system. The benefit is that more users have access to PC systems, and the speed of these systems is sufficient to run the code. With each release of FRAPCON-3, PNNL sends the code to the user group as an executable that can be run on any PC system capable of executing a WIN32 application. PNNL also distributes the FORTRAN source code so users can compile the code and make changes if they wish. Due to the number of different systems and compilers used to develop and maintain the code, the source code was not compatible with all FORTRAN compilers. Therefore, PNNL made the extensive (non-modeling) revisions to bring the code into compliance with the FORTRAN 90 standard. Now, any compiler that can compile a FORTRAN 90 program will be able to compile the program regardless of the operating system or computer type in use.

During this process of bringing the code into compliance with the FORTRAN 90 standard, an extensive quality assurance program was in place whereby the output of the code was checked electronically relative to the output of the original code after each set of changes were made. This program ensured that the output of the FORTRAN 90 compliant code was identical to the output of the original code.

7.0 REFERENCES

Adamson, M.G., E.A. Aitken, and R.W. Caputi. *Journal of Nuclear Materials*, vol. 130 p. 245. 1985.

Bagger, C., H. Carlson, and P. Knudson. *Details of Design Irradiation and fission Gas Release for the Danish UO_2-Zr Irradiation Test 022*, RISP-M-2152, Riso National Laboratory, Denmark. 1978.

Balfour, M.G. *BR-3 High burnup Fuel Rod Hot Cell Program, Final Report, Vol. 1*. D0E/ET/34073-1, Westinghouse Electric Corporation, Pittsburgh, Pennsylvania. 1982.

Balfour, M.G., E. Roberts, E. DeQuidt, and P. Blanc, *Zorita Research and Development Program Volume 1: Final Report*, WCAP-10180, Westinghouse Electric Corporation, Pittsburgh, Pennsylvania. 1982.

Barner, J.O., M.E. Cunningham, M.D. Freshley and D.D. Lanning, *High Burnup Effects Program: Final Report*, HBEP-61, Pacific Northwest National Laboratory, Richland, Washington. 1990.

Berna. G.A., C.E. Beyer, K.L. Davis and D. D. Lanning. *FRAPCON-3: A Computer Code for the Calculation of Steady-State, Thermal Mechanical Behavior of Oxide Fuel Rods for High Burnup*, NUREG/CR-6534, volume 2 (PNNL-11513 v.2, Pacific Northwest National Laboratory, Richland, Washington). 1997.

Blanpain, P, L. Brunel, X. Thibault, and M. Trotabas. "MOX Fuel Performance in the French PWRs: Status and Development," in *Proceedings of the ANS/ENS Topical Meeting on Light Water Reactor Fuel Performance*, Park City, Utah, April 10-13, 2000, pp. 973-989. 2000.

Carrol, J.C., R.A. Gomme, and N.A. Leech. "Thermal Diffusivity Measurements on Unirradiated Archive Fuel, and Fuel Irradiated in the Halden IFA-558 Experiment," paper 13 in *Proceedings of the Enlarged HPG Meeting on High Burnup Fuel Performance, Safety and Reliability and Degradation of In-Core Materials and Water Chemistry Effects and Man-Machine Systems Research*, 1994 HWR-345, Bolkesjo, Norway Limited Distribution. 1994.

Chantoin, P.M., E. Sartori, and J.A. Turnbull. "The Compilation of a Public Domain Database on Nuclear Fuel Performance for the Purpose of Code Development and Validation," presented in *Proceedings of the ANS/ENS International Topical Meeting on Light Water Reactor Fuel Performance*, Portland, Oregon, March 2-6, 1997, pp. 515-522. 1997.

Cook, P., B. Christiansen, G. Dassel, E. Matthews, I. Robins. R. Stratton, C. Walker, and R. Weston. "Performance of BNFL MOX Fuel," in *Proceedings of the ENS TopFuel 2003 Meeting*, March 16 to 19, 2003, Wurzburg, Germany, p. 117. 2003.

De Meulemeester, E., N. Hoppe, G. de Contenson, M. Watteau "Review of Work Carried out by BELGONUCLEAIRE and CEA on the Improvement and Verification of the COMETHE Computer Code with the Aid of In-Pile Experimental Results," paper ECS-EEC-73-595, BNES *International Conference on Nuclear Fuel Performance*. 1973.

Devold, H., and H. Wallin. PIE *Results from the High Burnup Rods CD/CH (IFA 429) and Comparison with In Pile Data*, HWR 409. Halden Reactor Project, Halden, Norway. 1994.

Djurle, S. *Final Report of the Super Ramp Project*, D0E/ET/34032 1. U.S. Department of Energy, Washington, D.C. 1985.

Duriez, C., J.-P. Allesandri, T. Gervais, and Y. Philipponneau. "Thermal Conductivity of Hypostoichiometric Low Pu Content $(U,Pu)O_{2-x}$ Mixed Oxide," *Journal of Nuclear Materials*, vol. 277, pp. 143-158. 2000.

FRAMATOME (website http://www.framatech.com/pdf/m5.pdf)

Forsberg, K. and A.R. Massih, "Fission Theory of Fission Gas Migration in Irradiated Nuclear Fuel UO_2," *Journal of Nuclear Materials*, vol. 135, pp. 140-148. 1985.

Fukushima, S. T. Oishi, A. Maeda, and H. Watanabe. "The Effect of Gadolinium Content on the Thermal Conductivity of Near-Stoichiometric $(U,Gd)O_2$ Solid Solutions," *Journal of Nuclear Materials* vol.105, pp. 201-210. 1982.

Garlick, A., A.L. Goldsmith, P.D. Kennedy, P. Mellor and J.F.W. Thompson, *Destructive Examinations of KWU/CE and BNFL Rods at Windscale Task 2A*, HBEP 24. Pacific Northwest Laboratory, Richland, Washington. 1982.

Hagrman, D.L., A. Reymann, and R.E. Mason. *MATPRO-Version II (Revision 2): A Handbook of Materials Properties for Use in the Analysis of Light Water Reactor Fuel*, NUREG/CR 0497 (TREE-1280), Rev.2. 1981.

Hejzlar, P., D. Feng, Y. Yuan, M.S. Kazimi, He Feinroth, B. Hao, E.J. Lahota and H. Hamilton. 2004. "The Design and Manufacturing of Annular Fuel For High Power Density and Improved Safety in PWRs," the ANS/ENS/JAES International Meeting on Light Water Reactor Fuel Performance, Orlando Florida, September 19-22, 2004, p.41. 2004

Hermansson, P., and A.R. Massih, "An Effective Method for Calculation of Diffusive Flow in Spherical Grains," *Journal of Nuclear Materials*, vol. 304, pp. 204-211. 2002.

Hirai, M. and S. Ishimoto. "Thermal Diffusivities and Thermal Conductivities of UO_2-GD2O3," *Journal of Nuclear Science and Technology*, vol. 28, pp. 995-1000. 1991.

Hodge, S.A., and L.J. Ott. 2004. "Irradiation Tests of Mixed Oxide Fuel Prepared with Weapons Derived Plutonium," the ANS/ENS/JAES International Meeting on Light Water Reactor Fuel Performance, Orlando Florida, September19-22, 2004, p. 273. 2004

Hodge, S.A., L.J. Ott, and F.P. Griffin. *Implications of the PIE Results for the 40-GWd/MT-Withdrawal MOX Capsules*, ORNL/MD/LTR-241, Oak Ridge National Laboratory, Oak Ridge, Tennessee, vol. 2. 2003.

In de Betou, J., L.O.Jernkvist, A.R. Massih, P. Rudling, G. Ronnberg, M. Stepniewski, and G. Wiksell. 2004. "Assessment of Burnup Dependent Fuel Rod Failure Threshold under Reactivity Initiated Accidents in Light Water Reactors," the ANS/ENS/JAES International Meeting on Light Water Reactor Fuel Performance, Orlando Florida, September 19-22, 2004, p.516. 2004

Ishimoto, S., T. Kubo (NFD), R.B Adamson, (GE Nuc.Energy), Y. Etoh (Hitachi), K. Ito (Toshiba), and Y. Suzawa (TEPCO). "Development of New Zirconium Alloys for Ultra-High Burnup Fuel," *ANS/ENS Topical Meeting on LWR Fuel Performance*, April 10-13, 2000, Park City, Utah, pp. 499 -510. 2000.

Itagaki, N., K., Kakuichi, F. Yasuhiro, and T. Furuya, (NFI) and O. Kubota, (TEPCO), "Development of New High Corrosion Resistance Zr Alloy 'HIFI," in *ENS TopFuel 2003 Meeting*, March 16-19, 2003, Wurzburg, Germany. 2003.

Janvier, J C., de Bernardy de Sigoyer, B, and Delmas, R., *Irradiation of Uranium Oxide in Strong Cladding Effect of Initial Diametral Gap on Overall Behavior*, Program CC 7, 1st and 2nd Sections, CEA R 3358. Centre d'Etudes Atomique, France. 1967.

Kaiser, R.S., W.J. Leech, and A.L. Casadei. "The fuel duty index (FDI) – a New Measure of Fuel Rod Cladding Performance," in *ANS/ENS Topical Meeting on LWR Fuel Performance*, April 10-13, 2000, Park City, Utah, pp. 393-400. 2000.

Kakiuchi, K., N. Itagaki, T. Furuya. (NFI), A. Miyazaki, Y. Ishii, and S. Susuki (TEPCO) and M. Yamawaki (U. of Tokyo). "Effect of Iron for Hydrogen Absorption Properties of Zirconium Alloys," in *ENS TopFuel 2003 Meeting*, March 16-19, 2003, Wurzburg, Germany. 2003.

Kearns, J.J., "Terminal solubility and Partitioning of Hydrogen in the Alpha Phase of Zirconium, Zircaloy-2 and Zircaloy-4," *Journal of Nuclear Materials*, Vol. 22, pp. 292-303. 1967.

Khoruzkii, O.V., V.D. Kanyukova, V.V. Likhanskii, and A.A. Sorokin. 2004. "Thermophysical Modeling of High Burnup WWER Fuel by the RTOP Code," the ANS/ENS/JAES International Meeting on Light Water Reactor Fuel Performance, Orlando Florida, September 19-22, 2004, p. 770. 2004

Kim, Y.S., and C.B. Lee. 2004. "Two-Step, Two-Stage Fission Gas Release Model," the ANS/ENS/JAES International Meeting on Light Water Reactor Fuel Performance, Orlando Florida, September 19-22, 2004, p.727. 2004

Knott, R.P., R.L. Kesterson, L.G. Hallstadius, and M.Y. Young (Westinghouse-Columbia). "Advanced PWR Fuel Designs for High Duty Operation" in *ENS TopFuel 2003 Meeting*, March 16-19, 2003, Wurzburg, Germany. 2003.

Knudsen, P., C. Bagger, H. Carlsen, I. Misfeldt, and M. Mogensen. Riso Fission Gas Release Project Final Report, DOE/ET/34033 1. 1983. U.S. Department of Energy (Prepared for DOE by Riso Laboratory (Metallurgical Department), Roskilde, Denmark.

Komatsu, J., T. Tachibana, and K. Konashi. "The Melting Temperature of Irradiated Oxide Fuel," *Journal of Nuclear Materials*, Volume 154, pp. 38-44. 1988.

Lanning, D.D. Irradiation History and Final Postirradiation Data for IFA-432, NUREG/CR-0862, PNL-2948, Pacific Northwest Laboratory, Richland, Washington. 1986.

Lanning, D.D., M.E. Cunningham, J.O. Barner, and E.R. Bradley. *Qualification of Fission Gas Release Data from Task 2 Rods*, HBEP 25, Final Report. Pacific Northwest Laboratory, Richland, Washington. 1987.

Lanning, D.D., and C.E. Beyer. "Revised UO_2 Thermal Conductivity for NRC Fuel Performance Codes." *Transactions of the American Nuclear Society, 2002 Annual Meeting*, vol. 86, pp 285-287. June 9-13, 2002, Hollywood, Florida. 2002.

Lippens, M. "A European Investigation of MOX Fuel Performance in Light Water Reactors," in *Proceedings of the ANS/ENS Topical Meeting on Light Water Reactor Fuel Performance*, Williamsburg, Virginia, April 17-20, 1988, pp. 54-68. 1988.

Long, Y., Y. Yuan, A. Romano, and M.S. Kazimi. 2004. "Fission Gas Release of Heterogeneous Fuels for Plutonium Burnup," the ANS/ENS/JAES International Meeting on Light Water Reactor Fuel Performance, Orlando Florida, Sept 19-22, 2004, p. 596. 2004

Lucuta, P.G., H.S. Matzke, and I.J. Hastings, "A Pragmatic Approach to Modeling Thermal Conductivity of Irradiated UO_2 Fuel: Review and Recommendations," *Journal of Nuclear Materials*, vol. 232 (1996), pp 166-180.

Mardon, J.P., and N. Waeckel (FRAMATOME-ANP and EdF). "Behavior of M5^{TM} Alloy Under LOCA Conditions," in *ENS TopFuel 2003 Meeting*, March 16-19, 2003, Wurzburg, Germany. 2003.

Massih, A.R., S. Persson and Z. Weiss. "Modeling of $(U,Gd)O_2$ Fuel Behavior in Boiling Water Reactors," in *Proceedings of Symposium E on Nuclear Materials for Fission Reactors of the 1991 E-MRS Fall Conference; Journal of Nuclear Materials* vol. 188, pp 323-330. 1992.

Matsson, I., and J.A. Turnbull. *The Integral Fuel Rod Behaviour Test IFA-597.3: Analysis of the Measurements*, HWR-543 Halden Reactor Project, Norway (Limited distribution). 1998.

Mogard, H., project manager. *Final Report of the Inter Ramp Project*, STIR 53. ABB Atomenergi, Studsvik Laboratory, Nykoping, Sweden. 1979.

Newman, L.W. *Development and Demonstration of an Advanced Extended-Burnup Fuel Assembly Design Incorporating Urania-Gadolinia*, DOE/ET/34212-36, BAW-1681-2. Babcock and Wilcox Inc., Lynchburg, Virginia. 1982.

Newman, L.W., project manager. *Thermal and Physical Properties of Urania-Gadolinia Fuel*, DOE/ET/34212-43, BAW-1759. Babcock and Wilcox Inc., Lynchburg, Virginia. 1984.

Newman, L.W., project manager. *The Hot Cell Examination of Oconee 1 Fuel Rods after Five Cycles of Irradiation*, DOE/ET/34212 50, BAW 1874. Babcock and Wilcox Inc., Lynchburg, Virginia. 1986.

Notley, M.J.F., and J.R. MacEwan. *The Effect of UO_2 Density on Fission Gas Release and Sheath Expansion*, AECL-2230, Atomic Energy of Canada, Ltd., Chalk River, Canada. 1965.

Notley, M.J.F., R. DesHais, and J.R. MacEwan. *Measurements of the Fission Product Gas Pressures Developed in UO2 Fuel Elements During Operation*, AECL-2662, Atomic Energy of Canada, Ltd., Chalk River, Canada. 1967.

Ogata, K., T. Karasawa, T. Anegawa, S. Koizumi, and K. Ito. "Japanese BWR Fuel Performance and Recent R& D Activities," in *ANS/ENS Topical Meeting on LWR Fuel Performanc*e, April 10-13, 2000, Park City, Utah, pp. 108-117. 2000.

Ohira, K., and N. Itagaki. "Thermal Conductivity Measurements of High Burnup UO_2 Pellet and a Benchmark Calculation of Fuel Center Temperature," in *Proceedings of the ANS International Topical Meeting on LWR Fuel Performance*, pp. 541-549. March 2-6, 1997, Portland, Oregon. 1997.

Peititprez, B., *Ramp Tests with Two High Burnup MOX Fuel Rods in IFA-629.3*, HWR 714, Halden Reactor Project, Norway (Limited Distribution), 2002.

Popov, S.G., J.J. Carbajo, VK. Ivanov, and G.L. Yoder, *Thermophysical Properties of MOX and UO_2 Fuels Including the Effects of Irradiation*, ORNL/TM 2000/351, Oak Ridge National Laboratory, Oak Ridge, Tennessee. 2000.

Potts, G.A. "Recent GE BWR Fuel Experience," *ANS/ENS Topical Meeting on LWR Fuel Performance*, April 10-13, 2000, Park City, Utah, pp. 95-107. 2000.

Ronchi, C., M. Sheindlin, M. Musella, and G.J. Hyland. "Thermal Conductivity of Uranium Dioxide Up to 2900K from Simultaneous Measurement of the Heat Capacity and Thermal Diffusivity." *Journal of Applied Physics* 85(2):776-789. 1999.

Ronchi, C., M. Sheindlin, D. Staicu, and M. Kinoshita. "Effect of Burnup on the Thermal Conductivity of Uranium Dioxide up to 100,000 MWd/t," *Journal of Nuclear Materials*, volume 327, pp. 58-76. 2004.

Sabol, G.P., R.J. Comstock, R.A. Weiner, P. Larouere, and R.N. Stanutz. "In-Reactor Corrosion Performance of ZIRLO™ and Zircaloy-4," in *Zirconium in the Nuclear Industry: Eighth International Symposium*, ASTM STP 1023, L.F.P Van Swam and C.M. Euken, Eds., ASME, Philadelphia, Pennsylvania, pp. 227-244. 1989.

Sabol, G.P., G.R. Kelp, M.G. Balfour, and E. Roberts. "Development of a Cladding Alloy for High Burnup," in *Zirconium in the Nuclear Industry: Tenth International Symposium*, ASTM STP 1245, A.M. Garde and E.R. Bradley, Eds., ASME, Philadelphia Pennsylvania. pp. 724-744. 1994.
Sakurai, H., Y. Wakashima, K. Ito, M. Sasaki, T. Nomata, Y. Tsukuda, H. Hayashi, and D. Kubota. "Irradiation Characteristics of High burnup BWR Fuels," in *ANS/ENS Topical Meeting on LWR Fuel Performance*, April 10-13, 2000, Park City, Utah, pp. 128-138. 2000.

Sawatzky, A., and Wilkins, B.J.S, "Hydrogen Solubility in Zirconium Alloys Determined by Thermal Diffusion", *Journal of Nuclear Materials*, Vol. 22, pp. 304-310. 1967.

Smith, G. P. Jr., Project Manager, et al., *The Evaluation and Demonstration of Methods for Improved Nuclear Fuel Utilization*, DOE/ET/34013 15. 1994. Prepared for the U.S. Department of Energy by Combustion Engineering, Inc., Windsor Lock, Connecticut. 1994

Tolonen, P., M. Pihlatie, and H. Fuji, *The MOX Fuel Behaviour Test IFA-597.4/5/6: Thermal and Gas Release Data to a Burnup of 25 MWd/kgMOX*, HWR-652, Halden Reactor Project, Halden, Norway (Limited Distribution), 2001.

Tsukuda, Y., Y. Kosaka, T. Kido, S. Doi, T. Sendo, P. Gonzales, and J.M. Alonso (Japan-NUPEC, NDC, MHI, and KEPCO; Spain-ENDESA and ENUSA). "Performance of Advanced Fuel Materials for High Burnup," in *ENS TopFuel 2003 Meeting*, March 16-19, 2003, Wurzburg, Germany. 2003.

U.S. Department of Energy Office of Fissile Materials Disposition. *Surplus Plutonium Disposition Final Environmental Impact Statement*, DOE/EIS – 0283. 1999.

Vallejo, I., M.T. del Barrio, and L.E. Herranz. 2004. "Major Sensitivities of Fission Gas Release Modeling within the FRAPCON-3 Code," the ANS/ENS/JAES International Meeting on Light Water Reactor Fuel Performance, Orlando Florida, September 19-22, 2004, p. 263. 2004

Vrtilkova, V., J. Jaos, J. Cmakal, and L. Belovsky (Czech, SKODA). "Corrosion of Zr-Alloys," in *ANS/ENS Topical Meeting on LWR Fuel Performance*, April 10-13, 2000, Park City, Utah, pp. 401-415. 2000.

Waterman, M.E. *Corrected and Updated Data for IFA 429 from Beginning of Life Through June 1978*, NUREG/CR 0478, Tree 1269. 1978.

Wesley, D., A., K Mori, and S. Inoue. "Mark BEB Ramp Testing Program" presented in the *Proceedings of the 1994 ANS/ENS International Topical Meeting on Light Water Reactor Fuel Performance, West Palm Beach, Florida*. American Nuclear Society, p. 343. 1994.

White, R.J. "The Re-Irradiation of MIMAS MOX Fuel in IFA-629.1," HWR-586 Halden Reactor Project, Halden, Norway. 1999.

White, R.J., S.B. Fisher, P.M.A. Cook, R. Stratton, C.T. Walker, and I.D. Palmer. "Measurement and Analysis of Fission Gas Release from BNFL's SBR MOX Fuel." *Journal of Nuclear Materials*, vol. 288, pp. 43-56. 2001.

Wiesenack, W., and T. Tverberg. "Thermal Performance of High Burnup Fuel - In-Pile Temperature Data and Analysis," in *Proceedings of the ANS International Topical Meeting on Light Water Reactor Fuel Performance*, pp. 730-737. April 2000, Park City, Utah. 2000.

Wright, J. "The SBR MOX and UO_2 Comparison Test in Gas Flow Rig IFA-633: Results after Seven Cycles of Irradiation," HWR-764, Halden Reactor Project, Halden, Norway. 2004.

Appendix A

Code-Data Comparisons for MOX Fuel Temperatures

Appendix A

Code-Data Comparisons for MOX Fuel Temperatures

A.1 Introduction

Recent instrumented fuel tests in the Halden test reactor are of interest to FRAPCON-3.3 MOX fuel thermal performance confirmation because they include re-fabricated high-burnup pressurized water reactors (PWR) mixed plutonia-urania oxide MOX fuel segments. A total of four rod segments are represented in the five high-burnup tests, with pre-test burnups ranging from 50 to 65 MWd/kgM. These comparisons include fuel temperature as a function of time and burnup and include fission gas release (FGR) in the case of experiments IFA 606 and 629.3 (see Sections A.2 through A.5).

Fuel temperature, rod elongation, and FGR data are also available from two additional PWR MOX fuel rod segments tested in the IFA-629.1 experiment. The base-irradiation burnup for these two rods was 27 and 29 MWd/kgHM. The maximum linear heat generation rates (LHGRs) during the test were significant (35 to 40 kW/m). Code-data comparisons are shown in Section A.6.

Beginning-of-life (BOL) fuel temperatures have been measured for both UO_2 (urania) and MOX fuel in IFA-633. The IFA-633 code-data comparisons in particular confirm the magnitude of the conductivity difference between MOX and urania. These are shown in Section A.7.

A.2 IFA-606 Temperature and FGR Data and Calculations

The IFA-606 test assembly consisted of four re-fabricated rod segments from a full-length PWR MOX rod irradiated in the Beznau-1 reactor (Switzerland) at nominal LHGRs to a burnup of 50 MWd/kgM. Two test rods were instrumented with a fuel thermocouple and a pressure transducer, and irradiated under Halden conditions for approximately 30 days at elevated LHGR in "Phase 2" of the test, to determine FGR behavior (Mertens et al., 1998; Mertens and Lippens, 2001). The code-data comparisons presented here are for one of these rods with "nominal" (12.5-micron) grain size.

A.2.1 Description of Test Rod and Base Irradiation

The design and operating parameters available for the full-length ("mother") rod and for the instrumented rod segments ("daughter rods") are given in Tables A.2.1 and A.2.2, respectively. Table A.2.2 does not list the thermocouple well diameter for the instrumented rod, which is assumed to be 2.5 mm based on other Halden irradiation specifications. The rod was base-irradiated at nominal LHGRs for ~1500 days, as shown in Figure A.2.1. The rod segment reached a burnup of 49.5 MWd/kgM.

A.2.2 Test Rod Instrumentation and Test Conduct

The fuel rod segment was instrumented with a pressure transducer and a fuel centerline thermocouple. FGR was determined from the rise in pressure readings and was later confirmed by postirradiation examination puncture. The LHGR history during the test (the segment-average LHGR) is shown in Figure A.2.2. The neutron flux at the thermocouple position happens to be very close to the rod-average value; however, this value is adjusted downward by 10% for FRAPCON input because of the effect of the thermocouple well, which in this case is 30% of the radius and hence about 10% of the fuel volume.

A.2.3 Code-Data Comparisons

The measured and calculated fuel center temperatures vs. burnup are shown in Figure A.2.3. The data are overpredicted by about 50°C at the highest LHGR but the comparison is closer elsewhere. The FGR was measured as about 12% by end-of-test compared to a calculated increase in FGR (during the test) of 13.1%.

Table A.2.1. IFA 606 Mother Rod

Pellet OD:	9.293 mm
Pellet ID:	0.000 mm
Pellet Ht:	12.555 mm
Dish & Chamfer Volume:	1.2%
RMS Roughness:	0.0025 mm
Avg. Grain Diameter:	0.012 mm
As-Fabricated Density:	95.585%
Resinter Densification:	0.65%
Open Porosity:	0.1%
Pu Content:	5.97 w/o HM
U-235 Enrichment:	0.278 w/o
Pu isotopes:	65.86, 23.83, 7.38, 3.33 est.
(Pu-239, Pu-240, 241, 242) at. %	
Fuel Type:	AUC
Clad Material:	Zr-4
Clad OD:	10.72 mm
Clad ID:	9.48 mm
RMS Roughness:	0.00063 mm
Stack Length:	3028.7 mm
Upper Plenum Volume:	8.96 cm^3
Lower Plenum Volume:	0.0 cm^3
Total Free Volume:	21.42 cm^3
He Backfill Pressure:	2.4 Mpa
Backfill Temperature:	25°C

Table A.2.2. IFA 606 Daughter Rod

Fuel Rod Diametral Gap:	0.0 mm
Stack Length:	398.2 mm
Upper Plenum Length:	45.0 mm
Upper Plenum Volume:	3.14 cm^3
Lower Plenum Volume:	0.0 cm^3
Total Free Volume:	3.91 cm^3
He Backfill Pressure:	0.511 Mpa
Backfill Temperature:	25°C
Mass Flux:	3280.0 kg/m^2s
Hydraulic Diameter:	25.90 mm
Equivalent Heated Diameter:	27.00 mm
Inlet Temp:	220°C
Coolant Pressure:	33.6 bar

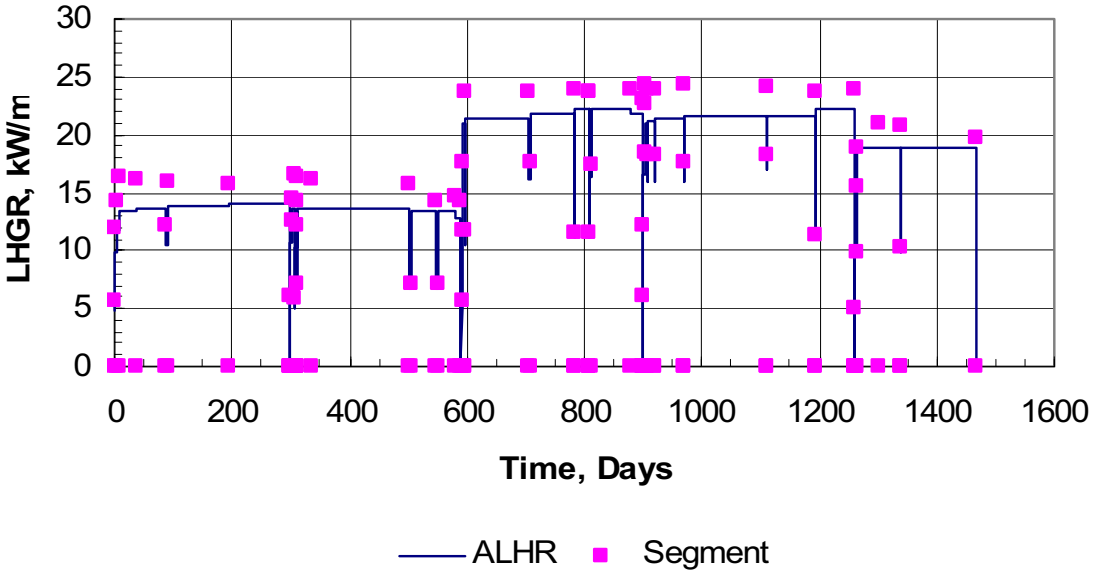

Figure A.2.1. IFA-606 Base Irradiation Power History. ("ALHR" is Average Linear Heat Rate; "Segment" Shows Heat Rating for the Segment of Interest, which was Re-Fabricated to a Test Rod)

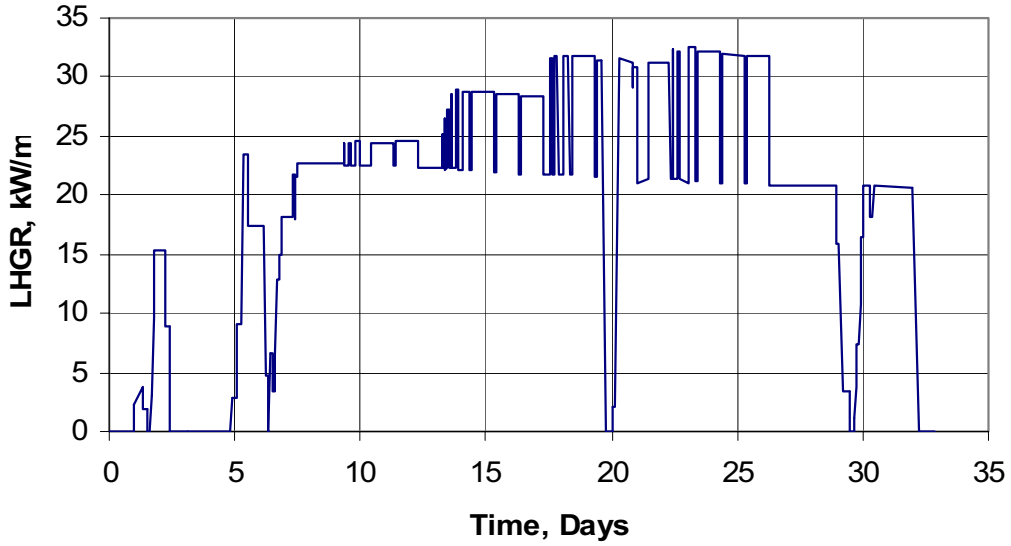

Figure A.2.2. Test Irradiation LHGR History for Phase 2

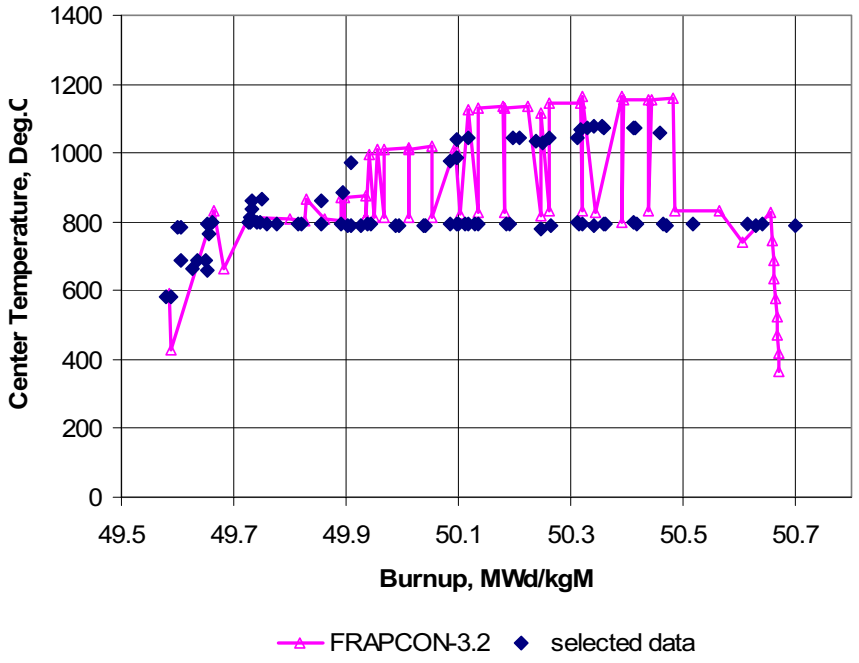

Figure A.2.3. Calculated and Measured Fuel Center Temperature vs. Burnup for IFA-606, Phase 2

A.3 IFA-610.2 and 610.4 Fuel Temperature Data and Calculations

One segment from 4-Cycle PWR MOX EdF Rod N016 (which was base-irradiated for four cycles in the French Gravelines-4 reactors to a burnup of approximately 55 MWd/kgM) was re-fabricated and instrumented for use in the sequential IFA-610.2,4 cladding liftoff experiments (Nishi and Lee, 2001). The rod was tested under simulated PWR conditions in a pressurized water loop within the Halden reactor. The rod was connected to a gas supply system, and temperature measurements were made in both helium and argon fill gases at varying pressures. Fuel temperature data from helium gas fill periods are compared to calculations herein.

A.3.1 Description of the Test Rod and Base Irradiation

The design and operating parameters available for the mother (full-length) rod and daughter rod segment are given in Tables A.3.1 and A.3.2, respectively. The rod was base-irradiated at nominal LHGRs for ~1500 days, as shown in Figure A.3.1. The final burnup for the segment was 54.5 MWd/kgM.

A.3.2 Test Rod Instrumentation and Test Conduct

The rod was instrumented with a fuel center thermocouple and a rod elongation sensor. Internal gas pressure was varied throughout the ~100-day IFA-610.2 test to investigate the threshold for cladding liftoff (Beguin, 1999; Fujii and Claudel, 2001). The LHGR level during the IFA-610.2 test was steady at about 14 kW/m to 15 kW/m, and LHGR at the thermocouple was about 13.5 to 14 kW/m.

In IFA-610.4, the LHGRs were similar at the beginning and drifted downward to 12.5 and 12.0 kW/m for rod-average and thermocouple location, respectively (Fujii and Claudel, 2001). The test duration was similar to that of IFA-610.2 (100 days); however, after 50 days, questions of potential thermocouple degradation were raised, and code data comparison was only conducted over the first 50 days of the test.

A.3.3 Code-to-Data Comparisons

The measured and predicted temperatures throughout the IFA-610.2 test are shown in Figure A.3.2. FRAPCON-3 tracked the measured temperatures very closely (+/- 10°C) for this test. For information, this comparison is plotted vs. rod-average burnup in Figure A.3.3. The fuel picked up about 3.5 MWd/kgM during the test.

The calculated center temperature is shown vs. time-in-test for IFA-610.4 in Figure A.3.4. The code continued to track the measured center temperature closely in this follow-on test < 20°C overprediction). During the first half of each test, the rod internal overpressure was 150 to 200 bar, with little apparent effect upon fuel temperatures.

Table A.3.1. IFA 610 Mother Rod

Pellet OD:	8.193 mm
Pellet ID:	0.000 mm
Pellet Ht:	11.770 mm
Dish diameter and depth:	4.897, 0.281 mm
RMS Roughness:	0.002 mm est.
Diametral gap:	167 microns
As-Fabricated Density:	94.43%
Resinter Densification:	0.503%
Grain size:	8 microns
Pu Content:	5.95 w/o HM
U-235 Enrichment:	0.229 w/o
Pu isotopes:	0.953, 65.187, 23.215, 7.317, 3.298 (Pu-238, Pu-239, Pu-240, 241, 242) at. %
O/M Ratio:	1.997
Clad Material:	Zr-4 (SR)
Clad OD:	9.50 mm
Clad ID:	8.36 mm
RMS Roughness:	0.001 mm estimated
Stack Length:	3655.9 mm
Lower Plenum Volume:	0.0 mm^3
Total Free Volume:	19.7 cm^3
He Backfill Pressure:	2.6 Mpa
Backfill Temperature:	25°C

Table A.3.2. IFA 610 Daughter Rod

Fuel Rod Diametral Gap:	0.0 mm
Thermocouple well diameter:	2.3 mm
Stack Length (enriched):	400 mm
Total Free Volume:	3 cm^3 est.
He Backfill Pressure:	2.6 Mpa
Backfill Temperature:	25°C
Inlet Temp:	300°C
Outlet Temp:	310°C
Coolant Pressure:	160 bar

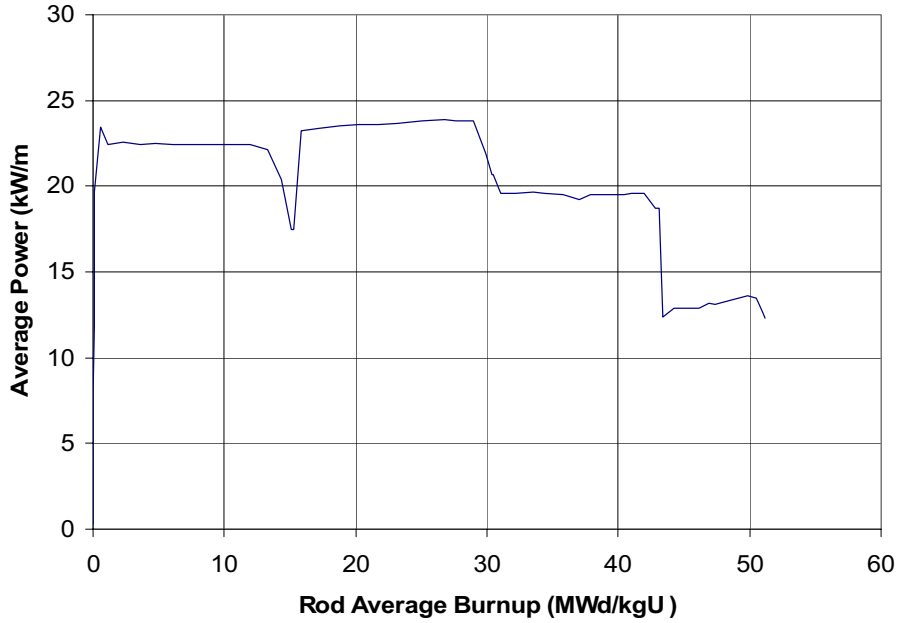

Figure A.3.1. Base Irradiation History of IFA-610.2,4 Rod Segment

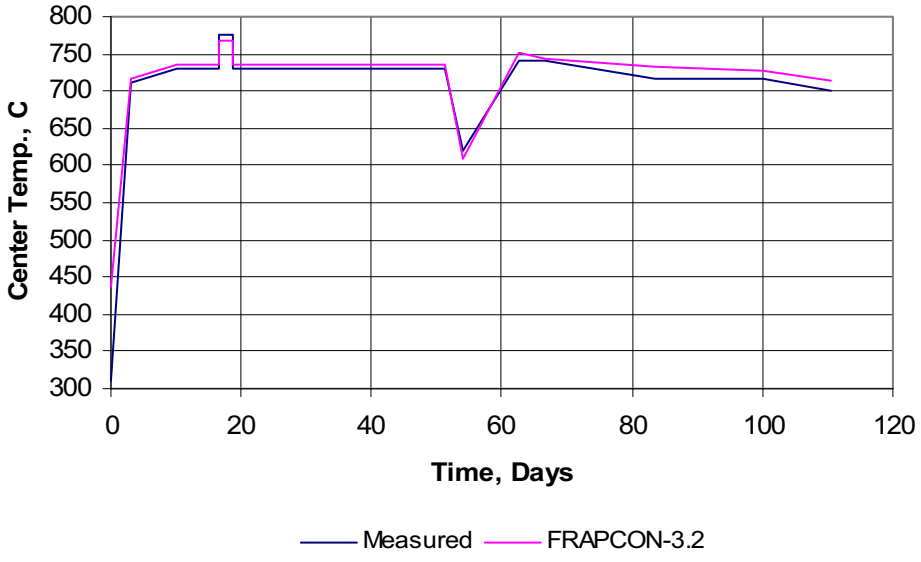

Figure A.3.2. Measured and Calculated Fuel Center Temperatures vs. Time-in-Test for IFA-610.2

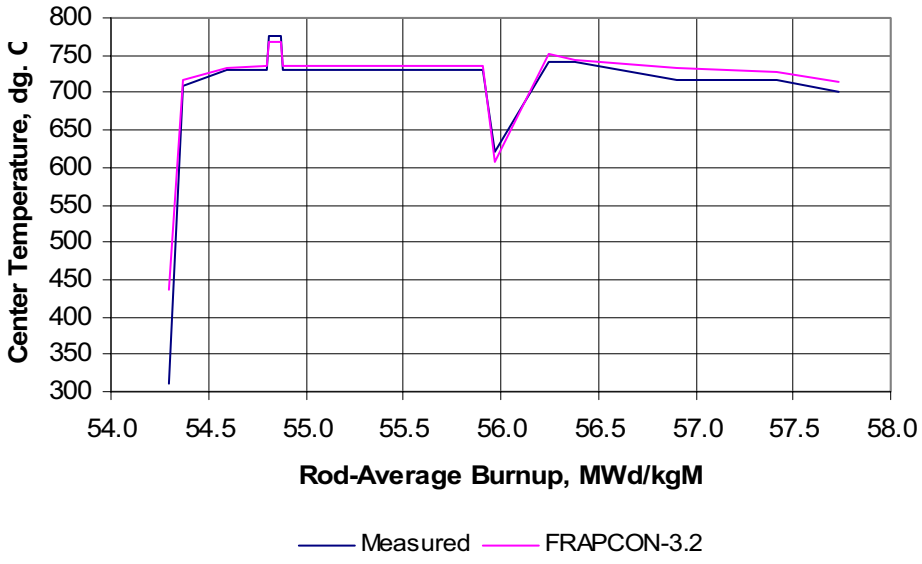

Figure A.3.3. Measured and Calculated Fuel Center Temperatures vs. Rod-Average Burnup for IFA-610.2

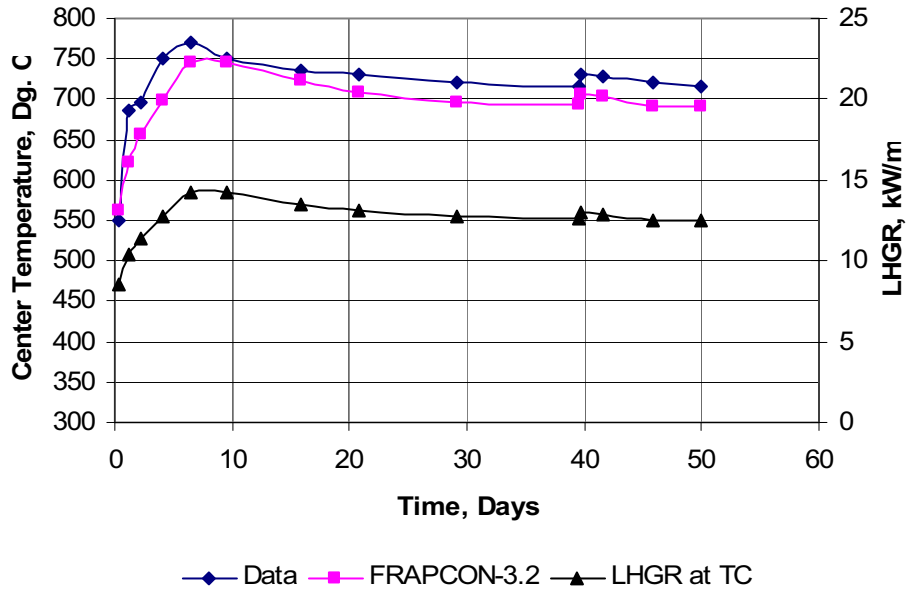

Figure A.3.4. Measured and Calculated Fuel Center Temperatures vs. Time-in Test for IFA-610.4 (first 50 days)

A.4 IFA-648.1 Temperature Data and Calculations

The IFA-648.1 irradiation was simply a burnup extension at low LHGR for two re-fabricated instrumented segments from Gravelines-4 four-cycle PWR MOX rods, one segment each from Rods N12 and P16. The irradiation was carried on at low LHGR under simulated PWR conditions in a pressurized water loop within the Halden reactor. The rods were then power-ramped in the follow-on IFA-629.3 test to investigate FGR and rod elongation behavior.

A.4.1 Test Rod Description and Base Irradiation

The design and operating parameters available for the mother (full-length) rods and daughter rod segments are given in Tables A.4.1 and A.4.2, respectively (Nishi and Lee, 2001). The mother rods were base-irradiated at nominal LHGRs for ~1200 days, as shown in Figure A.4.1 and A.4.2. The final burnup for the Rods N12 and P16 were 57 and 53 MWd/kgM, respectively.

A.4.2 Test Rod Instrumentation and Test Conduct

The two rods were instrumented differently upon refabrication. Rod 1 carried a fuel center thermocouple and a rod elongation sensor. Rod 2 carried a fuel center thermocouple and a pressure transducer. The LHGRs were kept deliberately low to accumulate more burnup without inducing FGR (Claudel and Huet, 2001). The LHGRs at the thermocouple locations are shown in Figures A.4.3 and A.4.4, respectively. Note that the LHGRs for Rod 1 are slightly higher than those for Rod 2. The rod-average LHGRs were about 10% higher than those shown in the figures.

A.4.3 Code-to-Data Comparisons

The measured and predicted temperatures throughout the IFA-648.1 irradiation are shown for Rods 1 and 2 in Figures A.4.5 and A.4.6, respectively. Note that the measured temperatures for Rod 1 are slightly higher than for Rod 2, reflecting the difference in LHGRs. FRAPCON-3 tracked the measured temperatures very closely for Rod 1 (within 15°C) and underpredicted the temperatures for Rod 2 by 20 to 30°C).

For information, the measured temperatures for the two rods are plotted vs. rod-average burnup in Figures A.4.7 and A.4.8. The segments accumulated an additional ~7 MWd/kgM burnup during the IFA-648.1 irradiation.

Table A.4.1. IFA 648.1 Mother Rods (1st value for Rod N12, 2nd value for Rod P16)

Pellet OD:	8.193,8.190 mm
Pellet ID:	0.000 mm
Pellet Ht:	11.936, 11.897 mm
Dish diameter:	4.864,4.972 mm
Dish depth:	0.292, 0.293 mm
RMS Roughness:	0.002 mm estimated
Diametral gap:	167, 170 microns
As-Fabricated Density:	94.72, 94.62%
Resinter Densification:	0.086, 0.385%
Grain size:	8.0, 6.5 microns
Pu Content:	5.93, 4.69 w/o in HM
U-235 Enrichment:	0.231, 0.225 w/o
Pu isotopes:	0.957, 65.211, 23.175, 7.356, 3.302
(Pu-238, Pu-239, Pu-240, 241, 242) at. %	1.047, 65.296, 23.209, 7.004, 3.444
O/M Ratio:	1.996, 2.000
Clad Material:	Zr-4 (SR)
Clad OD:	9.50 mm
Clad ID:	8.36 mm
RMS Roughness:	0.001 mm estimated
Stack Length:	3656.3, 3658.0 mm
Total Free Volume:	19.7, 19.6 cm^3
He Backfill Pressure:	2.6 Mpa
Backfill Temperature:	25°C

Table A.4.2. IFA 648.1 Test Rods (Rods 1 and 2)

Fuel Rod Diametral Gap:	0.0 mm
Thermocouple well diameter:	2.5 mm
Stack Length: (enriched):	453.6, 451.3 mm
Total Free Volume:	2.81, 2.81 cm^3
Instrumentation:	TF/EC, TF/PF
He Backfill Pressure:	2.6 Mpa
Backfill Temperature:	25°C
Coolant Temp:	315 to 325°C
Coolant Pressure:	160 bar

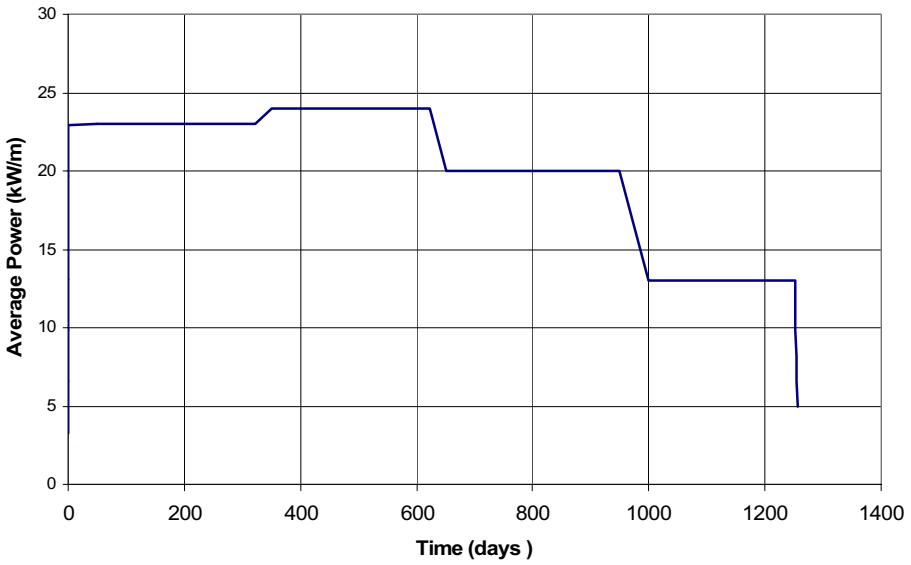

Figure A.4.1. IFA-648.1 (Rod 1) Base Irradiation Power History (Full-Length Rod N12)

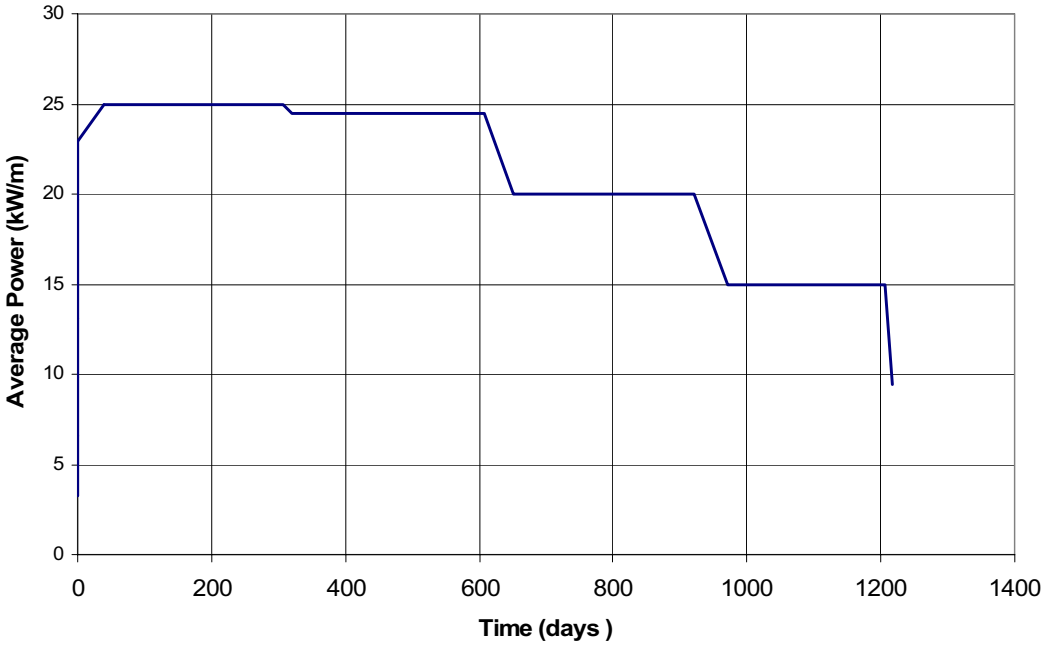

Figure A.4.2. IFA-648.1 (Rod 2) Base Irradiation Power History (Full-length Rod P16)

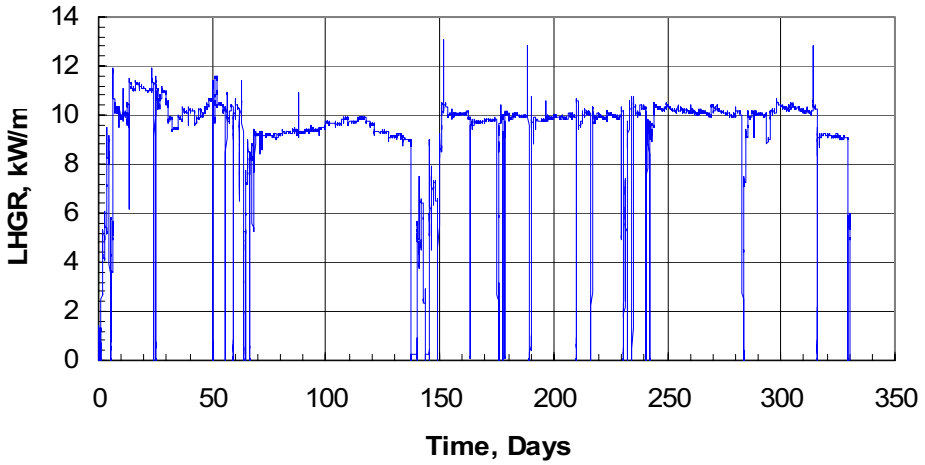

Figure A.4.3. LHGR at thermocouple location vs. time-in-test for Rod 1, IFA-648.1

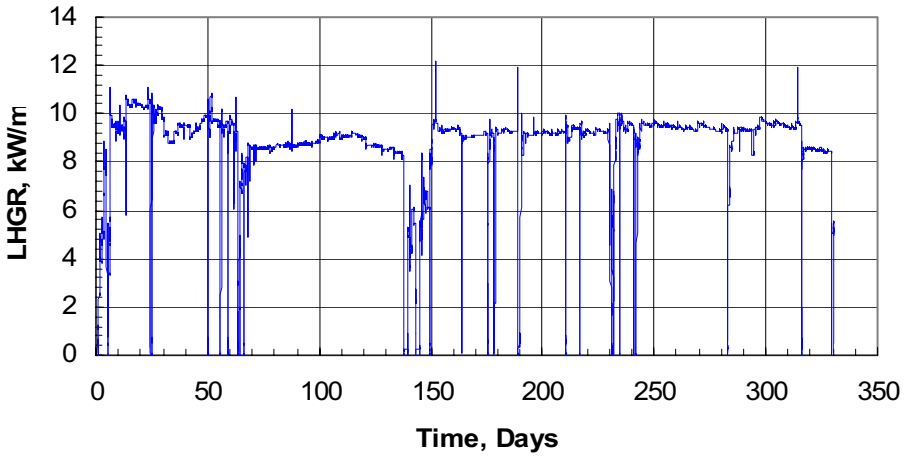

Figure A.4.4. LHGR at thermocouple location vs. time-in-test for Rod 2, IFA-648.1

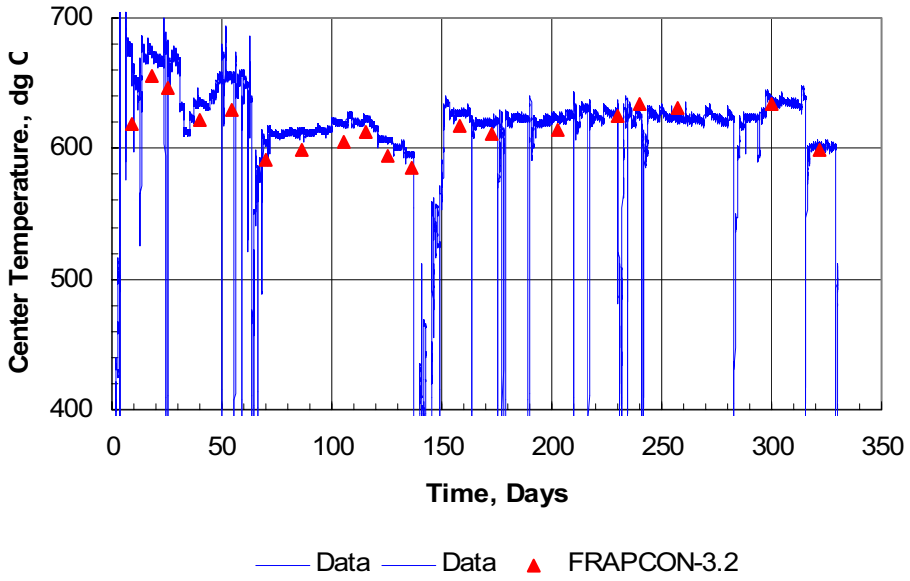

Figure A.4.5. Measured and Calculated Fuel Center Temperatures for Rod 1 of IFA-648.1, vs. Irradiation Time

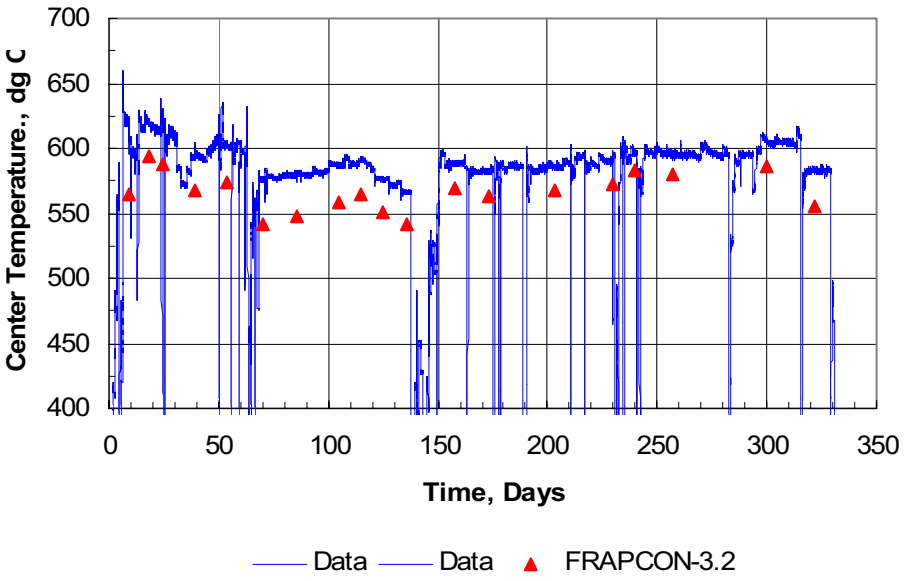

Figure A.4.6. Measured and Calculated Fuel Center Temperatures for Rod 2 of IFA-648.1, vs. Irradiation Time

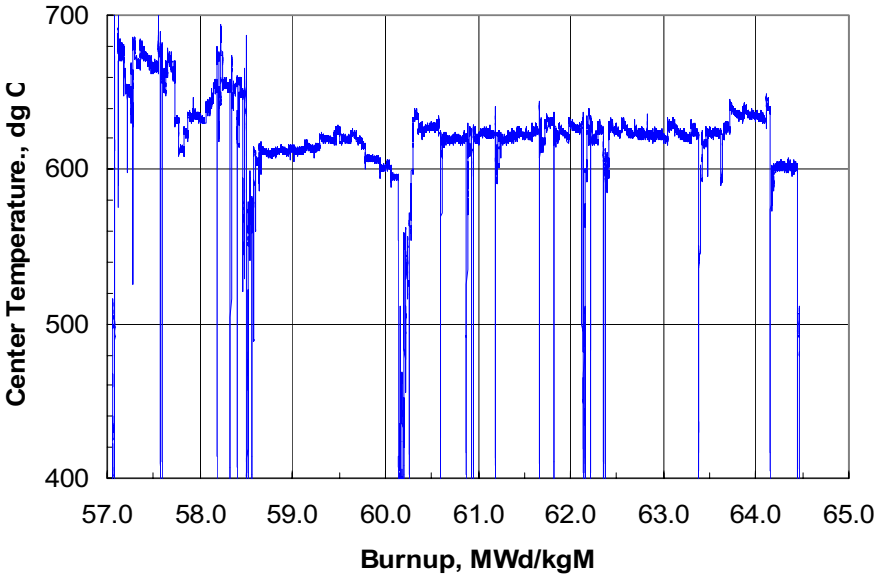

Figure A.4.7. Measured Fuel Center Temperature for Rod 1 vs. Burnup

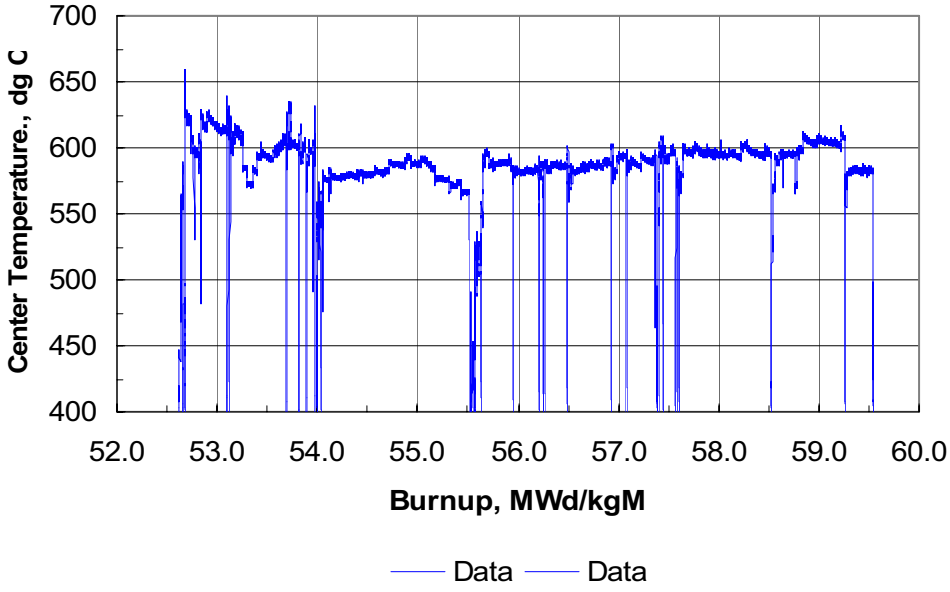

Figure A.4.8. Measured Fuel Center Temperature for Rod 2 vs. Burnup

A.5 IFA-629.3 DATA AND CALCULATIONS

The IFA-629.3 test was carried out in a standard Halden Reactor test position under the normal Halden Reactor coolant conditions (~240°C temperature, 500 psia pressure). The test involved the same rod segments that were irradiated in IFA-648.1 in a pressurized water loop under simulated PWR coolant conditions (320°C temperature, 2350 psia pressure). The rod designations changed: Rod 1 in IFA-648.1 is called Rod 5 in IFA-629.3 and Rod 2 is called Rod 6. Between the two tests, Rod 6 was fitted with a new type of thermocouple not subject to in-reactor decalibration. The LHGRs in IFA-629.3 were much higher (up to 30 kW/m) since FGR at high burnup was being investigated. Data from the first 30 days of the irradiation are compared to FRAPCON-3.2 calculations for fuel center temperatures from both rods, gas pressure/FGR from Rod 6.

A.5.1 Test Rod Description and Base Irradiation

The design and operating parameters available for the mother (full-length) rod and daughter rod segments are given in Tables A.4.1 and A.4.2, respectively. The mother rods were base-irradiated at nominal LHGRs for ~1200 days, as shown in Figures A.4.1 and A.4.2 (Nishi and Lee, 2001). The final burnup for the Rods N12 and P16 were 57 and 53 MWd/kgM, respectively. Following the IFA-648.1 low-power irradiation, these burnups had increased to approximately 64.5 and 59.5 MWd/kgM.

A.5.2 Test Rod Instrumentation and Test Conduct

The two rods were instrumented differently upon refabrication. Rod 5 carried a fuel center thermocouple and a rod elongation sensor. Rod 6 carried a new type of fuel center thermocouple (replacing the one used in IFA-648.1) and a pressure transducer. The LHGRs during the first 30 days of the test were increased slowly in a stepwise fashion to probe for the gas release threshold (Petitprez, 2002). The LHGRs at the thermocouple locations are shown in Figures A.5.1 and A.5.2, respectively.

A.5.3 Code-to-Data Comparisons

The measured and predicted temperatures through the first 30 days of the IFA-629.3 irradiation are shown for Rods 5 and 6 in Figures A.5.3 and A.5.4, respectively. Note that the measured temperatures for Rod 5 are slightly higher than for Rod 6, reflecting the difference in LHGRs. FRAPCON-3 tracked the measured temperatures very closely for Rod 5 (within about 10°C). For Rod 6, the temperatures are over-predicted by 30 to 40°C.

The fact that center temperatures for Rod 2 of IFA-648.1 are underpredicted, whereas the temperatures for Rod 6 of IFA 629.3 are overpredicted, is remarkable since Rod 2 and Rod 6 are just two different designations for the same rod segment. The measured center temperatures show small differences for Rod 1/Rod 5 but a larger difference exists for Rod 2/Rod 6, as shown in Figures A.5.5 and A.5.6, respectively. To make these plots, the data from IFA-648.1 were corrected downward by the difference in coolant temperatures (320°C versus 240°C = 80°C).

The thermocouple was replaced in Rod 2/6 between the two irradiations, and this may have contributed to the difference in measurements. The uncertainty in quoted LHGRs at the thermocouple position between Rod 2 and Rod 6 may also be a contributing factor.

The FGR deduced from pressure measurements on Rod 6 is given in Petitprez (2001) for the first 15 days of the test. These data are plotted in Figure A.5.7 in comparison with the FRAPCON-3.2 calculation of FGR. The agreement is fairly close regarding the onset of FGR during the power ascensions, and the predicted FGR at the end of 15 days is fairly close to the measured value.

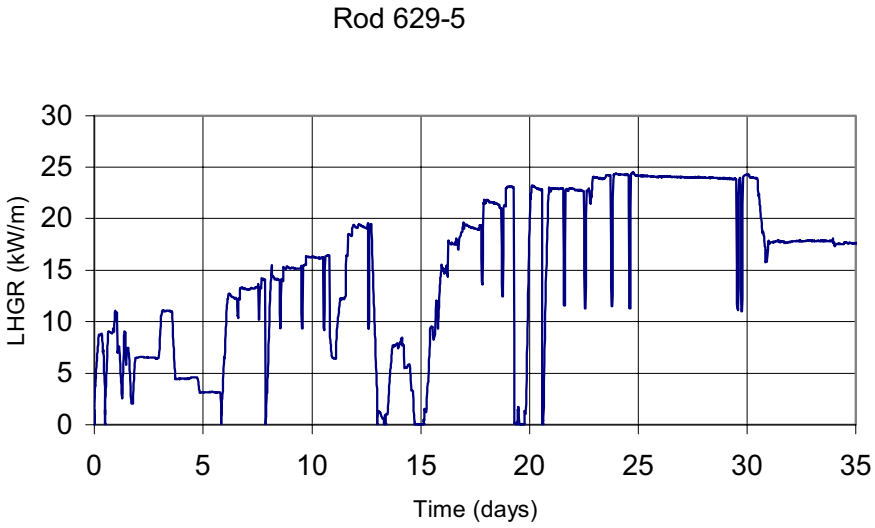

Figure A.5.1. LHGR at the Thermocouple location for Rod 5, IFA-629.3

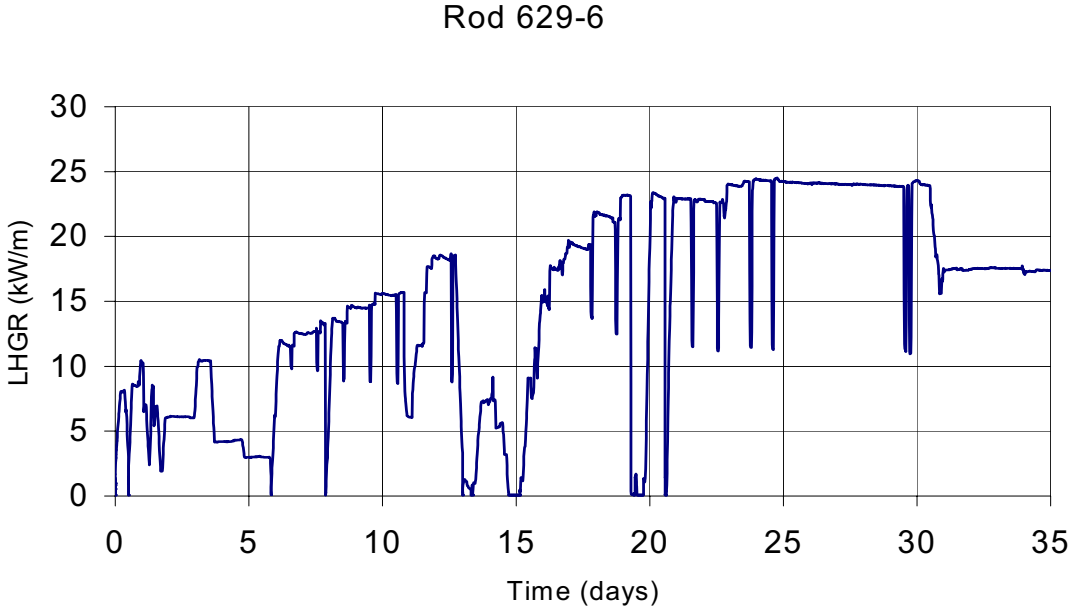

Figure A.5.2. LHGR at the Thermocouple location for Rod 6, IFA-629.3

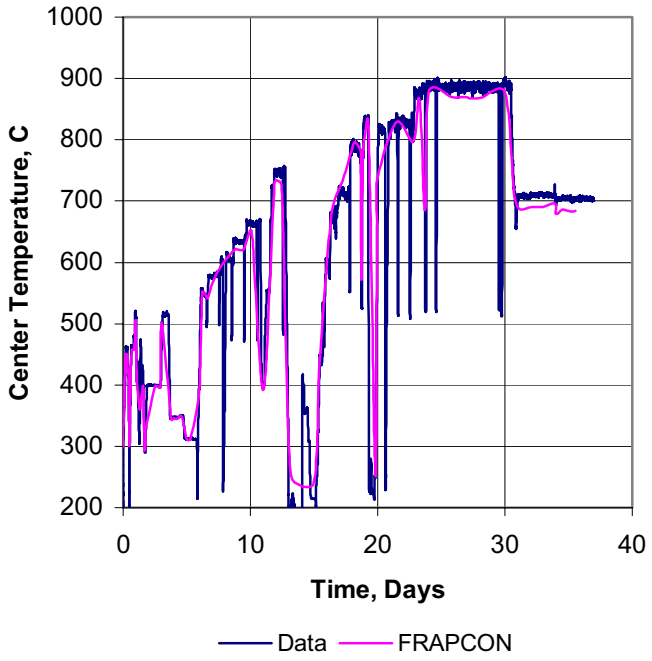

Figure A.5.3. Measured and Predicted Fuel Center Temperatures for Rod 5

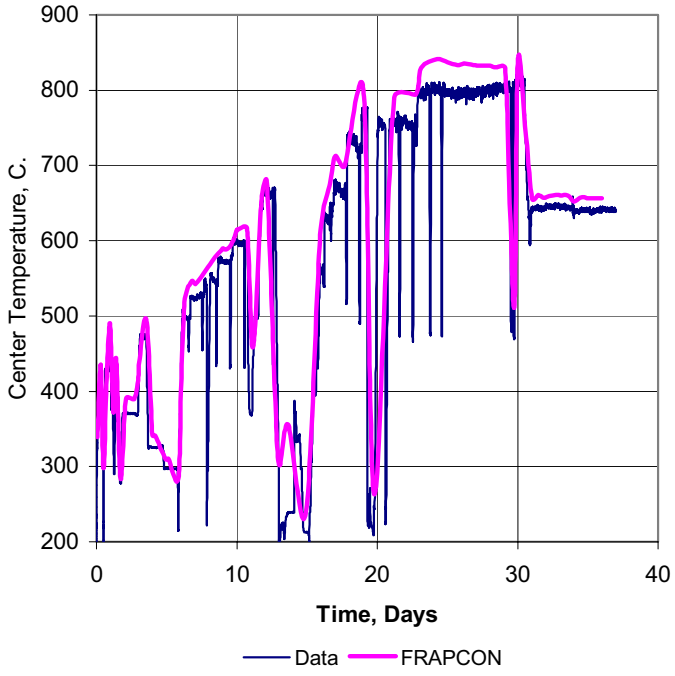

Figure A.5.4. Measured and Predicted Fuel Center Temperatures for Rod 6

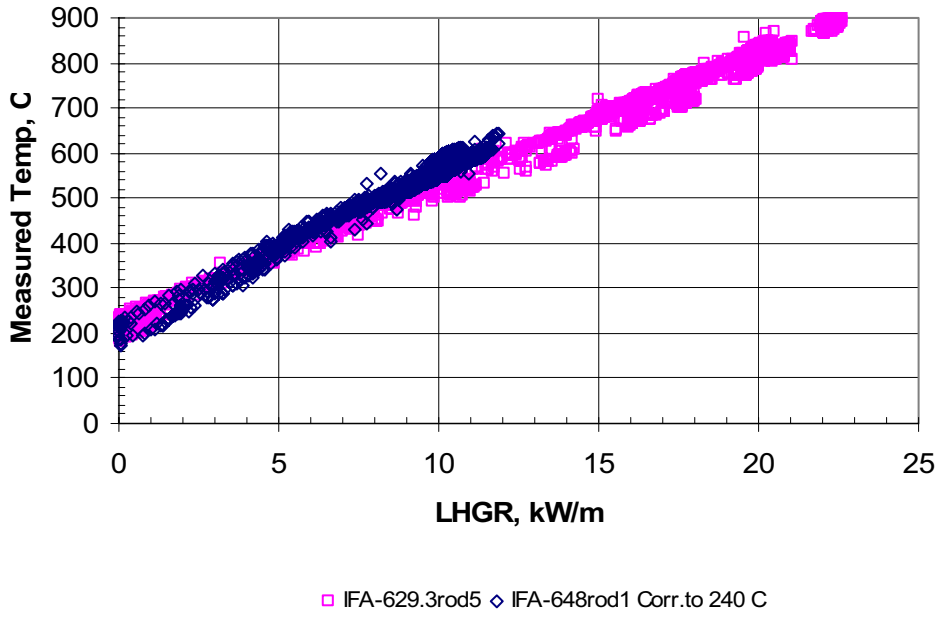

Figure A.5.5. Fuel Center Temperatures for IFA-648 Rod 1 and IFA-629.3 Rod 5

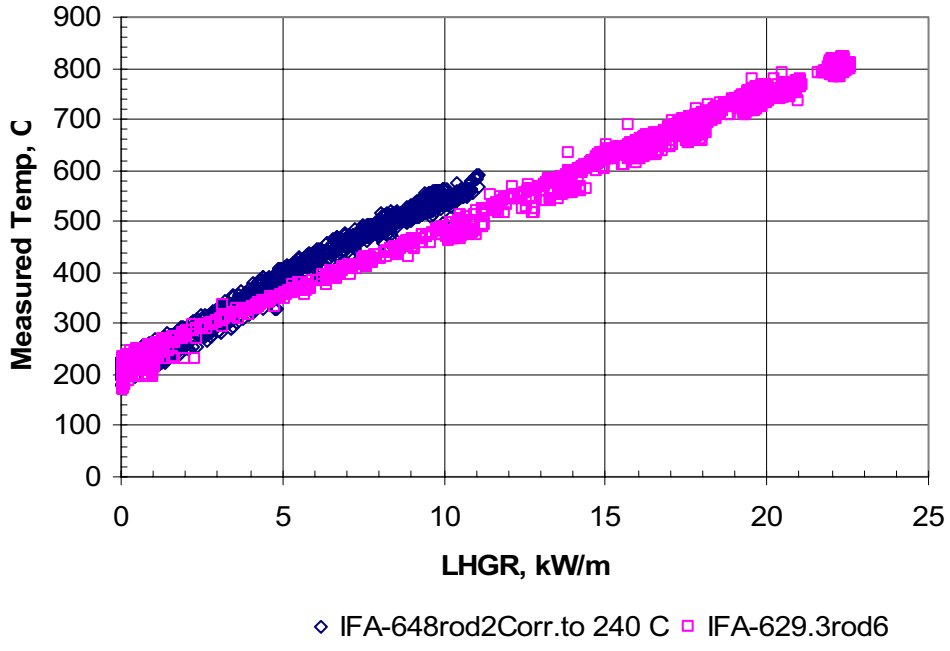

Figure A.5.6. Fuel Center Temperatures for IFA-648 Rod 2 and IFA-629.3 Rod 6

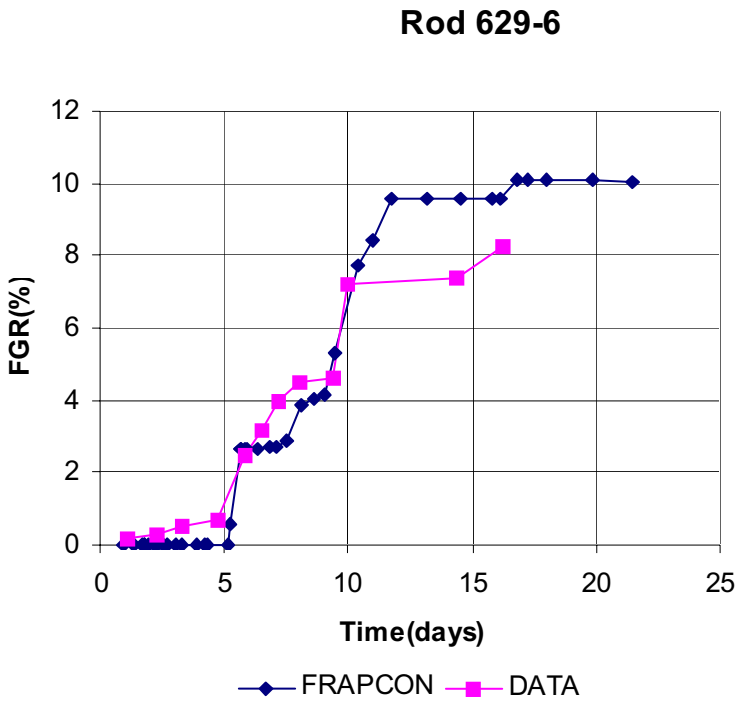

Figure A.5.7. Predicted FGR for IFA-629.3 Rod 6 Compared to Measured FGR in First 15 Days of the Test (Based on Measured Rod Internal Pressure)

A.6 Data and Calculations for the IFA-629.1 Test

Fuel temperature, rod elongation, and FGR data are available from two additional base-irradiated PWR MOX fuel rod segments tested under Halden Reactor coolant conditions in the IFA-629.1 experiment. The base-irradiation burnups for Rods 1 and 2 were 27 and 29 MWd/kgHM, respectively, which were extended to 33 and 40 MWd/kgM, respectively, during the Halden irradiation. The maximum LHGRs were significant (35 to 40 kW/m).

A.6.1 Description of the Test Rods and Base Irradiation

The mother rod for the IFA-629.1 test rods was a full-length PWR MOX rod irradiated for two cycles in the Gravelines-4 PWR. The design and operating parameters available for the mother (full-length) rod and daughter rod segment are given in Tables A.6.1 and A.6.2, respectively (Nishi and Lee, 2001). The mother rod was base-irradiated at (segment-specific) LHGRs ranging from 18 to 25 kW/m.

Table A.6.1. IFA 629.1 Mother Rod J09

(Ranges for pellet dimensions and density reflect ranges given for pellet lots used.)

Pellet OD:	8.192 to 8.195 mm
Pellet ID:	0.000 mm
Pellet Ht:	11.83 to 12.02 mm
Dish diameter:	4.879 to 4.907 mm
Dish depth:	0.295 to 0.306 mm
RMS Roughness:	0.002 mm estimated
Diametral gap:	167 microns nominal
As-Fabricated Density:	95.22 to 95.41%
Resinter Densification:	0.669%
Grain size:	11.8 microns
Pu Content:	5.93w/o in HM
U-235 Enrichment:	0.253 w/o
Pu isotopes:	1.187, 60.744, 24.373, 8.957, 4.74
(Pu-238, Pu-239, Pu-240, 241, 242) at. %	
O/M Ratio:	1.996 estimated
Clad Material:	Zr-4 (SR)
Clad OD:	9.50 mm
Clad ID:	8.36 mm
RMS Roughness:	0.001 mm estimated
Stack Length:	3657 mm estimated
Lower Plenum Volume:	0.0 mm^3
Total Free Volume:	19.7 cm^3 estimated
He Backfill Pressure:	2.6 Mpa
Backfill Temperature:	25°C

Table A.6.2. IFA 629.1 Test Rods (Rods 1 and 2)

Fuel Rod Diametral Gap:	0.0 mm
Thermocouple well diameter:	1.8 mm
Stack Length: (enriched):	380.7, 451.0 mm
Total Free Volume:	2.81, 3.31 cm^3
Instrumentation:	TF/EC, TF/PF
He Backfill Pressure:	2.6 Mpa
Backfill Temperature:	25°C
Coolant Temp:	232°C
Coolant Pressure:	160 bar

A.6.2 Test Rod Instrumentation and Test Conduct

The two rods were instrumented differently upon refabrication. Rod 1 carried a fuel center thermocouple and a rod elongation sensor. Rod 2 carried a fuel center thermocouple and a pressure transducer. The LHGRs during the first 30 days of the test were increased slowly to probe for the gas release threshold (White, 1999). The LHGRs at the thermocouple locations and the rod-average LHGRs are shown in Figures A.6.1 and A.6.2, respectively. Note that (White, 1999) covers only the first 120 days of operation, whereas LHGR and temperature data plots presented here cover the full 180 days of operation.

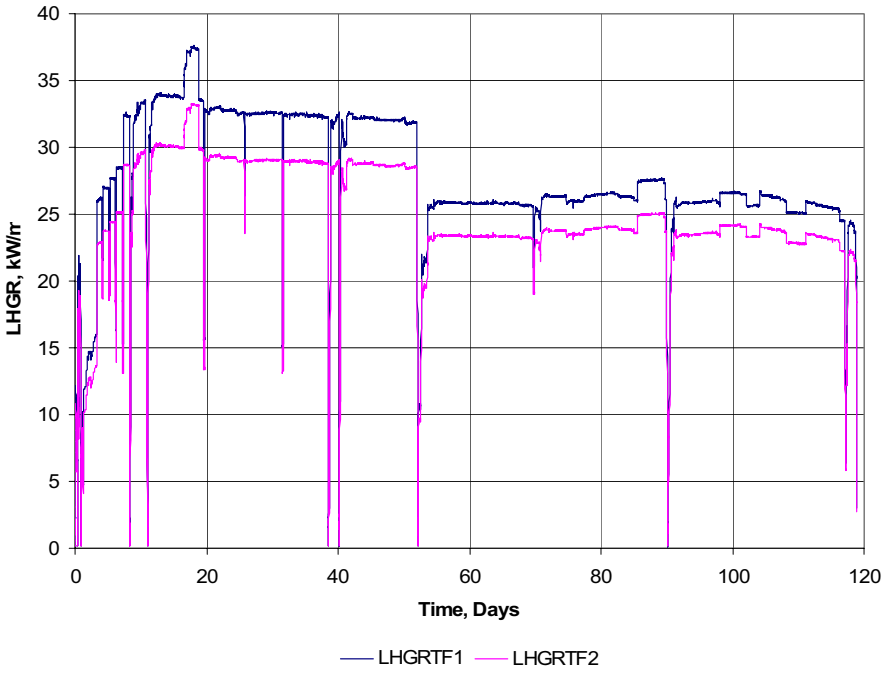

Figure A.6.1. LHGR at the Thermocouple Location for IFA-629.1 Rods and 2

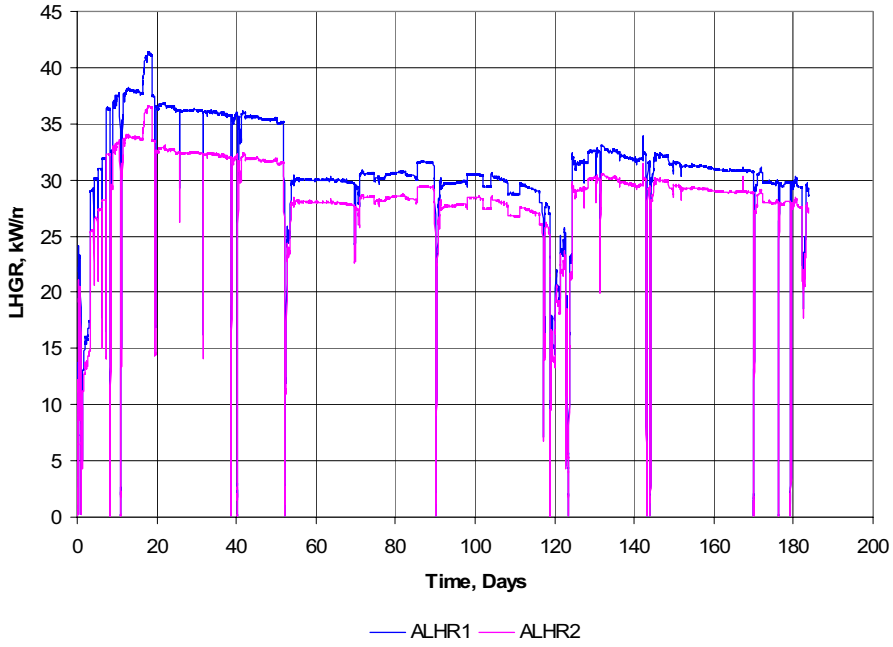

Figure A.6.2. Rod-Average LHGRs for IFa-629.1 Rods and 2

A.6.3 Code-to-Data Comparisons

The measured and predicted temperatures through the first 120 days of the IFA-629.1 irradiation (spanning the published data set) are shown for Rods 5 and 6 in Figures A.6.3 and 6.4, respectively. Note that the measured temperatures for Rod 1 are slightly higher than for Rod 2, reflecting the difference in LHGRs. FRAPCON-3 underpredicts the measured temperatures by 30 to 60°C in the first half of the irradiation but is much closer thereafter. The code predictions appear closer to data for Rod 2 than for Rod 1, but this is mainly a consequence of the lower LHGRs for Rod 2.

The FGR was deduced for Rod 2 by rod puncture and gas analysis (Oberlander et al., 2000), as 21.7%. The predicted value for Rod 2 (at the end of 180-day test) was 13.5%. The calculated FGR is calculated in comparison to the measured rod pressure in Figure A.6.5. It is apparent that the onset of FGR is well predicted, even though the total FGR is somewhat underpredicted in this case.

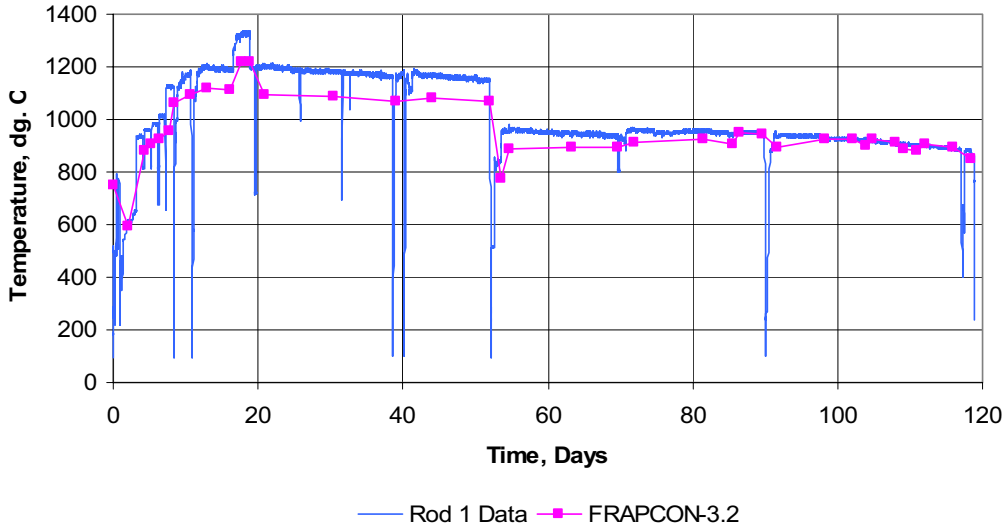

Figure A.6.3. Fuel Temperature Data and Predictions for IFA-629.1, Rod 1

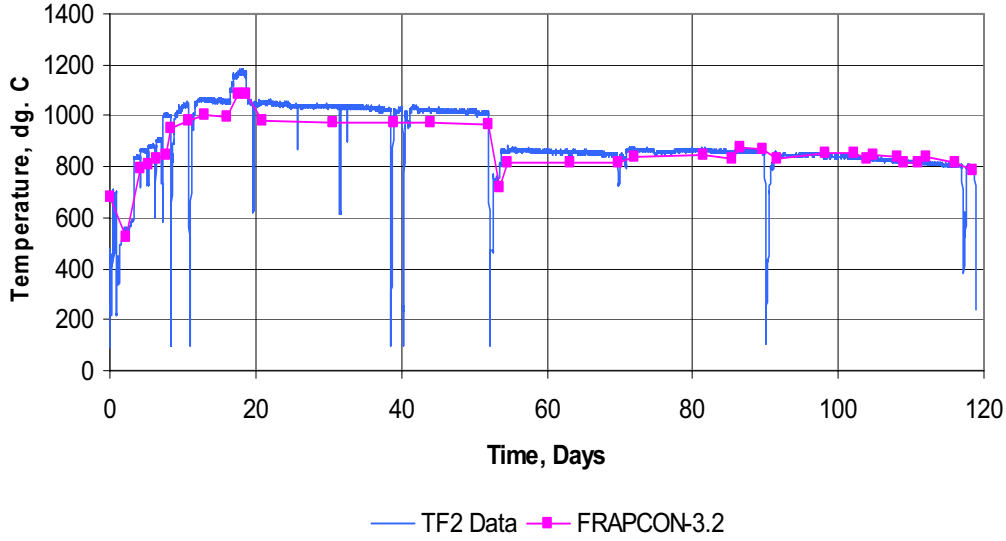

Figure A.6.4. Fuel Temperature Data and Predictions for IFA-629.1, Rod 2

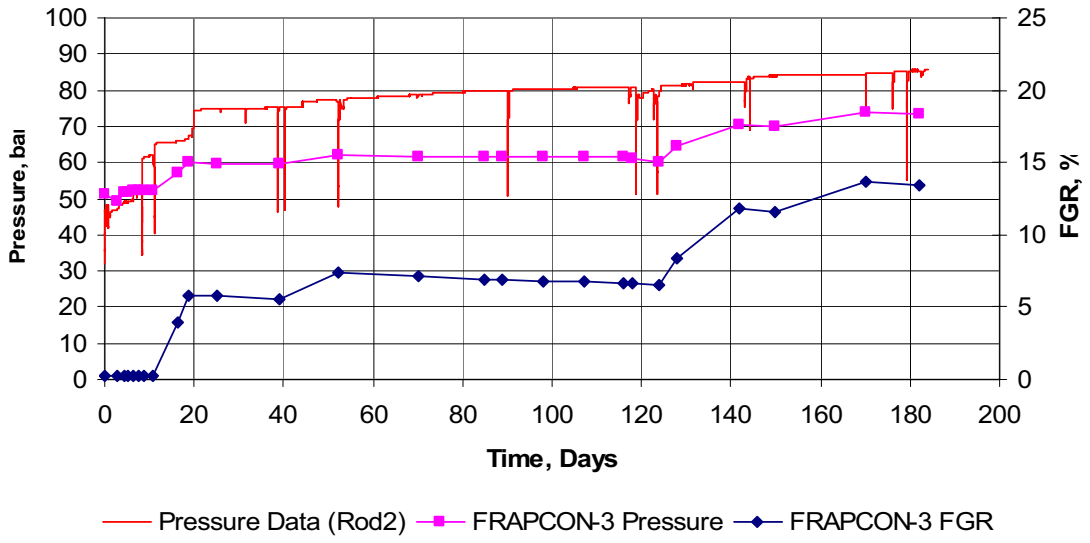

Figure A.6.5. Calculated FGR and Measured/Calculated Rod Pressure vs. time-in-test for IFA-629.1, Rod 2

A.7 Data and Calculations for the IFA-633 Test

Fuel temperature, rod elongation, pellet stack elongation, and FGR data are becoming available from six instrumented rods (three MOX rods and three urania rods) irradiated from BOL under Halden Reactor coolant conditions in the IFA-633 gas flow experiment. Data are available through a burnup of 25 MWd/kg oxide and include a power ramp to achieve fission gas bubble interlinkage (Wright, 2004). The code-data comparisons presented here are from BOL and used to confirm the difference between MOX and urania fuel thermal conductivity.

A.7.1 Description of the Test Rods

The test rods were short but had normal PWR 17 x 17 fuel rod radial dimensions (9.5 mm outer diameter). The rods were heavily instrumented and connected to a gas flow system, which permitted changes between various gas species and measurement of gas release for both short-lived and long-lived isotopes.

The short binderless route (SBR) MOX fuel pellets had a small grain size (7.5 microns) in contrast to the more normal urania pellet grain size (10 microns). Otherwise, the fuel pellets were high-density stable pellets dished on both ends, which is typical of commercial fuel.

A.7.2 Test Rod Instrumentation and Test Conduct

All six rods had fuel centerline thermocouples in the top and bottom of the fuel stack and were connected to rod elongation sensors and to gas flow lines. One urania rod and one MOX rod were fitted with pressure transducers. The remaining two rods of each type had stack elongation sensors. The rod design parameters are further describes in Table A.7.1.

Table A.7.1. IFA 633 Rod Dimensions and Fabrication Parameters

Pellet OD:	8.15 mm
Pellet ID:	0.000 mm (1.8 mm at top/bottom of stack)
Pellet Ht:	12.39 Urania, 12.41 MOX mm
Dish diameter:	6.4 mm
Dish depth:	0.2 mm
Land width:	0.65 mm
RMS Roughness:	0.002 mm estimated
Diametral gap:	210 microns nominal
As-Fabricated Density:	95.4% TD urania 95.4% TD MOX
Resinter Densification:	not given
Grain size:	9.95 microns urania, 7.42 microns MOX
Pu Content:	6.04 wt.% Pu-fissile in depleted U
Enrichment:	7.98 wt.% U-235 in urania rods
Pu isotopes (estimated) (Pu-238, Pu-239, Pu-240, 241, 242)	1.187, 60.744, 24.373, 8.957, 4.74
MOX Fuel Type:	SBR
O/M Ratio:	1.996 estimated for MOX 2.00 est. for urania
Clad Material:	Zr-4 (SR)
Clad OD:	9.50 mm
Clad ID:	8.36 mm
RMS Roughness:	0.001 mm estimated
Stack Length:	450 mm urania, 447 mm MOX
Lower Plenum Volume:	0.0 mm^3
Total Free Volume:	6.0 cm^3 with pressure transducer 5.1 cm^3 for remaining rods.
He Backfill Pressure:	2 bar nominal
Backfill Temperature:	25°C

A.7.3 Code-to-Data Comparisons for Fuel Center Temperature at Beginning of Test

The predicted and measured centerline temperatures as a function of LHGR in the startup ramps for urania and SBR MOX rods are shown in Figures A.7.1 and A.7.2, respectively. The agreement is very close. If the calculated fuel surface temperatures are subtracted from both the measured and calculated centerline temperature values, the resulting estimated temperature rises across the fuel can be used to estimate the relative value of the MOX and urania thermal conductivities. The result is shown in Figure A.7.3. The ratio of MOX conductivity to that of MOX is about 0.92 to 0.94.

Data were also recorded for the effect of exchanging argon gas for helium fill gas. Because the thermal conductivity of argon is much lower than that of helium, the fuel temperatures rise dramatically when argon is exchanged for helium gas. The code-to-data comparison for this effect for a urania rod is shown in Figure A.7.4. The excellent prediction of this dramatic effect indicates the predicted BOL effective gap sizes are very close to true values.

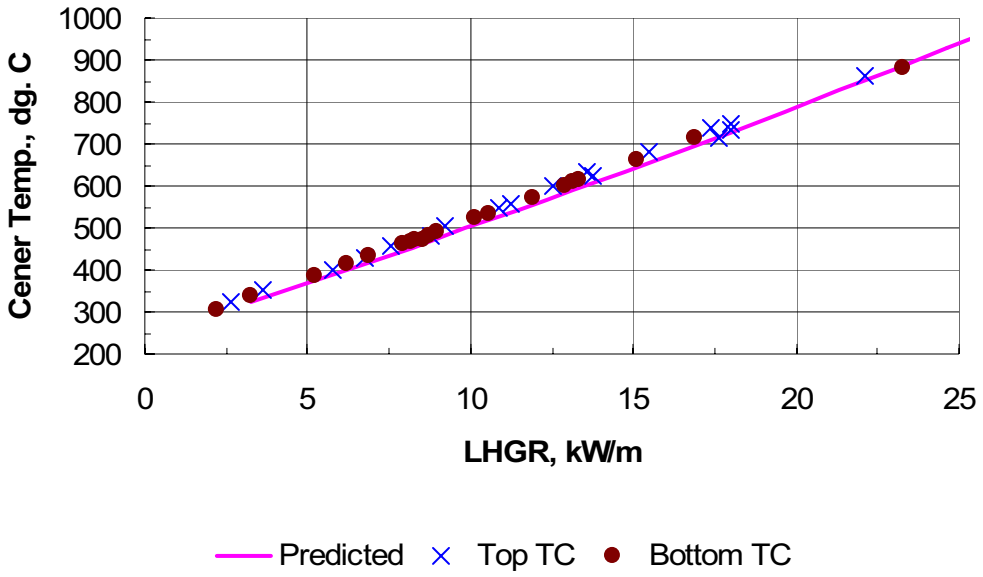

Figure A.7.1. Measured and Predicted BOL Fuel Center Temperatures for IFA-633 Urania Rod with Helium Fill Gas

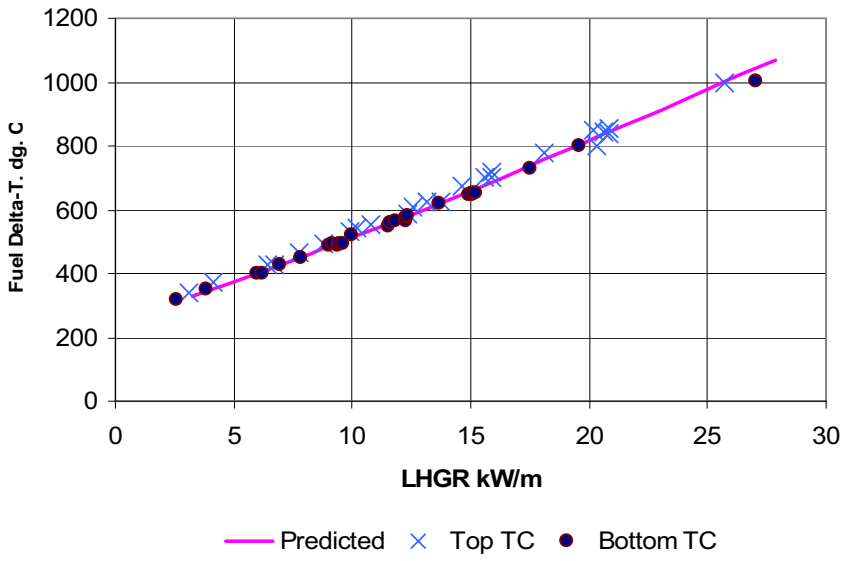

Figure A.7.2. Measured and Predicted BOL Fuel Center Temperature for IFA-633 MOX Rod with Helium Fill Gas

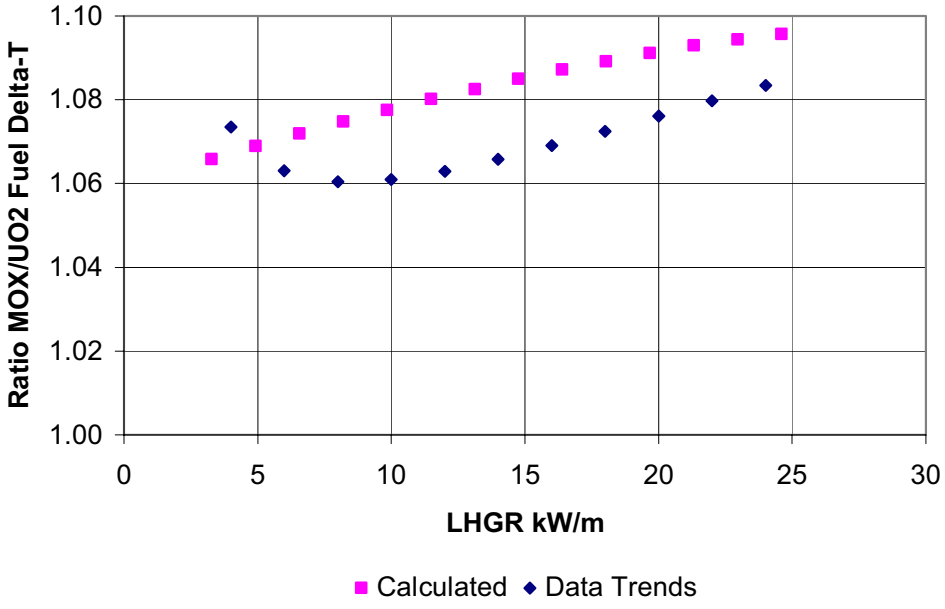

Figure A.7.3. Ratio of Predicted and Measured MOX Fuel Delta-T (Temperature Rise from Pellet Surface to Center) to Urania Fuel Delta-T for IFA-633

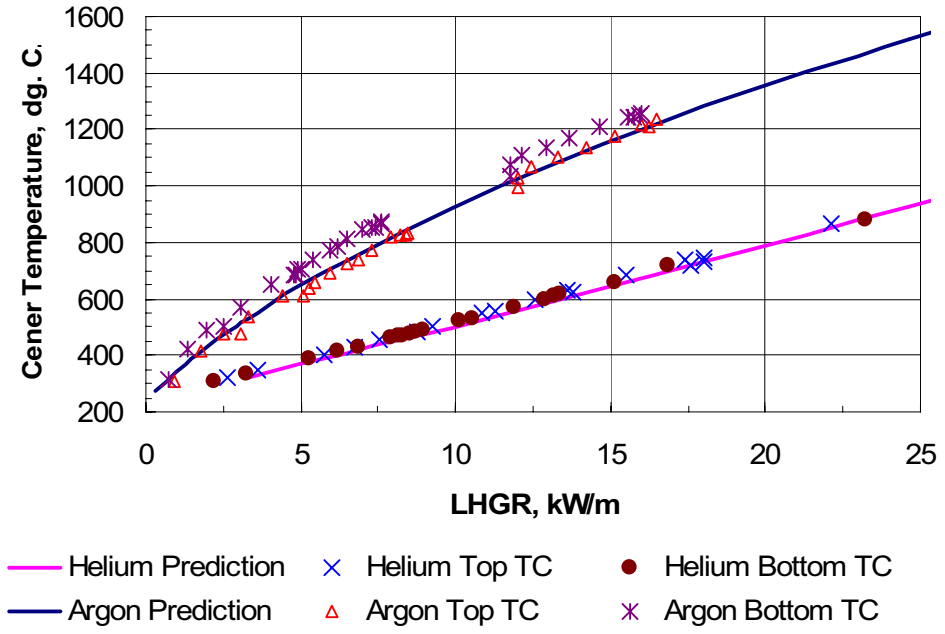

Figure A.7.4. Predicted and Measured Fuel Centerline Temperatures with Argon and Helium Fill Gases for a Urania Rod, IFA-633 Test

A.7.4 Code-to-Data Comparisons for Fuel Temperatures Through-Test to Date

Rod 6 (MOX) also had a pressure transducer, which permitted an estimate of the onset of FGR as a function of temperature. This was assessed during an "interlinkage test" (step-wise power ramp) performed at a rod-average burnup of approximately 20 MWd/kgHM. Measured and predicted fuel temperatures and FGR (estimated from measured rod pressures) are plotted in Figure A.7.5. The corresponding estimated and FRAPCON-calculated peak center temperatures (in solid pellets) are shown in Figure A.7.6. The predicted temperatures are close to measured values until the onset of FGR. Thereafter, the predicted temperatures are greater than the measured values. This overprediction is believed to occur because in this gas flow experiment, there is a large helium-filled volume of interconnected piping open to the rods, and fission gas can diffuse into this volume. The code does not model this volume (i.e., it only models the rod plenum volume) resulting in the code calculating more degradation in gap conductance (due to the higher fraction of low conductivity xenon and krypton gas) and higher fuel temperatures. The important aspect for FRAPCON-3 is that the code does predict onset of significant FGR (>1%) at a peak (solid-pellet) fuel temperature of 1200°C, followed by major FGR (6.2% quoted in the reference) as peak fuel temperatures approach 1400°C.

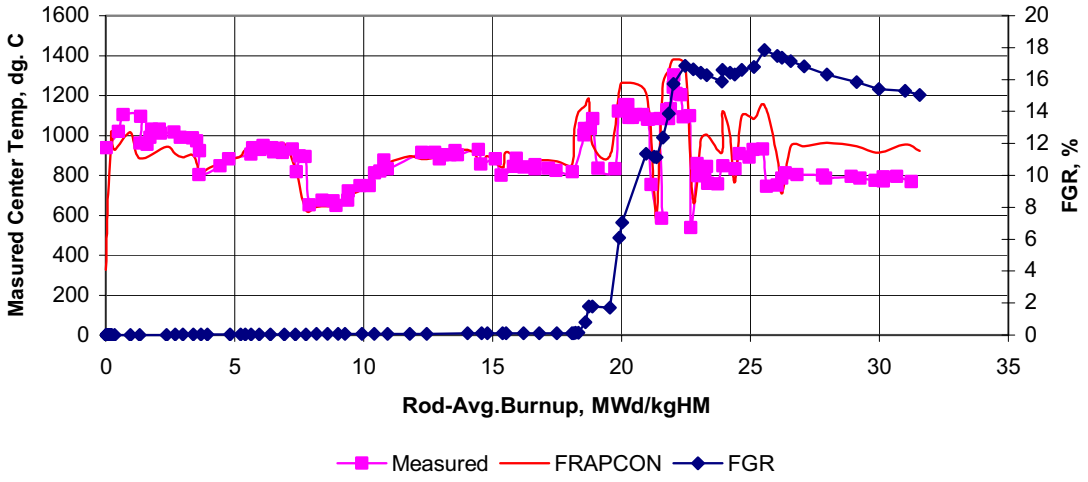

Figure A.7.5. Measured and Predicted (Lower Thermocouple) Fuel Temperatures and Predicted FGR for IFA-633, Rod 6

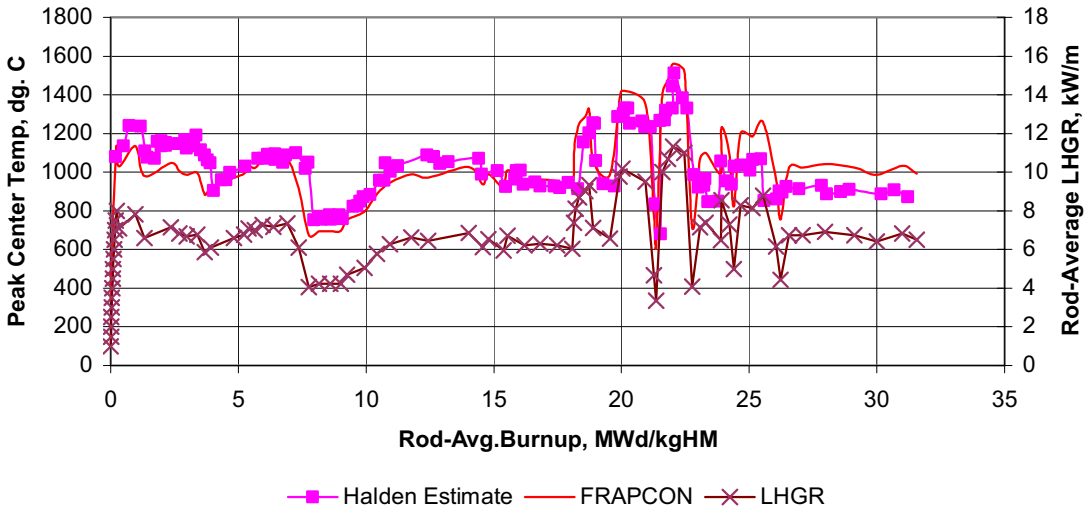

Figure A.7.6. Estimated and Predicted Fuel Peak (Solid Pellet) Center Temperatures for IFA-633, Rod 6

A.8 References

Beguin, S. *The Lift-Off Experiment with MOX Fuel Rod in IFA-610.2; Initial Results*, HWR-603, Halden Reactor Project, Halden, Norway. 1999.

Claudel, J., and F. Huet. *Results from the Burnup Accumulation Test with High Exposure (63 GWd/kg HM) MOX Fuel (IFA-648)*, HWR-651, Halden Reactor Project, Halden, Norway. 2001.

Fujii, H., and J. Claudel. *The Lift-Off Experiments IFA 610.3 (UO_2) and IFA610.4 (MOX): Evaluation of In-Pile Measurement Data*, HWR-650, Halden Reactor Project, Halden, Norway. 2001.

Mertens L., M. Lippens, and J Alvis. *The FIGARO Programme: The Behaviour of Irradiated MOX Fuel Tested in the IFA-606 Experiment, Description of Results and Comparison with COMETHE Calculation*, HPR 349/30 Halden Reactor Project, Halden, Norway. 1998.

Mertens, L., and M. Lippens. *Study of Fission Gas Release on High Burnup MOX Fuel*, ENS TOPFUEL Meeting, May 2001. Stockholm, Sweden. 2001.

Nishi, M., and B.H. Lee. *Summary of Pre-Irradiation Data on Fuel Segments Supplied by EdF/FRAMATOME and Tested in FA-610, 629 and 648*, HWR-664 Halden Reactor Project, Halden, Norway. 2001.

Oberlander, B.C., S. Thoshaug, and M. Espland, *DT PIE of Pre-irradiated and Re-Instrumented MOX Rod after Power Ramp Testing in IFA-629*, IFE/KR/F-2000/149 (Limited Distribution), Institute for Energiteknik, Kjeller Laboratory, Norway. 2000.

Petitprez, B. *Ramp Tests with Two high Burnup MOX Fuel Rods in IFA-629.3*, HWR-714 Halden Reactor Project, Halden, Norway. 2002.

White, R.J. *The Re-Irradiation of MIMAS MOX Fuel in IFA-629.1*, HWR-586 Halden Reactor Project, Halden, Norway. 1999.

Wright, J. *The SBR MOX and UO_2 Comparison Test in Gas Flow Rig IFA-633: Results after Seven Cycles of Irradiation*, HWR-764 Halden Reactor Project, Halden, Norway. 2004.

Appendix B

Summary of Code Changes Since FRAPCON Version 1.0

Appendix B

Summary of Code Changes Since FRAPCON Version 1.0

B.1 Changes Made for FRAPCON-3 v1.1

- Axial array of fast fluence was added to the output
- The input variable 'jdlpr' was set equal to 0 (output all axial nodes) when ntape > 0 (create a FRAPTRAN initialization file)
- The hydrogen concentration in the final summary page of the output was corrected to be the peak node hydrogen concentration
- The variable cladding permanent displacement was added to the FRAPTRAN start tape.

B.2 Changes Made for FRAPCON-3 v1.2

- The excess hydrogen concentration was added to the FRAPTRAN initialization file
- Corrected typographical error in function call statement
- Moved continuation markers from column 1 to column 6 in many places to make the code more compatible with different compilers.

B.3 Changes Made for FRAPCON-3 v1.3

- The volume of the central annulus, if present, was included in the calculation of the rod void volume for the gas pressure calculation
- External changes were made to allow the building of the PC version of FRAPCON.

B.4 Changes Made for FRAPCON-3 v1.3a

- A typographical error in the constant, 'a2', in the Massih fission gas release model was corrected. The new value of a2 is as specified in equation 40 by Forsberg and Massih (1985). The earlier value was in error.

B.5 Changes Made for FRAPCON-3.2

Many changes were made for the release of FRAPCON-3.2. In this section, the changes are divided into five categories: model changes, input changes, output changes, errors fixed, and changes to clean up FORTRAN.

B.5.1 Model Changes

- A new thermal conductivity model is now used in FRAPCON. This model is described in Section 2.0 of this report.

- Mixed oxide modeling capability was added. The changes made to model mixed oxide are described in Section 3.0 of this report.

- The pre- and post-transition values of hydrogen pickup fraction were made the same for boiling-water reactor and pressurized water reactor applications.

- The alternate fission gas release model, ANS54, was modified to calculate gas release based on the current time step radial power and burnup profile. Previously, it had used the beginning of life power and burnup profiles throughout life. (Note: no adjustments were made to the ANS54 gas release model parameters to account for the new thermal conductivity model. In addition, Pacific Northwest National Laboratory (PNNL) has not assessed the impact on that change on ANS54 predictions relative to data).

- Tuning parameters in the Massih fission gas release model were changed to better fit data. This change is due to changes in the new thermal conductivity model. This change is described in Section 4.0 of this report.

- Calculation of fraction gas release in the Massih fission gas release model was made a function of radial burnup profile rather than radial power profile. This change is described in Section 4.0 of this report.

- A four-term approximation, rather than the original three-term approximation, is now used as the integration kernel in the Massih fission gas release model as given by Hermansson and Massih (2002). This change is described in Section 4.0 of this report.

B.5.2 Input Changes

- Input variable 'time' was changed to 'ProblemTime' to avoid issues with some compilers for which ‘time’ is a reserved variable.

- The default value of ‘ngasr’ was changed to 45. This is the value PNNL recommends for the number of radial fuel nodes used in the gas release calculation.

- The input variable 'afsw' was removed. This variable was not described in the input instructions.

- The input variable 'ivoid' was removed. This variable was not described in the input instructions.

- The input variable 'linkt' was removed. This variable was not described in the input instructions.

- The input variable 'rhoh2o' was removed. This variable was not described in the input instructions.

- The input variable 'cldwkd' was removed. This variable was not described in the input instructions.

- The input variable 'grnsiz' was removed. This variable was not described in the input instructions.
- The input variable 'im93wc' and associated function emftc.f was removed. This function was not being used in the code.

B.5.3 Output Changes

- Write statements were changed to reflect the presence of a dish or a central hole.
- A misspelling in the plotter was corrected.
- The plotter was corrected to plot the bulk coolant temperature rather than the inlet temperature for each node.
- Error warnings were made to print to the output file, not a separate file.
- The output of 'fuel thermal conductivity degradation factor' is removed if FRACAS-1 is used. If FRACAS-2 is used, this value is output as 'cracked fuel thermal conductivity degradation factor.'
- Negative values calculated for uniform strain are changed to 0.0 and the user is warned.
- The problem with output value of relocation in microns not being the same as the output value of relocation in mils was corrected.
- A statement was added that the clad-coolant film coefficient includes the effect of the crud layer.
- The text in page headers was changed to reflect the current version of FRAPCON-3.
- Interface pressure output in peak node summary had been calculated before creep occurred. It was changed to be calculated after creep was calculated.
- In the plotter, one set of data is labeled “Fuel Surface Hoop Strain” but the values are for fuel surface axial strain. The label was changed to “Fuel Surface Axial Strain.”
- A rod average burnup selection was added under the 'data' tab in the plotter.
- The output of the 0th time step in the plotting routine was removed.
- A mechanical gap selection was added to '1D data' tab in the plotter.
- A Fission Gas Release was added to the list of variables that can be plotted in the ‘Data’ tab of the plotter.
- The variable, Yield Stress, was removed from the plotter. This variable is always 0.0.
- A relocation to initialization file for FRAPTRAN was added.

B.5.4 Errors Fixed

- Correctly calculate the initial cold void volume in rods with a central hole.
- Correctly calculate the fuel volume for dished pellets with a central hole.
- Correctly calculate the thermal expansion for annular pellets.
- Correct error in subroutine cmlimit under the calculation of uniform strain.
- Use the correct conversion factor in fudens.f to convert from MWs/kgU to MWd/kgU.
- Use the variable 'gadolin' correctly in calculating fuel enthalpy.
- The input variable, 'enrich', is in atom%. Use this variable in the appropriate manner in calculating the radial power profile.
- Use consistent value of 10.96 g/cc for the theoretical density of urania (UO_2) throughout the code.

B.5.5 Changes to clean up FORTRAN

- The dynamic dimensioning was completely removed, and the a-array was replaced by variables that make it easier to follow what the code is doing.
- The input variable, 'iplant' is used as the universal signal for plant type.
- The following subroutines that are never called were removed: fluxd.f, fluxdp.f, radar.f, and voidp.f.
- In turbin.f, only one call per ring to turbnp.f is needed to initialize atom concentrations.
- The variables drdt, dkdt, and cdkdt were removed. These variable store the uncertainty from models that are not being used in FRAPCON-3.
- 'icm' was made the universal index for cladding type (icm=2 - Zircaloy-2, icm=4 - Zircaloy-4), and the variables ‘iaaha’ and ‘iah’were removed.
- Default values were explicitly given to all variables that are not required input.

B.6 Changes made for FRAPCON-3.3

Many changes were made for the release of FRAPCON-3.2. In this section the changes are divided into five categories: model changes, input changes, output changes, errors fixed, and changes to clean up FORTRAN.

B.6.1 Model Changes

- The capability to run a case with no gas release up to a certain time step was added in order to model re-fabricated rods.

- The hydrogen solubility model was changed to the Kearns' hydrogen solubility to be more consistent with FRAPTRAN and available data.

- Oxidation and hydrogen pickup properties were added for ZIRLO™ and M5™. These changes are described in Sections 5.1 and 5.2 of this report, respectively.

- The cladding stress calculation was modified to account for the clad thinning that occurs as the cladding oxidizes. This change is described in Section 5.5 of this report.

- The code was changed to allow the user to set the cladding surface temperature axial profile for each time step. This option was added to allow the calculation of fuel rod behavior under spent fuel storage conditions. This change is described in Section 6.2 of this report.

- The burnup dependence for fuel melting temperature was changed from a reduction of 3.2 K/GWd/tHM to 0.5 K/GWd/tHM. This change is described in Section 3.7 of this report.

B.6.2 Input Changes

- The default value of fuel sintering temperature was changed to be the same value in regardless of whether SI or British input units are selected.

- If the same value is input for consecutive values of 'ProblemTime,' the code will stop and inform the user to fix the input.

- New warning statements have been added so the code stops and informs the user what line of input has a problem rather than crashing.

- The input of the axial power profiles was changed so they do not need to be normalized to an average value of 1.0. The code will automatically normalize the input axial power profile to a value of 1.0. This normalization procedure will not be applied to cases where the chopped cosine distribution is used.

- The check that ensured the maximum value of 'qf' was not less than 1.0, and the warning if the maximum value of 'qf' was 1.0, were removed now that the code automatically normalizes the input power profiles.

- The fuel grain size was re-added as an input value. The default grain size (effective diameter) is 10 microns.

- The ICM variable has the value 5 for M5™ cladding and 6 for ZIRLO™.

B.6.3 Output Changes

- When the input file is in SI units, the output of pitch was in meters and labeled in cm. The output was changed to cm to match the label.

- Changes were made to the page header to better track the current version.

- In SI units, the output of gap and oxide thickness were not being shown with enough detail. The output was changed to print out in microns with three digits before the decimal and one digit after the decimal.

- Some cosmetic glitches in the printout were corrected.

- The code was changed to output total hydrogen rather than excess hydrogen to the FRAPTRAN initialization file.

- The cladding fast neutron fluence for each axial node was added to the FRAPTRAN initialization file.

- The oxide surface temperature was added as an option in the plotter.

- The total hydrogen concentration was added as an option in the plotter.

- The cladding and fuel radii in the output file were changed to be consistent with the fuel and cladding radii elsewhere in the output file.

- The gas release value in the peak axial node summary table of the output file was specified as the rod average gas release.

- In the plotter, the value labeled "average power" plotted peak power if the chopped cosine axial power shape was used. This error was corrected so this item plots average power for all cases.

B.6.4 Errors Fixed

- A typographical error in the second call to print2.f was corrected.

- Changes were made to make the evaluation model options work correctly. (Note: PNNL has not evaluated the evaluation models and does not recommend using these options).

- Several typographical errors in gspres.f were corrected.

- The indexes on several variables used to calculate temperature and power were corrected.

- The alternate fission gas release mode, ANS5.4, had been excluding the thermal release from its calculation of gas release because of a typographical error. This error was corrected. (Note: no adjustments have been made to the ANS5.4 gas release model parameters to account for the new thermal conductivity model. In addition, PNNL has not assessed the impact on that change on ANS5.4 predictions relative to data).

- An error in the calculation of the plenum temperature was corrected.

- The initial cladding dimensions are written to the FRAPTRAN initialization file rather than to the dimensions that have been reduced due to cladding oxidation.

- An error was corrected where the calculation of cladding creep used the value of flux from the top axial node for every axial node. The code now uses the value of flux that corresponds with each axial node.

B.6.5 Changes to Clean Up FORTRAN

- The dimension statements in tapegn.f were changed to be consistent with the other dimension statements.

- The arrays 'porosnew,' 'densp, 'densf,' 'dpw,' and 'dpwpp' were explicitly initialized.

- The code was changed to be compliant with the standards of FORTRAN 90. This will ensure that the code can be compiled on any compiler that complies with FORTRAN 90. This change is described in Section 6.3 of this report.

B.7 References

Forsberg, K. and A.R. Massih, "Fission Theory of Fission Gas Migration in Irradiated Nuclear Fuel UO_2," *Journal of Nuclear Materials*, vol. 135, pp. 140-148. 1985.

Hermansson, P., and A.R. Massih, "An Effective Method for Calculation of Diffusive Flow in Spherical Grains," *Journal of Nuclear Materials, vol. 304*, pp. 204-211. 2002.

Appendix C

Input Instructions for FRAPCON-3.3

Contents

Appendix C

Input Instructions for FRAPCON-3.3

C.1 Input Structure

The NAMELIST input is divided into four sections: Case control integers (in $FRPCN), case design and operation descriptors (real and integer variables) located in ($FRPCON), evaluation model options (in $EMFPCN), and plutonium isotopic distributions (in $FRPMOX). The variables in the first group must be separated by commas and placed between the statement $FRPCN and $END. Similarly, the variables in the second, third, and fourth groups must be placed between $FRPCON and $END, between $EMFPCN and $END, and between $FRPMOX and $END, respectively.

Before the NAMELIST input, the following lines must be included in the input file

FILE05='nullfile', STATUS='UNKNOWN', FORM='FORMATTED',

CARRIAGE CONTROL='NONE'

This line sets up a file called “nullfile,” which is needed by FRAPCON-3.3.

FILE06=’file.out', STATUS='UNKNOWN', CARRIAGE CONTROL='LIST.'

This line specifies the name of the output file. In this case, the output file would be called “file.out.”

FILE66='file.plot', STATUS='UNKNOWN', FORM='FORMATTED',
CARRIAGE CONTROL='LIST.'

This line is needed if a plot output file is being created. (See definition of variable NPLOT in the table below.) In this case, the plot file would be called “file.plot.”

The above three lines should not exceed 72 spaces, and if they do, continue on the next line with no continuation symbols needed.

The line below, which is proceeded by the character “/,” tells the code that the lines specifying files are complete.

/***

The line immediately after this line is reserved for the case description that will be displayed in the page headers in the output. Up to 72 characters can be inserted here to describe the case.

After this line, the NAMELIST input can be entered. In the section above the NAMELIST input, any line with a "*" in column 1 is considered a comment and will not be read by the code. An example case input is given in Section C.2.

C.2 Input Variables Specifying Rod Design

The following tables describe the input variables to FRAPCON-3.3. Unless otherwise noted in the Limitations/Default value column, the variables should be placed in the $frpcon data input block.

C.2.1 Rod Size

Variable Name (type)	Description	Units British/SI	Limitations/Default Value
dco (R)	Cladding outer diameter	in./m	Required input
thkcld (R)	Cladding wall thickness	in./m	Required input
thkgap (R)	Pellet-cladding as-fabricated radial gap thickness	in./m	Required input
totl (R)	The total (active) fuel column length.	ft/m	Required input
cpl (R)	Cold plenum length	in./m	Required input
			(R) = real, (I) = integer

C.2.2 Spring Dimensions

Variable Name (type)	Description	Units British/SI	Limitations/Default Value
dspg (R)	Outer diameter of plenum spring	in./m	Required input (*dgpg* should be less than the clad inner diameter)
dspgw (R)	Diameter of the plenum spring wire	in./m	Required input
vs (R)	Number of turns in the plenum spring	Dimensionless	Required input
			(R) = real, (I) = integer

C.3 Input Variables Specifying Pellet Fabrication

C.3.1 Pellet Shape

Variable Name (type)	Description	Units British/SI	Limitations/Default Value
hplt (R)	Height (length) of each pellet	in./m	Required input
rc (R)	Radius of inner pellet	in./m	Default = 0.0
hdish (R)	Height (depth) of pellet dish, assumed to be a spherical indentation.	in./m	Default = 0.0
dishsd (R)	Width of pellet end-dish shoulder (outer radius of fuel pellet minus radius of dish)	in./m	Default = 0.0
			(R) = real, (I) = integer

C.3.2 Pellet Isotopics

Variable Name (type)	Description	Units British/SI	Limitations/Default Value
enrch (R)	Fuel pellet U-235 enrichment	Atom % U-235 in total U	Required input
imox (I)	Index for modeling MOX: 0 = urania (UO_2) fuel >0 = mixed oxide fuel 1 = use Duriez/Ronchi/NFI l thermal conductivity correlation 2 = use Halden thermal conductivity correlation (if *imox*>0, must include *comp* and namelist $FRPMOX)	Dimensionless	Default = 0
comp (R)	Weight percent of plutonia (PuO_2) in fuel (Must specify if *imox*>0)	wt.%	Default = 0.0
enrpu39 (R)	Fuel pellet Pu-239 content	Atom % Pu-239 in total Pu	Default = 0.0 (namelist frpmox)
enrpu40 (R)	Fuel pellet Pu-240 content	Atom % Pu-240 in total Pu	Default = 0.0 (namelist frpmox)
enrpu41 (R)	Fuel pellet Pu-241 content	Atom % Pu-241 in total Pu	Default = 0.0 (namelist frpmox)

Variable Name (type)	Description	Units British/SI	Limitations/Default Value
enrpu42 (R)	Fuel pellet Pu-242 content	Atom % Pu-242 in total Pu	Default = 0.0 (namelist frpmox)
fotmtl (R)	Oxygen-to-metal atomic ratio in the oxide fuel pellet	Dimensionless	Default = 2.0 (If MOX fuel is selected, *fotmtl* should be less than 2.0)
gadoln (R)	Weight fraction of gadolinia (Gd_2O_3) in urania-gadolinia fuel pellets	Dimensionless	Default = 0.0
ppmh2o (R)	Parts per million by weight of moisture in the as-fabricated pellets	ppm	Default = 0.0
ppmn2 (R)	Parts per million by weight of nitrogen in the as-fabricated pellets	ppm	Default = 0.0
			(R) = real, (I) = integer

C.3.3 Pellet Fabrication

Variable Name (type)	Description	Units British/SI	Limitations/Default Value
den (R)	As-fabricated apparent fuel density	% of theoretical density	Required input (theoretical density taken as 10.96 g/cc)
deng (R)	Open porosity fraction for pellets	% of theoretical density	Default = 0.0
roughf (R)	The fuel pellet surface arithmetic mean roughness, peak-to-average	in./m	Required input
rsntr (R)	The increase in pellet density expected during in-reactor operation (determined from a standard re-sintering test as per NUREG-0085 and regulatory Guide 1.126)	kg/m^3	Required input
tsint (R)	Temperature at which pellets were sintered	°F/K	Default = 2911 °F
			(R) = real, (I) = integer

C.4 Input Variables Specifying Cladding Fabrication

Variable Name (type)	Description	Units British/SI	Limitations/Default Value
icm (I)	Cladding type indicator: 2 = Zircaloy 2 4 = Zircaloy 4 5 = M5™ 6 = ZIRLO™	Dimensionless	Required input
cldwks (R)	Cold-work of the cladding (fractional reduction in cross-section area due to processing). PNNL recommends 0.5 for stress relief annealed cladding and 0.0 for fully recrystallized cladding.	Dimensionless	Default = 0.2
roughc (R)	The cladding surface arithmetic mean roughness, peak-to-average	in./m	Required input
catexf (R)	Cladding texture factor; defined as the fraction of cladding cells with basal poles parallel to the longitudinal axis of the cladding tube	Dimensionless	Default = 0.05
chorg (R)	As-fabricated hydrogen in cladding	ppm wt.	Default = 10.0
			(R) = real, (I) = integer

C.5 Input Variables Specifying Rod Fill Conditions

Variable Name (type)	Description	Units British/SI	Limitations/Default Value
Fgpav (R)	Initial fill gas pressure (taken to be at room temperature)	psia/Pa	Required input
Idxgas (I)	Initial fill gas type indictator: 1 = helium 2 = air 3 = nitrogen 4 = fission gas 5 = argon 6 = user-specified mix, using the *amfxx* variables *amfair* etc.	Dimensionless	Default = 1
amfair (R)	Mole fraction of air; use only if *idxgas* = 6.	Mole fraction	Default = 0.0
amfarg (R)	Mole fraction of argon; use only if *idxgas* = 6	Mole fraction	Default = 0.0
amffg (R)	Mole fraction of fission gas; use only if *idxgas* = 6 and if *amfxe* and *amfkry* = 0.0	Mole fraction	Default = 0.0
amfhe (R)	Mole fraction of helium; use only *idxgas* = 6.	Mole fraction	Default = 0.0 (note default on *idxgas* = 1 initializes pure He)
amfh2o (R)	Mole fraction of water vapor; use only if *idxgas* = 6.	Mole fraction	Default = 0.0
amfkry (R)	Mole fraction of krypton; use only if *idxgas* = 6.	Mole fraction	Default = 0.0
amfn2 (R)	Mole fraction of nitrogen; use only if *idxgas* = 6	Mole fraction	Default = 0.0
amfxe (R)	Mole fraction of xenon; use only if *idxgas* = 6.	Mole fraction	Default = 0.0
			(R) = real, (I) = integer

C.6 Input Variables Specifying Reactor Conditions

Variable Name (type)	Description	Units British/SI	Limitations/Default Value
iplant (I)	Signal for which type of reactor: -2 = PWR -3 = BWR -4 = HBWR	Dimensionless	Default = -2
nsp (I)	Signal for time-dependent input arrays for *p2*, *tw*, and *go*: If *nsp* = 0, single values for these three variables will be used for all time steps If *nsp* = 1, a value for each variable for each time step must be input	Dimensionless	Required input
p2(IT) (R)	Coolant System pressure. Must be input for each time step if *nsp* = 1	psia/Pa	Required input
tw(IT) (R)	Coolant inlet temperature. Enter a value for every time step if *nsp* =1	°F/K	Required input
go(IT) (R)	Mass flux of coolant around fuel rod. Input a value for each time step if *nsp* = 1. Note: *go* input may have to be adjusted to yield both desired coolant and desired cladding surface temperatures. Concurrent adjustment of *pitch* may also be required.	lb/hr-ft^2/ kg/s-m^2	Required input
pitch (R)	Center-to-center distance between rods in a square array	in./m	Required input (must be greater than *dco*)

Variable Name (type)	Description	Units British/SI	Limitations/Default Value
icor (I)	Index for Crud Model: *icor* = 0 or 1 yields constant crud thickness; 0.0 mil crud as default; input *crdt* as constant thickness. Maximum temperature rise permitted across this layer is 20 °F. *icor* = 2 yields time-dependent crud; growth rate is *crdtr*, starting from zero crud layer. There is no limit to the temperature rise across the crud when *icor*=2. The conductivity of the layer is 0.5 Btu/hr/ft-°F.	Dimensionless	Default = 0
crdt (R)	Initial thickness of crud layer on cladding outside surface	mils/m	Default = 0.0
crdtr (R)	Rate of crud accumulation (used if *icor* = 2)	mils/hr/m/s	Default = 0.0
flux(J) (R)	Conversion between fuel specific power (W/g) and fast neutron flux ($n/m^2/s$, E>1MeV). Input as an axial array; the second value of the array corresponds to the first axial node, the *na*+1 value corresponds to the top axial node.	n/m^2 /s/W/g of fuel	Default = 0.221×10^{17} (Maximum of 20 values)
			(R) = real, (I) = integer IT = Time Step Index J = 1 + Axial Node Index

C.7 Input Variables Specifying Power History

Variable Name (type)	Description	Units British/SI	Limitations/Default Value
im (I)	Number of time steps	Dimensionless	Greater than 1, less than 400 Required input (namelist frpcn)
ProblemTime(IT) (R)	Cumulative time at the end of each time step. Note: Time steps greater than 50 days are not recommended. If steady-state operation is being modeled, use time steps greater than 1 day. Time steps less than 1 day should only be used when modeling a fast power ramp.	Days	Required input Limit 400 steps
qmpy(IT) (R)	The linear heat generation rate at each time step. This equals the rod-average value if *iq* = 0 and the peak value if *iq* = 1. Note: Changes in local LHGR of greater than 1.5 kw/ft per time step are not recommended. Size *qmpy* accordingly.	kW/ft / kW/m	Required input Limit 400 steps
			R) = real, (I) = integer IT = Time Step Index

C.8 Input Variables Specifying Axial Power Profile

Variable Name (type)	Description	Units British/SI	Limitations/Default Value
iq (I)	Indicator for axial power shape: 0 = User-input power shapes, with *qmpy* = rod-average powers and power shapes defined by *qf*,*x*, and *fa* = 1.0 1 = Chopped-cosine shape, with *fa* = peak-to-average ratio and *qmpy* = peak power (use na=odd to have an axial node corresponding to the input peak power)	Dimensionless	Required input
x(N) (R)	The elevations in each *qf*, *x* array defining a power shape. Note the first value should be 0.0 and the last value must = *totl*	ft/m	Required input if *iq*=0 Maximum number of *qf*, *x* pairs is 40
qf(N) (R)	The ratio of the linear power at the *x*(N) elevation to the axially averaged value for the M-th power shape. The number of QF, X pairs for the Mth power shape is defined by *jn*(M). The code will automatically normalize to an average value of 1.0	Dimensionless	Required input if *iq* = 0 Maximum number of *qf*, *x* pairs is 40
jn(M) (I)	The number of *qf*, *x* value pairs for each axial power shape; required input if *iq* = 0. Input in the same sequence as the *qf* and *x* arrays.	Dimensionless	Required input if *iq*=0 Maximum number of shapes is 20. Maximum number of *qf*, *x* pairs is 40
jst(IT) (I)	The sequential number of the power shape to be used for each time step. One value of *jst* is required per time step if *iq* = 0.	Dimensionless	Required input if *iq*=0 Maximum number of power shapes = 20. Maximum time steps is 400.

Variable Name (type)	Description	Units British/SI	Limitations/Default Value
fa (R)	Peak-to-average power ratio for cosine-type axial power distribution (= 1.0, unless *iq* = 1; see description of *iq*)	Dimensionless	Required input
			(R) = real, (I) = integer N = Axial Node Index for Input Power Profile M = Power Shape Number IT = Time Step Index

C.9 Input Variables Specifying Axial Temperature Distribution (Optional)

Variable Name (type)	Description	Units British/SI	Limitations/Default Value
ifixedtsurf (I)	Indicator for using axial temperature distribution 0 = Cladding temperature will be calculated based on input power and coolant conditions 1 = Cladding temperature will be specified by the user for certain time steps. Each time step where the temperature will be set by the user, the input variable, *go*, should be set equal to 0.0.	Dimensionless	Default value = 0
xt(N) (R)	The elevations in each *cladt*, *xt* array defining a cladding temperature profile. Note: the first value should be 0.0, and the last value must = *totl* Begin the input elevations for the second temperature profile at xt(n+1), where n is the number of values in the first profile.	ft/m	Default value =0.0
cladt(N) (R)	The cladding surface temperature *xt*(N) elevation for the M-th temperature profile. The number of *cladt*, *xt* pairs for the Mth power shape is defined by *jnsurftemp*(M).	Dimensionless	Default value =0.0 Maximum number of *cladt*, *xt* pairs is 40
jnsurftemp(M) (I)	The number of *cladt*, *xt* value pairs for each axial temperature distribution; input in the same sequence as the *cladt* and *xt* arrays.	Dimensionless	Default value = 0 Maximum number of shapes is 20. Maximum number of *cladt*, *xt* pairs is 40

Variable Name (type)	Description	Units British/SI	Limitations/Default Value
jstsurftemp(IT) (I)	The sequential number of the temperature profile to be used for each time step. One value of *jstsurftemp* is required per time step if *ifixedtsurf* = 1.	Dimensionless	Default value = 0 Maximum number of shapes = 20. Maximum time steps is 400.
(R) = real, (I) = integer N = Axial Node Index for Input Surface Temperature Profile M = Surface Temperature Profile Number IT = Time Step Index			

C.10 Input Variables Specifying Code Operation

Variable Name (type)	Description	Units British/SI	Limitations/Default Value
nr (I)	Number of radial boundaries in the pellet (for temperature calculations and temperature distribution output). These are spaced by the code with greater fraction in the outer region to optimize definition of the heat generation radial distribution.	Dimensionless	Greater than 1, less than 25; suggested minimum number is 17 Default = 17 (namelist frpcn)
ngasr (I)	Number of equal-volume radial rings in the pellet for gas release calculations. ALSO SIGNALS WHICH GAS RELEASE MODEL THE CODE WILL USE. If *ngasr* is 10 or less, the ANS5.4 model is used; if 11 or greater, the MASSIH subroutine is used. It is not recommended to use ANS5.4 for burnups > 50 GWd/MTU	Dimensionless	Greater than 6, less than 50; suggested number is 45. Default = 45 (namelist frpcn)
na (I)	Number of equal-length axial regions along the rod, for which calculations are performed and output.	Dimensionless	Greater than 1, less than 18 Default = 9 (namelist frpcn)
nunits (I)	Signal for units system to be used for input and output: 1 = British units 0 = SI units Note that input of *nunits* >10 will activate "debug" output, which is significant in volume.	Dimensionless	Default = 1
crephr (R)	Subdivision for internal creep steps (should be set to a minimum of 10 creep steps per time step for smallest step)	hours	Default = 10.0

Variable Name (type)	Description	Units British/SI	Limitations/Default Value
sgapf (R)	Number of fission gas atoms formed per 100 fissions.	Dimensionless	Default = 31.0
slim (R)	Limit on swelling	Volume fraction	Default = 0.05
qend (R)	Fraction of end-node heat that transfers to the plenum gas	Dimensionless	Default = 0.3
igas (I)	Time step to begin calculation of fission gas release. For all time steps prior to *igas*, the calculated gas release will not be included in the gas in the rod void volume. (Note: this option only is available when using the Massih fission gas release model)	Dimensionless	Default = 0
			(R) = real, (I) = integer

C.10.1 Model Selection Variables Not Recommended by Pacific Northwest National Laboratory

Variable Name (type)	Description	Units British/SI	Limitations/Default Value
imswch (I)	Signal for EM models: = 1 All EM models = 0 No EM models = -1 Selected EM models, input signals in $EMFPCN	Dimensionless	Default = 0
impowr (R)	EM Power requirement index; = 0, not assumed to be required	Dimensionless	Default = 0 (namelist emfpcn)
imfuel (R)	Switch on dimensional changes: = 0, BE changes, =1, EM changes	Dimensionless	Default = 0 (namelist emfpcn)
imdens (R)	Switch on densification model	Dimensionless	Default = 0 (namelist emfpcn)
imrelo (R)	Switch on fuel relocation model	Dimensionless	Default = 0 (namelist emfpcn)

Variable Name (type)	Description	Units British/SI	Limitations/Default Value
imclad (R)	Switch on cladding deformation; = 1, no permanent deformation	Dimensionless	Default = 0 (namelist emfpcn)
imgapc (R)	Switch on gap conductance calculation	Dimensionless	Default = 0 (namelist emfpcn)
imenrg (R)	Switch on stored energy reference temperature: = 0 reference = 298 K = 1, reference = 273 K	Dimensionless	Default = 0 (namelist emfpcn)
			(R) = real, (I) = integer

C.11 Input Variables Specifying Code Output

Variable Name (type)	Description	Units British/SI	Limitations/Default Value
jdlpr (I)	Output print control for each time step: 0 = All axial nodes 1 = peak-power axial node -1 = axial summary for NO printout each step, see *nopt*	Dimensionless	Default = 1 Note: The code sets *jdlpr* to 0 (full output) when *ntape* is greater than 0, to assure full axial array of permanent radial deformations is passed to FRAPTRAN
nopt (I)	Control on printout = 0, printout each time step, controlled by *jdlpr* = 1, case input and summary sheet only	Dimensionless	Default = 0
nplot (I)	Control on output of plot file for excel plotting routine = 0, No output plot file will be created = 1, Plot output file will be created (File 66). Note: The name of the plot file should be specified in the input file below where the name of the ordinary output (File 06) is specified	Dimensionless	Default = 0
ntape (I)	Signal for creating a start tape for FRAPTRAN, from subroutine RESTFS. If *ntape* > 0, RESTFS is called and a tape (file 22= "restart") is incrementally written each time step	Dimensionless	Default = 0

Variable Name (type)	Description	Units British/SI	Limitations/Default Value
nread (I)	Signal to start up from a restart tape (File 13). The value of *nread* is the time step to start from. Note: user must switch his restart-write tape file number from 12 to 13 to make it a restart-read tape. Note: the restart tape does not currently contain complete restart information for the fission gas release models.	Dimensionless	Default = 0
nrestr (I)	Signal for writing a restart tape for FRAPCON-3. If *nrestr* not equal to 0, subroutine TAPEGEN generates a restart tape (file 12) at each time step. Note: the restart tape does not currently contain complete restart information for the fission gas release models.	Dimensionless	Default = 0
			(R) = real, (I) = integer

C.12 Example Case with MOX Fuel

```
*************************************************************************
*       frapcon3, steady-state fuel rod analysis code
*
*-------------------------------------------------------------------------------
*
*
*
*        CASE DESCRIPTION: MOX example rod
*
*
*
*UNIT     FILE DESCRIPTION
*
*------     ----------------------------------------------------------------Output:
*
*        Output :
*
*    6       STANDARD PRINTER OUTPUT
*
*
*
*        Scratch:
*
*    5       SCRATCH INPUT FILE FROM ECH01
*
*
*
*  Input:   FRAPCON3 INPUT FILE (UNIT 55)
*
*
*
*************************************************************************
* GOESINS:
FILE05='nullfile', STATUS='UNKNOWN', FORM='FORMATTED',
       CARRIAGE CONTROL='NONE'
*
* GOESOUTS:
FILE06='MOXexample.out',  STATUS='UNKNOWN', CARRIAGE CONTROL='LIST'
FILE66='MOXexample.plot', STATUS='UNKNOWN', FORM='FORMATTED',
      CARRIAGE CONTROL='LIST'
/*************************************************************************
       MOX Example Rod
 $frpcn
 im=50, na=4,
 ngasr = 45,
 $end
```

```
$frpcon
cpl = 2., crdt = 0.0, thkcld = 0.0224, thkgap = 0.0033,
dco = 0.374, pitch = 0.5,nplot=1,
rc = 0.0453, fotmtl = 1.997,dishsd=0.06488,
den = 94.43, dspg = 0.3,fa = 1.,
dspgw = 0.03, enrch = 0.229, fgpav = 382, hdish = 0.011,
hplt = 0.5, icm = 4, imox = 1, comp = 5.945,
idxgas = 1, iplant =-2, iq = 0, jdlpr = 0,
jn = 5,5,
totl = 1.31, roughc = 3.94e-5, roughf = 7.9e-5, vs = 10.0,
nunits = 1, rsntr = 52., nsp = 1,
p2(1) = 44*2250., p2(45) = 6*2352,
tw(1) = 44*570, tw(45) = 6*590
go(1) = 50*2.0e6,
jst = 44*1, 6*2
qf(1) = 1.0, 1.0, 1.0, 1.0, 1.0
x(1) = 0.0, 0.3275, 0.6650, 0.9925, 1.31
qf(6) = 0.9, 1.0, 1.1, 1.0, 0.9
x(6) = 0.0, 0.3275, 0.6650, 0.9925, 1.31
ProblemTime=
0.1, 0.2, 0.3, 0.4, 0.5,
0.6, 30., 60., 90., 120.,
150., 180., 210., 240., 270.,
300., 331., 360., 390., 420.,
450., 480., 510., 540., 570.,
600., 625., 650., 700., 750.,
800., 850., 900., 945., 990.,
1000., 1050., 1100., 1150., 1200.,
1250., 1300., 1350., 1400
1401., 1402., 1403., 1404., 1405.,
1406.
qmpy =
1,2,3,4,5,
6., 6.7, 6.7, 6.7, 6.7,
5*6.7
6.7, 6.7, 7.0, 7.0, 7.0,
5*7.0,
7.0, 7.0, 7.0, 5.8, 5.8,
5*5.8,
5*4.11,
4.11, 4.11, 4.11, 4.11,
4.0, 3.5, 3.0,
2.5, 2.0, 1.5
slim = .05,
$end
$frpmox
enrpu39 = 65.83, enrpu40 = 23.45, enrpu41 = 7.39,
enrpu42 = 3.33
$end
```

C.13 Input Variables Arranged Alphabetically and by Input Block

$frpcn input block

Variable Name	Page Number
im	C.9
na	C.14
ngasr	C.14
nr	C.14

$frpmox input block

Variable Name	Page Number
enrpu39	C.3
enrpu40	C.3
enrpu41	C.3
enrpu42	C.4

$emfpcn input block

Variable Name	Page Number
imclad	C.16
imdens	C.15
imenrg	C.16
imfuel	C.15
imgapc	C.16
impowr	C.15
imrelo	C.15

$frpcon input block

Variable Name	Page Number	Variable Name	Page Number
amfair	C.6	imswch	C.15
amfarg	C.6	iplant	C.7
amffg	C.6	iq	C.10
amfh2	C.6	jdlpr	C.17
amfh2o	C.6	jn	C.10
amfhe	C.6	jnsurftemp	C.12
amfkry	C.6	jst	C.10
amfn2	C.6	jstsurftemp	C.13
amfxe	C.6	nopt	C.17
catexf	C.5	nplot	C.17
chorg	C.5	nread	C.18
cladt	C.12	nrestr	C.18
cldwks	C.5	nsp	C.7
comp	C.3	ntape	C.17
cpl	C.2	nunits	C.14
crdt	C.8	p2	C.7
crdtr	C.8	pitch	C.7
crephr	C.14	ppmh2o	C.4
dco	C.2	ppmn2	C.4
den	C.4	ProblemTime	C.9
deng	C.4	qend	C.15
dishd	C.3	qf	C.10
enrch	C.3	qmpy	C.9
fa	C.11	rc	C.3
fgpav	C.6	roughc	C.5
flux	C.8	roughf	C.4
fotmtl	C.4	rsntr	C.4
gadoln	C.4	sgapf	C.15
go	C.7	slim	C.15
hdish	C.3	thkcld	C.2
hplt	C.3	thkgap	C.2
icm	C.5	totl	C.2
icor	C.8	tsint	C.4
idxgas	C.6	vs	C.2
ifixedtsurf	C.12	x	C.10
igas	C.15	xt	C.12
imox	C.3		

NRC FORM 335 (9-2004) NRCMD 3.7

U.S. NUCLEAR REGULATORY COMMISSION

BIBLIOGRAPHIC DATA SHEET

(See instructions on the reverse)

1. REPORT NUMBER
(Assigned by NRC, Add Vol., Supp., Rev., and Addendum Numbers, if any.)

NUREG/CR-6534, Vol. 4
PNNL-11513

2. TITLE AND SUBTITLE

FRAPCON-3 Updates, Including Mixed-Oxide Fuel Properties

3. DATE REPORT PUBLISHED

MONTH	YEAR
May	2005

4. FIN OR GRANT NUMBER

Y6586

5. AUTHOR(S)

D. D. Lanning, C. E. Beyer, K.J.Geelhood

6. TYPE OF REPORT

Technical Report

7. PERIOD COVERED *(Inclusive Dates)*

2002 - 2005

8. PERFORMING ORGANIZATION - NAME AND ADDRESS *(If NRC, provide Division, Office or Region, U.S. Nuclear Regulatory Commission, and mailing address; if contractor, provide name and mailing address.)*

Pacific Northwest National Laboratory
P.O. Box 999
Richland, Washington 99352

9. SPONSORING ORGANIZATION - NAME AND ADDRESS *(If NRC, type "Same as above"; if contractor, provide NRC Division, Office or Region, U.S. Nuclear Regulatory Commission, and mailing address.)*

Division of Systems Analysis and Regulatory Effectiveness
Office of Nuclear Regulatory Research
U.S. Nuclear Regulatory Commission
Wasington, DC 20555-0001

10. SUPPLEMENTARY NOTES

11. ABSTRACT *(200 words or less)*

The FRAPCON-3 code has been altered by a number of additions to form version FRAPCON-3.3. The major changes include an improved model for the urania fuel pellet thermal conductivity; the addition of mixed plutonia-urania oxide (MOX) fuel pellet thermal properties and other parameters to facilitate analysis of MOX fuel rod performance; and the addition of corrosion and hydrogen pickup parameters appropriate to advanced cladding types. This volume contains descriptions and discussions of these and other revisions.

The document also contains code-data comparisons of MOX fuel temperatures used to verify the MOX fuel pellet thermal conductivity model, and similar comparisons for urania fuel rods. The total sequence of code revisions that have led from the last-published version of FRAPCON-3 (NUREG/CR-6534, Volume 2, 1997) to the latest issued version, FRAPCON-3.3, is also given.

12. KEY WORDS/DESCRIPTORS *(List words or phrases that will assist researchers in locating the report.)*

Computer Code
Cladding
Fission Gas Release
FRAPCON
Fuel Temperature
Mixed Oxide
Nuclear Fuel
Plutonium Dioxide (Plutonia)
Thermal Conductivity
Uranium Dioxide (Urania)

13. AVAILABILITY STATEMENT

unlimited

14. SECURITY CLASSIFICATION

(This Page)
unclassified

(This Report)
unclassified

15. NUMBER OF PAGES

16. PRICE

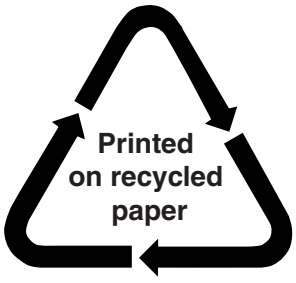

Federal Recycling Program